UNIVERSIDAD NACIONAL AUTÓNOMA DE MÉXICO

Maestría y Doctorado en Ciencias Bioquímicas

Propiedades amiloidogénicas de un fragmento derivado del dominio C-terminal de la proteína transferidora de ésteres de colesterol (CETP)

TESIS

QUE PARA OPTAR POR EL GRADO DE:
Maestro en Ciencias

PRESENTA:
VICTOR GUADALUPE GARCÍA GONZÁLEZ

TUTOR PRINCIPAL
JAIME MAS OLIVA (IFC, UNAM)

MIEMBROS DEL COMITÉ TUTOR
JULIO MORÁN ANDRADE (IFC, UNAM)
IGNACIO CAMACHO ARROYO (FQ, UNAM)

MÉXICO, D. F. noviembre, 2013

El presente trabajo se realizó bajo la dirección del Dr. Jaime Mas Oliva en el laboratorio 322N del departamento de Bioquímica y Biología Estructural del Instituto de Fisiología Celular de la Universidad Nacional Autónoma de México.

Dedicatoria

Este trabajo está dedicado a mi familia por todo el apoyo brindado, y especialmente a mis padres Maria Inés y Antonio, quienes han sido un ejemplo de trabajo incansable y lucha diaria.

Índice

Contenido **Página**

García-González, V.; Mas-Oliva, J. Amyloid fibril formation of peptides derived from the C-terminus of CETP modulated by lipids. *Biochem. Biophys. Res. Commun*. 2013, 434, 54-59.

García-González, V.; Mas-Oliva, J. Amyloidogenic Properties of a D/N Mutated 12 Amino Acid Fragment of the C-Terminal Domain of the Cholesteryl-Ester Transfer Protein (CETP). *Int. J. Mol. Sci.* 2011, 12, 2019-2035.

Mendoza-Espinosa, P.; García-González, V.; Moreno, A.; Castillo, R.; Mas-Oliva, J. Disorder-to-order conformational transitions in protein structure and its relationship to disease, *Mol. Cell. Biochem.* 2009, 330, 105-112.

Distinción

Premio de Investigación Médica "Jorge Rosenkranz 2010".

Área Básica. Categoria Consolidado. "Propiedades amiloidogénicas del péptido carboxilo-terminal de la Proteína Transferidora de Ésteres de Colesterol"

Jaime Mas Oliva y Victor Guadalupe García González

Resumen

La proteína transferidora de ésteres de colesterol (CETP) facilita la transferencia de ésteres de colesterol y triglicéridos entre lipoproteínas en el plasma, a través de una región critica para su función que está situada en el dominio C-terminal. Nuestro grupo de trabajo previamente ha demostrado que este dominio presenta cambios conformacionales en un ambiente sin lípidos y cuando se introduce la mutación $D_{470}N$. En este sentido, usando una serie de péptidos derivados de este dominio C-terminal, en el presente estudio se demostró que estos cambios favorecen la inducción de una estructura secundaria de tipo β, caracterización que fue realizada a través de estudios espectroscópicos y técnicas de microscopía electrónica. A partir de la estructura secundaria-β, se forman oligómeros y estructuras fibrilares con características de tipo amiloide que inducen citotoxicidad en células de microglia en cultivo. Estas estructuras supramoleculares promueven fenómenos de citotoxicidad a través de la formación de especies reactivas de oxígeno (ERO) y cambios en el balance de una serie de proteínas que controlan el proceso de endocitosis, condiciones que son similares a las que se han observado en el estudio de las fibras del péptido β-amiloide. No obstante, el grado de solvatación determinado por la presencia de grupos hidroxilo sobre la superficie de lípidos, como el ácido lisofosfatídico, es una condición clave que puede modular la estructura secundaria promoviendo la estructura nativa α-hélice, lo cual evita la formación de fibras amiloides en el dominio C-terminal de CETP. De manera que un delicado balance entre la altamente dinámica estructura secundaria del dominio C-terminal de CETP, su carga neta, y las propiedades fisicoquímicas del microambiente circundante de lípidos, como el grado de solvatación, definen el tipo de estructura secundaria adquirida. Cambios en este balance podrían favorecer el plegamiento anómalo en esta región, lo cual podría alterar la capacidad de

transferencia de lípidos conducida por CETP, favoreciendo la propensión a sustituir su función fisiológica.

Abstract

The cholesteryl-ester transfer protein (CETP) facilitates the transfer of cholesterol esters and triglycerides between lipoproteins in plasma, where the critical site for its function is situated in the C-terminal domain. Our group has previously shown that this domain presents conformational changes in a non-lipid environment when the mutation $D_{470}N$ is introduced. Using a series of peptides derived from this *C*-terminal domain, the present study shows that these changes promote the induction of a secondary β-structure, as characterized by spectroscopic analysis and microscopic techniques. From this type of secondary structure, the formation of peptide aggregates and fibrillar structures with amyloid characteristics induced cytotoxicity in microglial cells in culture. These supramolecular structures promote cell cytotoxicity through the formation of reactive oxygen species and change the balance of a series of proteins that control the process of endocytosis, similar to that observed when β-amyloid fibrils are employed. Notwithstanding, the degree of solvation determined by the presence of a free hydroxyl group on lipids such as lysophosphatidic acid is a key condition that can modulate the secondary structure and the consequent formation of amyloid fibrils in the C-terminal domain of CETP. Therefore, a fine balance between the highly dynamic secondary structure of the *C*-terminal domain of CETP, the net charge, and the physicochemical characteristics of the surrounding microenvironment, such as the degree of solvation, define the type of secondary structure acquired. Changes in this balance might favor misfolding in this region, which would alter the lipid transfer capacity conducted by CETP, favoring its propensity to substitute its physiological function.

1. Introducción

A la fecha un importante número de enfermedades causadas por la agregación de proteínas con un plegamiento anómalo han sido descritas. De éstas, aproximadamente 40 enfermedades se han asociado con péptidos y proteínas con propiedades de tipo amiloide que se agregan de manera extracelular e intracelular [1]. Sin embargo, el auto-ensamblaje hacia estructuras fibrilares del tipo amiloide no es una característica restringida hacia un grupo reducido de péptidos y proteínas con patrones específicos en la secuencia de aminoácidos o en la estructura tridimensional nativa. Desde hace más de tres lustros, se ha encontrado que varias secuencias peptídicas a pesar de presentar la propiedad de formar estructuras de tipo amiloide no están asociadas con alguna patología. En este sentido, se ha descrito la adaptación de funciones celulares específicas a la formación de amiloides, por ejemplo en la polimerización de moléculas precursoras durante la formación de la melanina dentro de los melanocitos [2]. De manera que actualmente la formación de estructuras amiloides se considera como una propiedad que pudiera ser genérica a muchas cadenas polipeptídicas, y en varios casos estar directamente relacionada con una función fisiológica [3]. De hecho, la diferencia entre amiloides funcionales y los que están asociados a enfermedad puede residir en los mecanismos celulares de regulación que están involucrados durante su formación [4].

Por varios años, nuestro laboratorio ha estado enfocado en el estudio de la relación entre estructura y función de proteínas asociadas con la unión y transporte de lípidos, como varias apolipoproteínas que forman parte de las partículas lipoproteínas, y la proteína transferidora de ésteres de colesterol (CETP). De forma colateral a los cambios encontrados en la estructura secundaria de regiones específicas de varias de estas proteínas, tales como la apolipoproteína C-I, hemos propuesto la posibilidad de que estas regiones responden a cambios específicos en el

microambiente de lípidos que las rodea, y a través de transiciones específicas desorden-al-orden poder actuar como interruptores moleculares que disparan o suprimen la función [5-7].

1.1 La proteína transferidora de ésteres de colesterol (CETP)

CETP es una glicoproteína hidrofóbica que promueve la transferencia de ésteres de colesterol y triglicéridos entre lipoproteínas, principalmente direccionando el flujo de colesterol de lipoproteínas de alta densidad (HDL) hacia lipoproteínas de baja y muy baja densidad (LDL y VLDL, respectivamente). Así mismo, CETP tiene la capacidad de transferir triglicéridos de las VLDL hacia HDL, lo cual origina un cambio en la composición, tamaño y estructura esférica de las HDL (Figura 1) [8]. A este respecto, extensos estudios sobre polimorfismos y deficiencias genéticas en CETP sugieren una relación directa entre su actividad, los niveles de colesterol en HDL y el potencial desarrollo de enfermedad cardiovascular [9]. Estudios de deleción y mutagénesis sitio-específica han mostrado que el dominio localizado en el extremo C-terminal (E_{465}-S_{476}), estructurado como una α-hélice anfipática, corresponde con una región clave para la transferencia de lípidos (Figura 1) [10-12].

CETP es una proteína plasmática de 476 residuos, con un peso molecular aproximado de 67 kDa, contiene cuatro glicosilaciones y un 44 % de los residuos son hidrofóbicos. La estructura cristalográfica de CETP refleja una estructura alargada en forma de *boomerang* con un plegamiento homólogo a la proteína BPI (bactericidal/permeability-increasin protein) [13,14]. La descripción estructural de CETP se puede realizar en cuatro dominios: un barril-β en cada costado de la proteína, denominados barriles N y C, una hoja β central conectora entre los dos

barriles y una extensión C-terminal nombrada hélice-*X*, la cual no se encuentra presente en la proteína BPI, siendo un dominio crítico para la actividad de transferencia de lípidos (Figura 1).

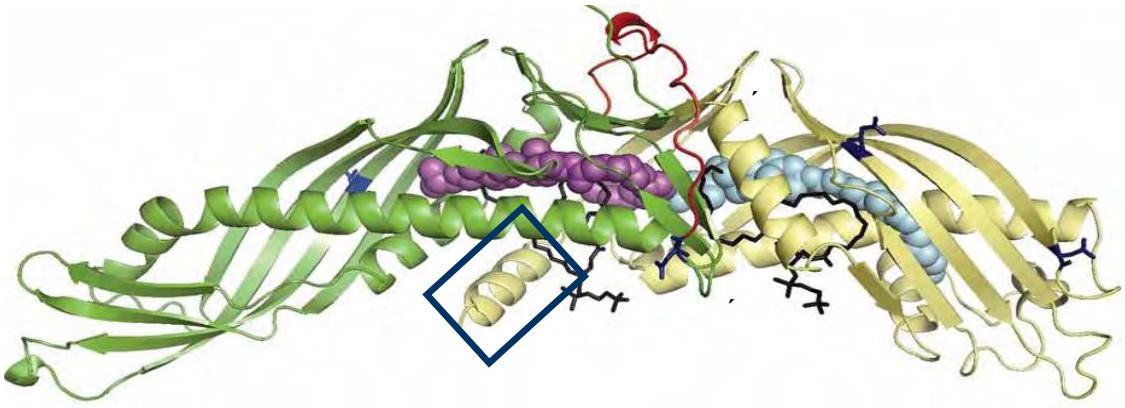

Figura 1. Estructura tridimensional obtenida a partir del cristal de CETP. En verde se muestra el barril N y en amarillo el C, la conexión entre ambos dominios se encuentra marcada en rojo. En magenta y cyan se presentan las moléculas de éster de colesterol, los fosfolípidos están representados en negro. El dominio C-terminal nombrado hélice-*X* está enmarcado en un recuadro azul. La estructura fue obtenida del Protein Data Bank (PDB), código de acceso: 2obd.

La Figura 2 muestra una imagen representativa de los últimos 24 residuos en el C-terminal de CETP (aa 453-476), integrado por una hebra-β (aa 453-462) y una estructura hélice-α (465-476), estas regiones están conectadas por un segmento de tres residuos (aa 462-464). La determinación de la estructura tridimensional ha sentado una base sólida para la propuesta de que CETP podría unirse sólo a una lipoproteína a la vez, y llevar a cabo su función a través de un mecanismo acarreador durante la transferencia de lípidos por medio del transporte de lípidos en el interior del túnel hidrofóbico que forma la proteína [13]; sin embargo no hay resultados concretos que expliquen la manera en como los ésteres de colesterol localizados en el núcleo de las partículas HDL alcancen el interior del túnel a través del medio acuoso. Estudios de nuestro laboratorio sugieren que el mecanismo de transferencia

puede estar directamente relacionado con la formación de un sistema micelar de acarreo de lípidos alrededor del dominio C-terminal de 12 residuos (465-476), como la manera de transferencia de ésteres de colesterol entre lipoproteínas a través de un ambiente acuoso, en donde la conservación de la estructura α-helicoidal de esta región es fundamental para que se lleve a cabo este proceso [15].

Durante la caracterización estructural de este dominio hemos encontrado que la interrupción del puente salino H_{466}-D_{470} por medio de la mutación $D_{470}N$ en la región α-helicoidal origina la pérdida de la estructura secundaria, de manera que este dominio se mantiene en un estado desordenado, debido en parte al cambio del grupo funcional carboxilato cargado negativamente en el ácido aspártico por el grupo amida presente en la asparagina (Figura 2) [10]. Durante este trabajo nos hemos enfocado sobre los 12 residuos del dominio C-terminal de CETP, a través del estudio de la estructura y función de dos péptidos derivados de este sitio, la secuencia nativa nombrada hélice-*X* y un péptido con la mutación $D_{470}N$, denominado hélice-*Z* (Figura 2).

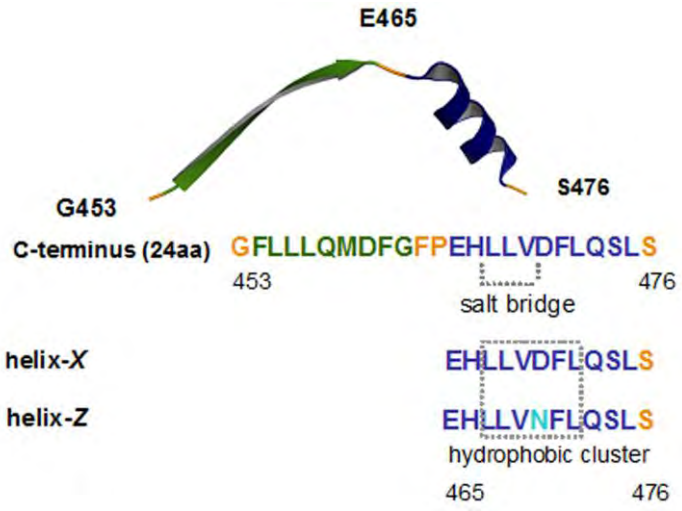

Figura 2. Representación estructural de la región C-terminal de CETP, mostrando la secuencia de aminoácidos de la hélice-*X* y hélice-*Z*. El puente salino H_{466}-D_{470} y el clúster hidrofóbico se encuentran marcados. La estructura fue obtenida del PDB: 2obd.

1.2 Cambios estructurales dependientes de lípidos

En un intento por definir la posibilidad de que las características clave del plegamiento en proteínas que participan en la unión y transporte de lípidos puedan proporcionarnos la manera de cómo explicar funciones básicas, como el reconocimiento a receptores, la actividad de transferencia de lípidos y el autointercambio llevado a cabo por varias apolipoproteínas, nuestro grupo de investigación ha estudiado estas propiedades a través de mediciones directas de los cambios de conformación molecular de varias apolipoproteínas en interfaces aire/agua y lípido/agua [5]. Esto se ha logrado empleando monocapas de Langmuir en conjunción con microscopía de ángulo de Brewster, microscopía de fuerza atómica en películas de proteínas de LB [16-19], difracción de rayos X en ángulo razante sobre monocapas de proteínas [20] y por medio de mediciones de fuerza superficial [21].

A diferencia de las proteínas altamente ordenadas, en las cuales las estructuras tridimensionales exhiben sólo pequeños cambios del eje central de átomos de carbono sobre sus posiciones de equilibrio, se ha descrito la existencia de proteínas desordenadas, las cuales se visualizan como ensamblajes dinámicos, en donde las posiciones de los átomos y los ángulos de torsión φ y ψ del espacio de Ramachandran pueden variar de forma significativa en el tiempo. Es precisamente esta propiedad la que permite la propuesta del concepto del *desorden en proteínas* [22–24].

Aunque la función que depende de manera específica de las proteínas completamente desordenadas representa el caso extremo, el concepto de tener segmentos desordenados en proteínas que sólo responden y adquieren una estructura secundaria definida bajo la unión a ligandos específicos, puede ser un fenómeno más común de lo que se ha visualizado. Este concepto se ha extendido a varias proteínas de unión a lípidos como la apolipoproteína C-I, en donde se ha determinado la

adquisición de una rápida conformación α-helicoidal dependiente de lípidos a partir de una transición desorden-al-orden en el dominio C-terminal [7]. Incluso, en el estudio de péptidos derivados de regiones específicas de la apolipoproteína A-I, cuando se mantienen en incubación a 4 °C, una muy lenta transición desorden-al-orden se desarrolla durante el curso de semanas, desde un estado desordenado hacia una bien definida estructura secundaria-β [25]. Esta condición apoya la propuesta de que las propiedades fisicoquímicas del microambiente que rodea a las proteínas pueden ser un factor clave en el desplazamiento del equilibrio hacia la formación de hélices-α o cadenas-β en segmentos específicos de proteínas [26].

1.3 Amiloides

Un importante número de enfermedades humanas encuentran su origen en el auto-ensamblaje anómalo de proteínas formando depósitos de fibras amiloides [27,28]. Aunque el establecimiento absoluto de esta conexión no ha sido demostrado, una evidencia sólida indica una fuerte conexión entre la formación de fibras amiloides y la presencia de toxicidad [29-31]. En este contexto, los amiloides son agregados de proteínas que se depositan en los tejidos durante el transcurso de diversas enfermedades. En condiciones normales, estas proteínas se encuentran en su plegamiento nativo, debido a múltiples factores adquieren un plegamiento anómalo, se vuelven insolubles y pueden resistir la degradación enzimática. A pesar de que la secuencia de aminoácidos es diferente de una proteína amiloide a otra, todas se depositan formando una estructura común, la fibra de tipo amiloide. Cada fibra está constituida por un solo tipo de proteína que se ensambla en forma repetitiva, y por lo general la proteína adquiere la conformación de hoja-β plegada.

Tomando en cuenta que existen varias estrategias de control y regulación que han evolucionado en los sistemas biológicos para proteger los mecanismos del plegamiento de proteínas, es sólo cuando éstos fallan que la condición patológica

asociada al plegamiento anormal se torna evidente. Aunque las enfermedades relacionadas con amiloides poseen diferentes características, sus orígenes moleculares pueden tener puntos en común. Por ejemplo, la agregación de proteínas es un proceso complejo que progresa de oligómeros pequeños a estructuras más organizadas como los protofilamentos, antes de la formación de las fibras amiloides bien definidas. Sin embargo, también la agregación puede generar grandes ensamblajes desorganizados que generalmente se describen como estructuras *amorfas*.

1.4 Endocitosis mediada por clatrina

La membrana plasmática es una estructura altamente dinámica que separa el medio intracelular del ambiente extracelular y regula la entrada y salida de diversas moléculas. Existen varias vías de entrada a las células: fagocitosis, macropinocitosis, endocitosis medida por clatrina, endocitosis mediada por caveolina y endocitosis independiente de clatrina y de caveolina. Inicialmente la formación de vesículas cubiertas de clatrina se caracterizó en las terminales nerviosas, donde es importante para el reciclaje de los componentes de las vesículas sinápticas después de la liberación de los neurotransmisores. La endocitosis mediada por clatrina constituye la principal vía para la internalización selectiva de receptores y sus ligandos en eucariotas superiores [32].

El proceso por el cual se producen las vesículas cubiertas de clatrina involucra interacciones tanto con proteínas adaptadoras multifuncionales como con la membrana plasmática, así como con la misma clatrina y varias proteínas accesorias y fosfoinosítidos. A través de este mecanismo, las moléculas que van a entrar son empaquetadas en vesículas cubiertas con la proteína clatrina. Este mecanismo es fundamental para la neurotransmisión, la transducción de señales y la

regulación de muchas actividades celulares que ocurren sobre la membrana plasmática [33].

Se ha descrito que la endocitosis dependiente de clatrina normalmente ocurre en sitios especializados de la membrana [34]. De forma general, la formación de vesículas recubiertas de clatrina procede a través de cinco etapas: iniciación, la selección del ligando, el ensamblaje del pozo, la fisión de la vesícula en la superficie de la membrana y el desensamblaje dentro de los endosomas [33].

Dentro del mecanismo de endocitosis mediada por clatrina, se han descrito más de 30 proteínas, muchas de las cuales son moléculas adaptadoras implicadas en la formación de los pozos cubiertos de clatrina. En este sentido, las proteínas α-, β-, μ-, y σ-adaptina integran el complejo adaptador AP2, un componente estructural clave durante las fases iniciales de la endocitosis [35]. Además de clatrina y el complejo AP2, proteínas tales como CALM, epsina, dinamina, anfifisina y eps15 también juegan un papel importante durante este mecanismo [35].

1.5 Formación de fibras amiloides modulada por lípidos

Se ha reportado que bajo condiciones específicas, moléculas de lípido pueden inducir cambios conformacionales en varias proteínas precursoras de amiloides, además de la función que ya se ha descrito los lípidos pueden tener durante la formación y en la posterior estabilización de las fibras de tipo amiloide [7,26,36]. En este sentido, se ha descrito que la interacción de las especies precursoras oligoméricas sobre dominios específicos de la membrana celular es un evento primario que puede desencadenar la aparición de los efectos citotóxicos iniciales asociados con la enfermedad [4,37].

En este caso, el papel de la composición específica de lípidos sobre la interface hidrofílica/hidrofóbica, determinada por las características químicas de

estas moléculas, puede ser una condición importante como sitio de reconocimiento que module posibles cambios conformacionales en la estructura secundaria de dominios específicos de proteínas, que a su vez podría modificar la formación de estructuras amiloides controladas por transiciones conformacionales desorden-al-orden y orden-al-desorden [4,7,26,38,39]. En este respecto, se ha descrito que moléculas como el ácido lisofosfatídico (LPA), un fosfolípido derivado de la acción enzimática de varias fosfolipasas extracelulares a partir de moléculas precursoras como la lisofosfatidilcolina y el ácido fosfatídico (PA), pueden promover *in vitro* la formación de fibras amiloides en la proteína β2-microglobulina [40,41]. Sin embargo, el mecanismo a través de la enzima autotaxina que particularmente produce una alta cantidad de LPA a partir de lisofosfatidilcolina es todavía poco entendido [42,43].

De esta forma, empleando al péptido hélice-*Z* (portador de la mutación $D_{470}N$) como una secuencia modelo, nos ha permitido demostrar un cambio conformacional en el dominio C-terminal de CETP, de una estructura α-helicoidal hacia una cadena-β, siendo la carga neta de la secuencia peptídica uno de los parámetros determinantes en dicha transición.

De manera secundaria a la formación de la estructura en hoja-β, el fragmento hélice-*Z* muestra la consiguiente formación de oligómeros y estructuras fibrilares de tipo amiloide que a su vez causan efectos citotóxicos asociados a la producción de especies reactivas de oxígeno, similares a los producidos por el péptido β-amiloide. Sin embargo, de forma interesante se ha encontrado que moléculas como el LPA y la lisofosfatidilcolina promueven un cambio estructural de una cadena-β hacia la estructura nativa hélice-α, incluso la incubación de la hélice-*Z* con concentraciones de LPA por arriba de 2.5 mM inhibe la formación de las fibras amiloides, de manera que las interacciones del péptido sobre la superficie de las micelas de LPA deben mantenerlo retenido sobre la superficie y de forma consecuente prevenir fenómenos

como el auto-ensamblaje de los péptidos cuando se mantienen en solución. Estas condiciones deben permitir a la hélice-*Z* recuperar y mantener la estructura funcional hélice-α del dominio C-terminal de CETP.

2. Materiales y métodos

2.1 Materiales

Todos los reactivos para cultivo celular fueron adquiridos de Gibco-Invitrogen (Carlsbard, CA, E.U.), mientras que las cajas de cultivo y el material de plástico se obtuvieron de Nulgene Nunc (Rochester, NY, E.U.). Las sales para la preparación de las soluciones amortiguadores se obtuvieron de Baker. El terbutil hidroperóxido (TBH), la tioflavina T (ThT), el rojo-Congo, el dodecil sulfato de sodio (SDS) y el 3-(4,5-dimetiltiazol-2-ilo) 2,5 bromuro difeniltetrazolio (MTT) se obtuvieron de Sigma-Aldrich (St. Louis, MO, E.U.). Los anticuerpos usados en la detección de las proteínas β-actina, CALM, β-adaptina y eps-15 fueron de Santa Cruz Biotechnology (Santa Cruz, CA, E.U.), así como los anticuerpos secundarios.

El colesterol, el éster de colesterol, el dipalmitoil ácido fosfatídico (PA), la dipalmitoil fosfatidiletanolamina (PE), la dipalmitoil fosfatidilcolina (DPPC) se obtuvieron de Sigma-Aldrich (St. Louis, MO, E.U.). Los lípidos L-α-fosfatidilcolina (PC), 1-palmitoil-2-oleoil-sn-glicero-3-fosfocolina (POPC), 1-palmitoil-2-oleoil-sn-glicero-3-fosfo-1-glicerol (POPG), 1-lauroil-2-hidroxi-sn-glicero-3-fosfocolina (liso-C_{12}PC) y el 1-oleoil-2-hidroxi-sn-glicero-3-fosfato (LPA) se obtuvieron de Avanti Polar Lipids (Alabaster, AL, E.U.).

2.2 Síntesis de péptidos y preparación

Basados en la función del C-terminal de CETP, dos péptidos fueron sintetizados, uno nombrado hélice-*X* que corresponde a la secuencia nativa, y el segundo denominado hélice-*Z* que contiene la mutación $D_{470}N$ (Genscript, NJ, E.U.). Los péptidos liofilizados se disolvieron en una solución amortiguadora de

carbonato de amonio (pH 9.5) a una concentración de 1 mg/ml, a partir de esta solución se llevó a cabo una dilución 1:5. Para evaluar la estructura a un pH de 3.8 y 4.8 se usó un amortiguador de acetatos; para pH 6.3 y 7.2 se usó un amortiguador de fosfatos, y para un pH de 8.6 y 9.5 fue empleado un amortiguador de carbonatos.

El fragmento 25-35 del péptido β-amiloide (βA_{25-35}) se empleó como una molécula de referencia para los ensayos de citotoxicidad (Figura 3). Los experimentos realizados con este péptido se llevaron a cabo en dos condiciones de pH, usando un regulador de fosfatos (pH 7.2) y con H_2O ultrapura (pH 5.5), ambas condiciones con la misma concentración de péptido (1.5 mg/ml). Todas las soluciones reguladoras se usaron bajo una concentración 50 mM, y se filtraron a través de membranas con un poro de 0.22 µm.

DAEFRHDSGYEVHHQKLVFFAEDVGSNKGAIIGLMVGGVVIA

1 25 35 42

βA_{25-35} **GSNKGAIIGLM**

βA_{35-25} **MLGIIAGKNSG**

Figura 3. Secuencia primaria del péptido β-amiloide (1-42), en azul se encuentra marcada la región considerada como de mayor citotoxicidad, la cual abarca los residuos G_{25}-M_{35}, así como la secuencia inversa M_{35}- G_{25}.

La pureza de los péptidos fue mayor al 98 % (Genscript, NJ, E.U.). Su identidad y pureza se confirmó por espectrometría de masas y por análisis de HPLC (datos no mostrados). La concentración fue determinada a través de la absorbancia del enlace peptídico a 205 y 218 nm.

2.3 Momento hidrofóbico (μH)

El cálculo del momento hidrofóbico se realizó a través de la ecuación 1.

$$\mu H = \frac{1}{N}\sqrt{\left[\sum_{n=1}^{N} H_n \sin(\partial n)\right]^2 + \left[\sum_{n=1}^{N} H_n \cos(\partial n)\right]^2} \quad \text{.....(1)}$$

μH Momento hidrofóbico

N Número total de aminoácidos del segmento peptídico

H_n Hidrofobicidad del enésimo residuo

∂ Ángulo expresado en radianes entre dos residuos

n Enésimo residuo

2.4 Espectroscopía de dicroísmo circular

Los espectros de dicroísmo circular (DC) en el espectro ultravioleta (UV) se registraron en un espectropolarímetro Aviv 62DS en una celda de cuarzo de 0.1 cm, usando un tiempo promedio de integración de 2.5 s y un tamaño de paso de 0.5 nm. Los resultados de DC son reportados en valores de elipticidad molar media (Θ, deg cm^2 $dmol^{-1}$) considerando la corrección realizada con las soluciones amortiguadoras, los cuales fueron obtenidos con base en la ecuación 2. En los estudios de pH, los espectros de DC se obtuvieron en una escala de pH de 3.8–9.5. Así mismo, se realizaron experimentos de desnaturalización por temperatura en un rango de 4–90 °C.

$$[\Theta] = \frac{[\Theta_{experimental}]}{[CMR]\,[Longitud\ de\ la\ celda]\,[10]} \quad \text{..... (2)}$$

A su vez, la concentración media por residuo (CMR) se determinó con base en la siguiente ecuación:

$$[CMR] = \frac{[\text{Concentración en mg/ml}]\,[\text{número de aminoácidos}]}{[\text{Peso molecular}]} \quad \ldots\ldots (3)$$

2.5 Espectroscopía con rojo-Congo y fluorescencia acoplada a tioflavina-T (ThT)

Los ensayos con rojo-Congo se realizaron con base en el protocolo establecido por Klunk *et al* [44]. Empleando una concentración de 10.6 μM de rojo-Congo y 180 μg/ml de péptido, se midió la absorbancia cada 2 nm dentro de un rango de 360–700 nm en un espectrofotómetro Perkin Elmer UV/Vis Lambda 2S. La presencia de la estructura secundaria-β estuvo caracterizada por un pico máximo de absorbancia en ~540 nm. Los espectros obtenidos de los péptidos se corrigieron restando el espectro de las soluciones amortiguadoras, bajo las mismas condiciones experimentales.

Adicionalmente, la presencia de la estructura-β se determinó con el ensayo de tioflavina-T (ThT). Los espectros de emisión de fluorescencia se registraron a 37 °C en un rango de 470–530 nm con una longitud de onda de excitación de 450 nm. Los registros se llevaron a cabo con una velocidad de barrido de 73 nm/min en un fluorímetro Olis DM45. Las concentraciones de la ThT y de los péptidos fueron 10 μM y 36 μM respectivamente.

2.6 Cultivo celular

Células EOC (microglia de ratón, American Type Culture Collection) fueron cultivados en medio DMEM (Dulbecco´s modified Eagles´s) suplementado con 10 % de suero fetal bovino y 20 % de medio condicionado LADMAC, obtenido de cultivos celulares de medula ósea de ratón que producen el factor de crecimiento estimulador de colonias 1. Así mismo, se adicionaron penicilina (50 U/ml) y estreptomicina (50 µg/ml) a los medios de cultivo. Antes de realizar los experimentos, se recambió el medio de cultivo por medio mínimo Opti-MEM (sin rojo de fenol y una concentración baja de suero fetal), llevándose a cabo todos los experimentos en esta condición para evitar posibles interferencias debidas al suero fetal y al medio LADMAC.

2.7 Ensayos de viabilidad celular

La citotoxicidad de los péptidos se evaluó a través del ensayo de reducción de la molécula 3-(4,5-dimetiltiazol-2-ilo) 2,5 bromuro difeniltetrazolio (MTT) en células EOC tratadas con hélice-*X*, hélice-*Z* y el péptido β-amiloide (βA_{25-35}). Las células se cultivaron en placas de 96 pozos con una densidad de 10,000 células por pozo en 100 µl de medio de cultivo, y se mantuvieron hasta una confluencia del 80 %. Posteriormente, el medio de cultivo fue reemplazado por medio Opti-MEM. Después de 2 h en esta condición, las células fueron tratadas bajo una serie de concentraciones graduales de péptido durante 20 h. Finalmente, 30 µl de una solución stock de MTT en medio Opti-MEM (2.1 mg/ml) fueron adicionados a los cultivos con la finalidad de alcanzar una concentración 0.5 mg/ml.

Los cristales de azul de formazán que se producen después de 4 h de incubación se disolvieron con la adición de buffer de lisis (20 % SDS, 50 % *N*,*N*-dimetilformamida, pH 3.7). A las 12 h de incubación se midió la absorbancia a 570 nm usando un lector de microplacas.

2.8 Inmunotransferencia tipo Western

Con una confluencia del 80%, las células fueron expuestas a diferentes dosis de los péptidos por 20 h. Después de este procedimiento, las células se lavaron con PBS y se lisaron por 45 min a 4 °C en buffer de lisis [150 mM NaCl, 10 mM Tris pH 7.4, Triton X-100 al 1%, NP40 al 0.5%, 1 mM EDTA, 1 mM EGTA, 0.2 mM de ortovanadato de sodio, 10 mM benzamidina, 10 μg/ml leupeptina, 10 μg/ml aprotinina y 250 μM PMSF]. Los lisados celulares se pasaron 5 veces por una jeringa de insulina y posteriormente se centrifugaron a 8,000 rpm por 10 min, y el sobrenadante fue recuperado para su análisis. La concentración de proteína fue determinada con el método del ácido bicinconílico (Pierce, IL, E.U.), en un siguiente paso muestras de la fracción total de proteínas (14 μg/carril) fueron analizadas a través de geles SDS-PAGE al 8%, los cuales fueron transferidos a membranas de PVDF (Millipore, MA, E.U.).

Las membranas fueron bloqueadas toda la noche a 4 °C en una solución salina amortiguada con Tris (TBS), 1 % tween-20, y 5 % de leche sin grasa. Para la detección de las proteínas, los siguientes anticuerpos policlonales provenientes de cabra fueron usados: anti-β-adaptina (1:600), anti-CALM (1:600), así como el de conejo anti-eps 15 (1:2500) y un monoclonal anti-β-actina (1:500). Las membranas previamente bloqueadas se incubaron con los anticuerpos primarios durante 1 h a 37 °C. Después de lavados sucesivos, las membranas se incubaron con anticuerpos

secundarios específicos acoplados a peroxidasa de rábano (1:5,000) por 1 h a 37 °C. Los anticuerpos usados fueron los siguientes: IgG anti-cabra para la detección de β-adaptina y CALM, un IgG anti-conejo para eps15, y un IgG anti-ratón para β-actina. Posteriormente, las membranas fueron lavadas con una solución TBS/1 % tween, y la actividad de peroxidasa fue detectada con el kit Immobilon Western (Millipore).

2.9 Microscopía óptica

Bajo las diferentes condiciones experimentales, y usando concentraciones variables de los péptidos hélice-*X*, hélice-*Z* y el péptido$\beta A_{25\text{-}35}$, las células EOC fueron visualizadas. Las imágenes fueron tomadas con un microscopio Olympus IX71 (100 y 400 X, aumentos).

2.10 Preparación de micelas de lípidos

Preparación de mezclas formadas de fosfatidilcolina (PC)/ésteres de colesterol

Los lípidos se mezclaron en cloroformo, posteriormente fueron secados por 6 h bajo un flujo suave de N_2, y un periodo adicional de 24 h en un concentrador SpeedVac (Savant). Las mezclas fueron preparadas con una relación molar de PC 2 mM y ésteres de colesterol 100 μM (relación molar 20:1). Posterior al secado, los lípidos se resuspendieron en una solución amortiguadora pH 6.8 y subsecuentemente fueron sonicados con 4 ciclos de 10 min (pulsos de 15 s encendido/30 s descanso) en un baño de hielo y bajo un flujo de N_2, a través de un ultrasonicador Sonifier 250 (Branson). Las muestras se dejaron equilibrar por 2 h y fueron centrifugadas a 13,000 rpm por 10 min.

Preparación de micelas de lyso-C_{12}PC, LPA y PA

Las cantidades requeridas de lisofosfatidilcolina-C12 (lyso-C_{12}PC) disuelta en cloroformo fueron colocadas bajo un flujo suave de N_2 por 4 h. La completa evaporación del solvente se alcanzó con un tratamiento adicional por 22 h en el equipo de vacío SpeedVac. Posteriormente, las muestras fueron resuspendidas en un amortiguador de fosfatos pH 6.8 a 37 °C (50 mM), se mantuvieron 2 h a 25 °C y fueron centrifugadas a 13,000 rpm por 10 min a 12 °C.

Por otra parte, las muestras de ácido lisofosfatídico (LPA) se colocaron bajo un flujo suave de N_2 por 6 h, y 12 h adicionales en un equipo de vacío. Las muestras fueron hidratadas en el amortiguador de fosfatos para ser procesadas a través de 4 ciclos de congelamiento en N_2 líquido, y descongelamiento a 37 °C. Las muestras se dejaron equilibrar por 2 h y fueron centrifugadas a 13,000 rpm por 10 min. Bajo las mismas condiciones experimentales, micelas de ácido fosfatídico (PA) fueron preparadas con una etapa adicional de sonicación por 4 ciclos de 10 min.

Preparación de micelas de fosfolípidos y LPA

Los lípidos PC y LPA fueron mezclados en cloroformo y secados por 6 h bajo un flujo de N_2, así mismo mediante un tratamiento adicional en el equipo de vacío por 22 h. Las mezclas de lípidos fueron preparadas con una relación molar de PC 3.06 mM y LPA 0.92 mM. Después del secado, las mezclas de lípido fueron resuspendidas en un amortiguador pH 6.8 y posteriormente fueron sonicadas por 4 ciclos, como previamente se ha descrito. Las muestras se mantuvieron equilibradas por 2 h a 25 °C y al final fueron centrifugadas a 13,000 rpm por 10 min. Empleando la misma metodología, se prepararon micelas compuestas de DPPC/LPA y PE/LPA. De igual forma, micelas con una carga negativa fueron preparadas con la adición de LPA, bajo una relación de 75 % de POPC y 25 % de POPG.

2.11 Microscopía electrónica

Las muestras de péptido que fueron tratadas bajo las diferentes condiciones experimentales se procesaron a través de la técnica de tinción negativa y fueron visualizadas usando microscopía electrónica de transmisión (MET). Alícuotas de 10 µl de las soluciones se colocaron sobre rejillas de cobre recubiertas con una capa de carbón (400 pozos) y se contrastaron con una solución de acetato de uranilo (2 %). Después de una incubación por 5 min a 25 °C fueron secadas por 30 min. Las imágenes de MET fueron obtenidas utilizando un microscopio JEOL JEM-1200EX11, a 70 kV y con aumentos de 60,000X.

3. Resultados

3.1 Cambios conformacionales en el dominio C-terminal de CETP

Estudios previos realizados en nuestro grupo de trabajo han demostrado el papel clave del dominio C-terminal de CETP durante la transferencia de lípidos, específicamente cuando se conserva la estructura α-helicoidal (residuos E_{465}-S_{476}) [10,16], sin embargo no se ha determinado si este dominio presenta la capacidad de mantener cambios conformacionales bajo la incubación en diferentes ambientes de lípidos. De manera que para investigar si este dominio puede presentar cambios conformacionales a través de la modificación de las propiedades fisicoquímicas del medio circundante, dos péptidos fueron evaluados: el péptido nativo derivado del C-terminal denominado hélice-*X*, y uno que contiene la mutación $D_{470}N$, nombrado hélice-*Z* (Figura 2).

En un primer panel de experimentos, la hélice-*X* y la hélice-*Z* se incubaron en un rango de pH de 3.8-9.5, y a través de espectroscopía de dicroísmo circular (DC) fueron estudiadas. La estructura secundaria de la hélice-*X* fue consistente con la presencia de un estado desordenado en todo el intervalo de pH estudiado (Figura 4A). En contraste, los espectros de DC de la hélice-Z mostraron una respuesta específica dependiente del pH, con un desplazamiento del mínimo entre 201 a 219 nm asociado con un incremento en la elipticidad, lo cual es indicativo de la formación de una estructura secundaria de tipo-β (Figura 4B). Estos espectros se encontraron solamente en un rango de pH de 7-8, alcanzando el valor más alto en un pH de 7.2 (Inserto Figura 4B).

Así mismo, a través del empleo de ensayos de fluorescencia acoplados a tioflavina T (ThT) se registró un incremento en el espectro de emisión de la ThT únicamente en las muestras de la hélice-*Z*, con un pico máximo cercano a 482 nm (Figura 4C).

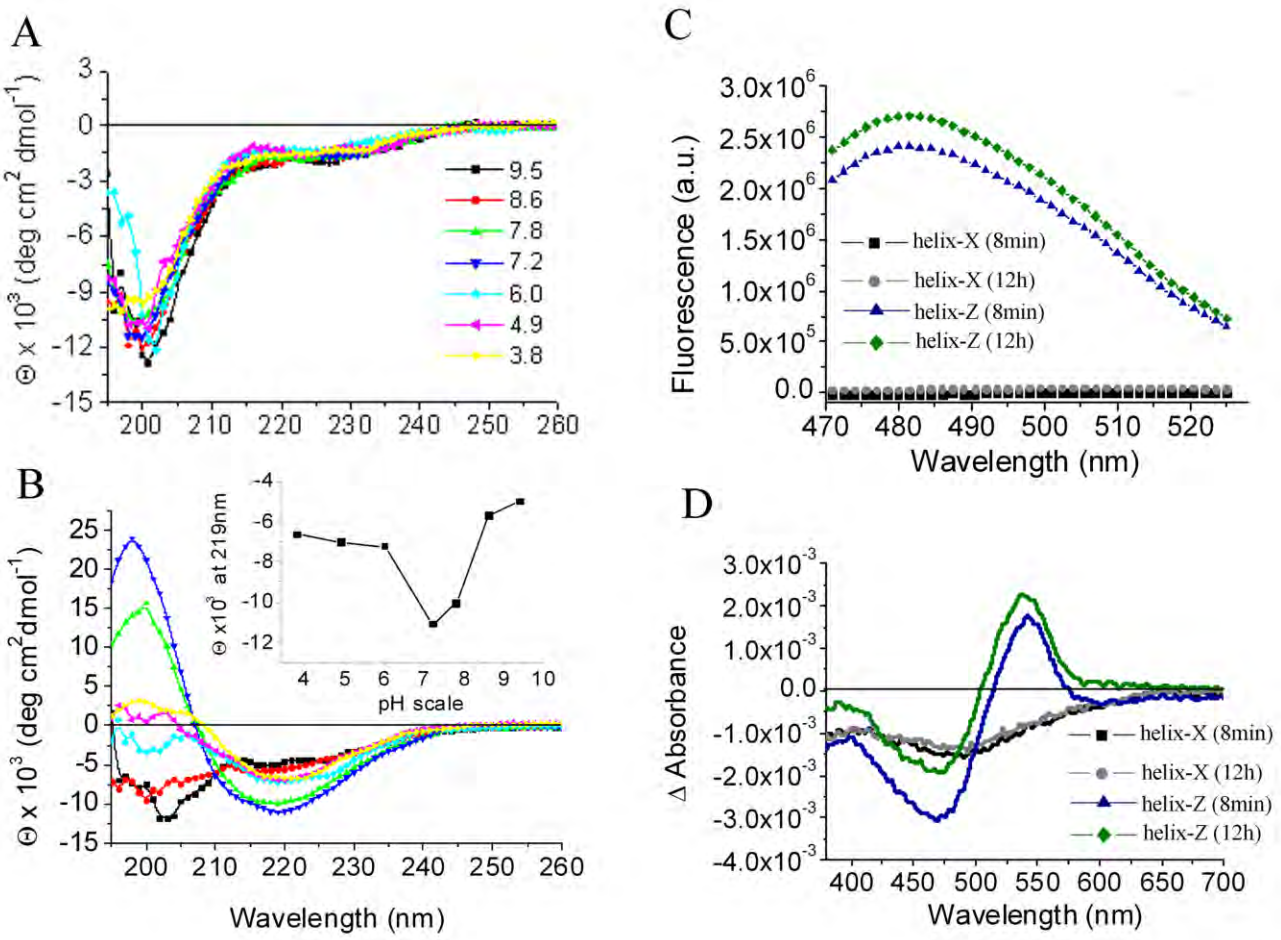

Figura 4. Espectros de DC de la hélice-*X* (**A**) y de la hélice-*Z* (**B**) en un rango de pH de 3.8–9.5. El inserto en **B** muestra los valores de elipticidad a 219 nm; (**C**) Ensayos de fluorescencia acoplados a ThT en la hélice-*X* y hélice-*Z*, mostrando el pico característico de estructura-β a 482 nm ; (**D**) Cambio de birrefringencia del rojo-Congo (Δ absorbancia) a diferentes tiempos de incubación. Los experimentos en (C) y (D) se realizaron en un pH de 7.2. La concentración de los péptidos en los ensayos de DC fue de 200 µg/ml, para los experimentos de ThT fue de 50 µg/ml, y en los ensayos con rojo-Congo de 180 µg/ml.

De forma paralela, realizando experimentos con la molécula rojo-Congo, se observó el cambio de birrefringencia característico de la presencia de estructuras-β, con una

señal máxima cercana a 540 nm (Figura 4D). Estos ensayos confirman la posibilidad de que bajo condiciones específicas como el pH, el C-terminal de CETP podría adquirir una estructura secundaria de tipo-β.

Por otra parte, durante la evaluación de la estabilidad de la hélice-*Z* a través del desplegamiento inducido por temperatura (4–90 °C), solamente en valores mayores a 65 °C se encontró una pérdida significativa en el contenido de la estructura secundaria de tipo-β monitoreada a través de DC, lo cual sugiere una alta estabilidad en la estructura secundaria de la hélice-*Z* (Figura 5A). En este sentido, la presencia de un punto isodicroíco cercano a 211 nm en los espectros de DC, y considerando un comportamiento de tipo sigmoideo durante el desplegamiento, sugieren la presencia de sólo dos estados conformacionales (Inserto figura 5A). Estos experimentos, junto con el hecho de que la hélice-*Z* mantiene el espectro característico de DC consistente con una hoja-β bajo el tratamiento con una fuerza iónica alta (hasta 2.4 M NaCl, figura 5B), muestran que la estructura-β en la hélice-*Z* no está determinada por interacciones electrostáticas de largo alcance, sino por interacciones fuertes inter- e intra-cadena, tales como puentes de hidrógeno.

En otra serie de experimentos, tanto la hélice-*X* como la hélice-*Z* fueron incubadas en un ambiente hidrofóbico compuesto de micelas de dodecil sulfato de sodio (SDS). Los resultados muestran que ambos péptidos adquieren y mantienen una estructura α-helicoidal (Figura 6A, B). Esta transición fue monitoreada en paralelo a través de la fluorescencia acoplada a ThT (Figura 6C) y siguiendo el cambio en la absorbancia del enlace peptídico a 205 nm (Figura 6D).

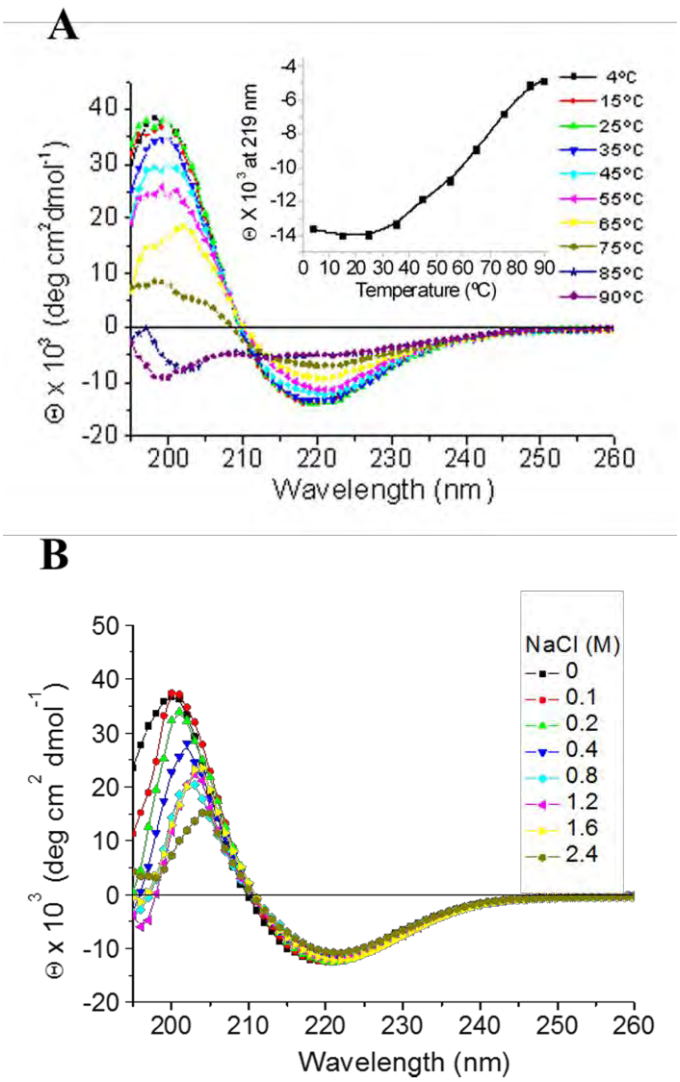

Figura 5. Evaluación de la estabilidad de la hélice-*Z*. (**A**) Desplegamiento inducido por temperatura en la hélice-*Z*, el recuadro muestra los valores de elipticidad a 219 nm (señal de estructura-β); (**B**) Espectros de DC de la hélice-*Z* bajo un tratamiento con concentraciones crecientes de NaCl.

Nuestros resultados sugieren que la interacción dentro de una interfase hidrofílica/hidrofóbica puede ser el parámetro clave para mantener a ambos péptidos en una conformación hélice-α, de forma importante, en el caso de la hélice-Z ésta es una condición clave para evitar la formación de la estructura-β [45].

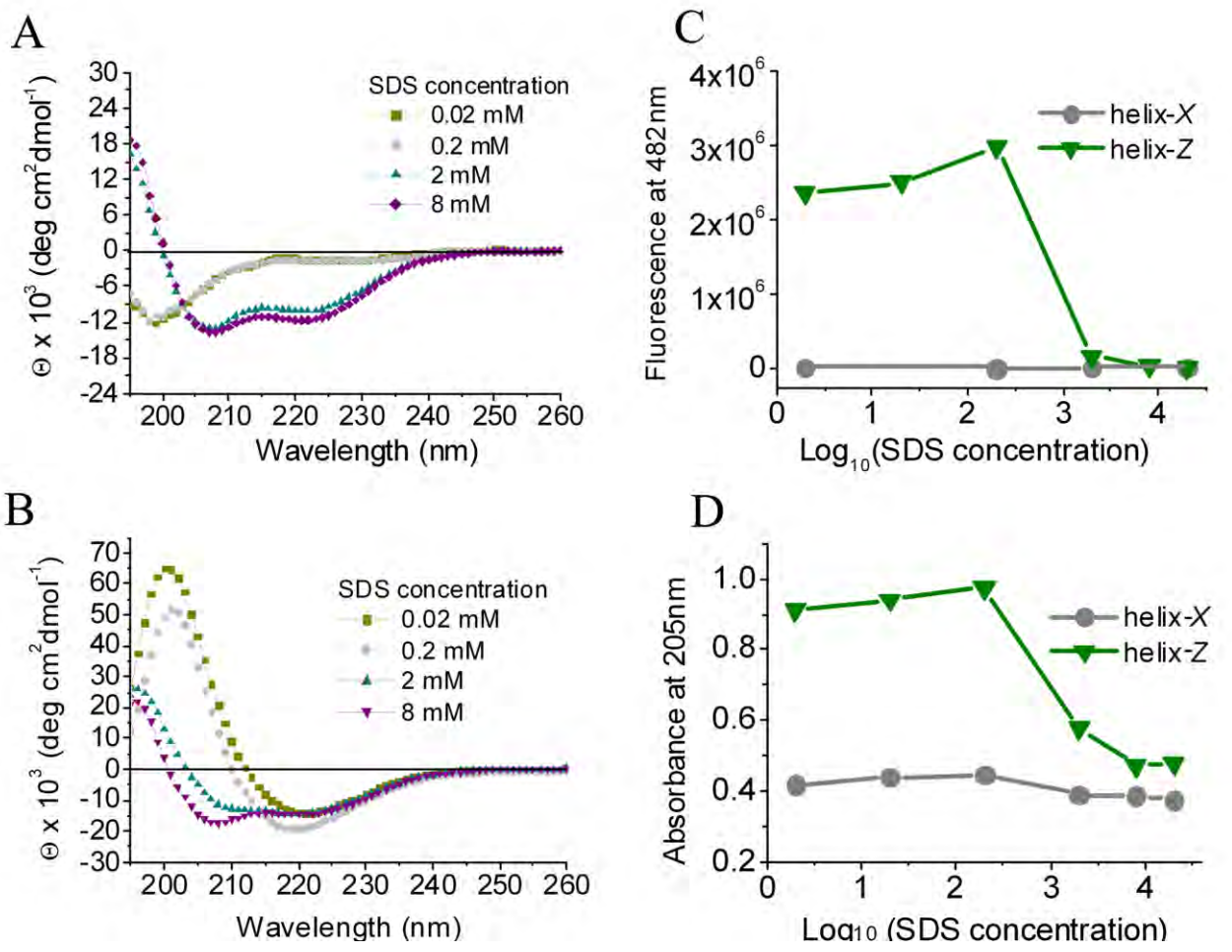

Figura 6. Efecto del SDS sobre la estructura secundaria de los péptidos, evaluado por DC. (**A**) hélice-*X*; (**B**) hélice-*Z*; (**C**) Fluorescencia acoplada a ThT a 482 nm; (**D**) Absorbancia del enlace peptídico a 205 nm. La concentración de los péptidos empleada en los ensayos de DC fue 200 µg/ml. Para los ensayos de ThT fue de 50 µg/ml, y para los ensayos de absorbancia 180 µg/ml.

3.2 La mutación $D_{470}N$ en el dominio C-terminal de CETP favorece la formación de fibras amiloides

Una característica de las proteínas y péptidos precursores de las fibras amiloides es que no se encuentran restringidos a un patrón común en la secuencia de aminoácidos, así mismo en su forma nativa o soluble presentan diferentes estructuras tridimensionales. No obstante, en la forma de fibras amiloides muestran características estructurales comunes, tales como un núcleo central compuesto principalmente de hojas-β y la propiedad de interaccionar con moléculas anfipáticas como el rojo-Congo y la tioflavina-T [46].

Con la finalidad de extender nuestro análisis estructural y considerando que un aumento en la señal de estructura-β no es una propiedad directa asociada con la formación de fibras de tipo amiloide, muestras de los péptidos fueron analizadas a través de microscopía electrónica de transmisión (MET). A lo largo del intervalo de pH evaluado (3.8-9.5), las muestras de la hélice-*X* no formaron algún tipo de material estructurado, lo cual está correlacionado con resultados mencionados previamente en los cuales la hélice-*X* permanece en un estado desordenado (Figura 7A). En cambio, cuando muestras de la hélice-Z fueron analizadas, incluso desde la primer muestra en donde el tiempo de incubación es reducido (tiempo 0 h) fueron identificados oligómeros de un tamaño reducido (Figura 7B, C), y solamente después de 1 h de incubación se registró la formación de protofilamentos (Figura 7D).

La incubación de la hélice-Z durante 6 h con agitación constante (200 rpm) fue la condición que permitió identificar una mezcla de estructuras oligoméricas, protofilamentos, y en algunos campos fibras maduras (Figura 7E). Muestras analizadas después de un tiempo de incubación de 72 y 120 h a 37 °C mostraron

claramente fibras maduras con una alta similitud estructural a las muestras derivadas del péptido βA, disminuyendo de forma importante en estas condiciones la cantidad de estructuras oligoméricas (Figura 7F, G). Durante esta etapa, es interesante mencionar que aunque la formación de fibras fue evaluada en un rango de pH de 3.8–9.5, los agregados y las fibras solamente se observaron en un intervalo reducido de pH entre 7 y 8, lo cual se encuentra correlacionado con la presencia de la estructura-β observada a través de DC. Cabe señalar que el tiempo de incubación es clave en la formación de las fibras maduras, mientras en tiempos de incubación menores a 12 h la población de estructuras oligoméricas es alta, en condiciones mayores a 72 h estas especies disminuyen de forma importante.

La mutación $D_{470}N$ en el extremo C-terminal de CETP ejemplifica el balance sutil que existe entre las interacciones que estabilizan a la conformación nativa y modificaciones mínimas que pueden originar estructuras anómalas como las fibras amiloides, en donde la hélice-*Z* a través de la formación de estructuras amiloides posiblemente encuentra el estado energético más bajo. En este sentido, en la siguiente etapa del proyecto se evaluaron las propiedades citotóxicas de la hélice-*Z*, manteniendo como control a la hélice-*X* en la condición de pH 7.2, considerando que en este punto se encontró el valor más alto en el contenido de estructura secundaria-β en la hélice-*Z*.

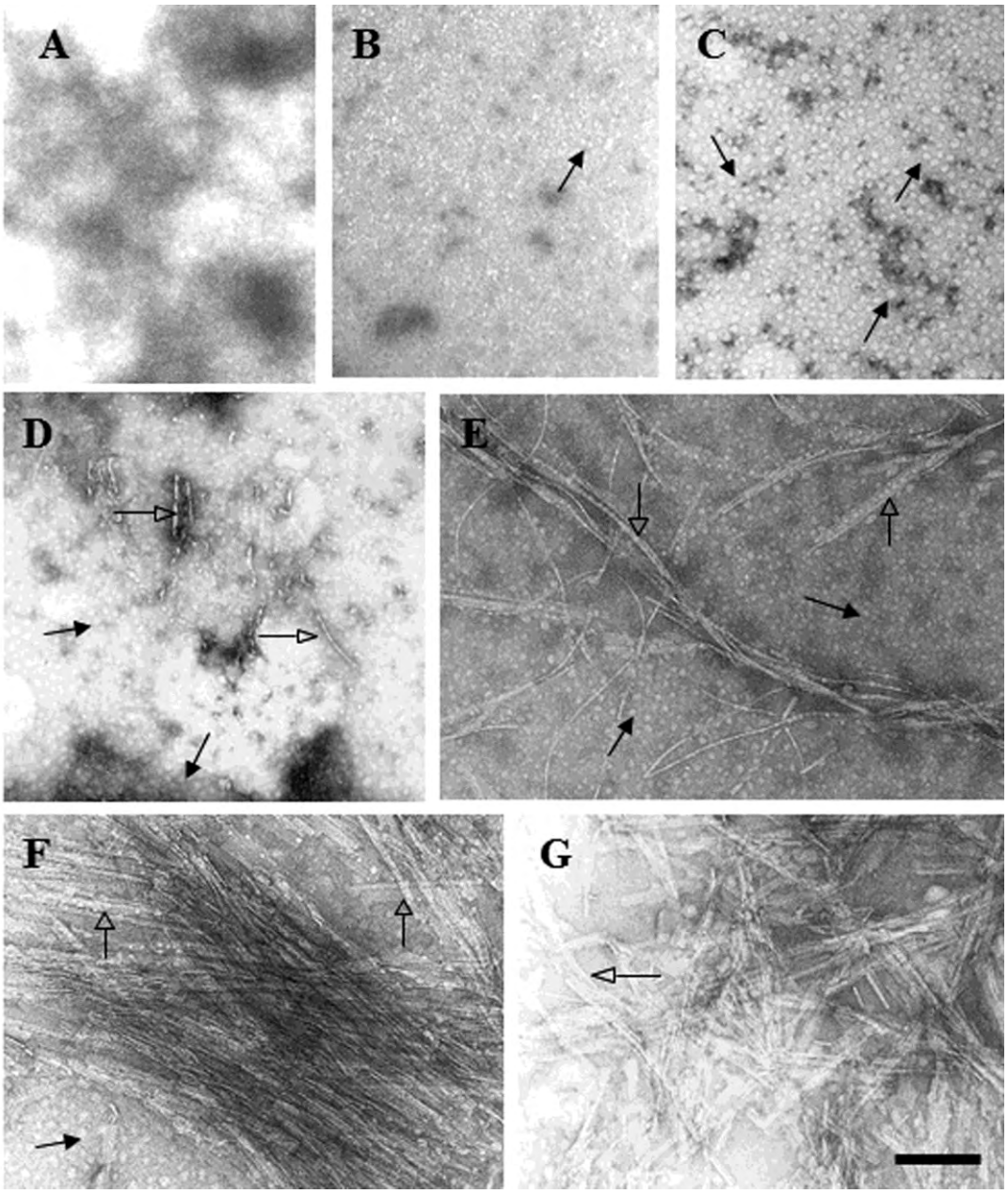

Figura 7. Análisis ultraestructural de los péptidos a través de MET; (**A**) La hélice-*X* después de 48 h de incubación a 37 °C (control); (**B**) La hélice-*Z* a 0 h de incubación; (**C**) Hélice-*Z* a 0.5 h de incubación; (**D**) Formación de protofilamentos en la hélice-*Z* a 1 h de incubación; (**E**) La hélice-*Z* a 6 h de incubación; (**F**) La hélice-*Z* a 48 h de incubación; (**G**) La hélice-*Z* a 120 h de incubación. Las flechas solidas indican estructuras oligoméricas, las flechas abiertas muestran protofilamentos y fibras de tipo amiloide. La concentración de péptido usada en todas las condiciones fue de 60 μg/mL. La barra indica una escala de 200 nm.

3.3 Efectos citotóxicos asociados a la hélice-*Z*

Tomando como base estudios previos que reportan el uso de macrófagos y microglia como modelos celulares durante la caracterización de los efectos citotóxicos del péptido βA [47-49], células de microglia fueron expuestas a incrementos graduales en la concentración de ambos péptidos. Solamente la hélice-*Z* mantuvo la capacidad de reducir significativamente la viabilidad celular evaluada a través del ensayo de reducción de la molécula 3-(4,5-dimetiltiazol-2-ilo) 2,5 bromuro difeniltetrazolio (MTT) (Figura 8). Es interesante observar que independientemente del tiempo de incubación usado para ambos péptidos en solución de manera previa al tratamiento celular (0, 6 o 120 h a 37 °C), la concentración más baja empleada de hélice-*Z* (1.7 μM) origina una reducción importante en la viabilidad celular, la cual se mantiene hasta 56 μM (Figura 8A-C). En este punto es importante mencionar que el tiempo 0 h corresponde en realidad al tiempo empleado en colocar a ambos péptidos, primero en la solución y posteriormente en la placa de cultivo celular. Este procedimiento dura aproximadamente 15 min, tiempo suficiente para producir oligómeros en la hélice-*Z* como se muestra en la Figura 7B-C

Debido a que la viabilidad celular se mantiene cercana al 50% independiente de la concentración de hélice-*Z* o del tiempo de incubación necesario para la formación de estructuras amiloides, nuestros experimentos indican que la forma oligomérica de la hélice-*Z* puede ser la especie más tóxica. En este sentido, las fibras maduras también son responsables de la toxicidad celular después de la incubación de la hélice-*Z* por 120 h, sin embargo tendremos que dilucidar en experimentos posteriores si bajo estas condiciones la presencia de oligómeros podría descartarse por completo. Una propuesta puede ser que a las 120 h se mantiene el 50 % de viabilidad, ya que solamente se observan fibras y no estructuras oligoméricas, las cuales pueden ser más tóxicas durante tiempos cortos de incubación (Figura 8A,B)

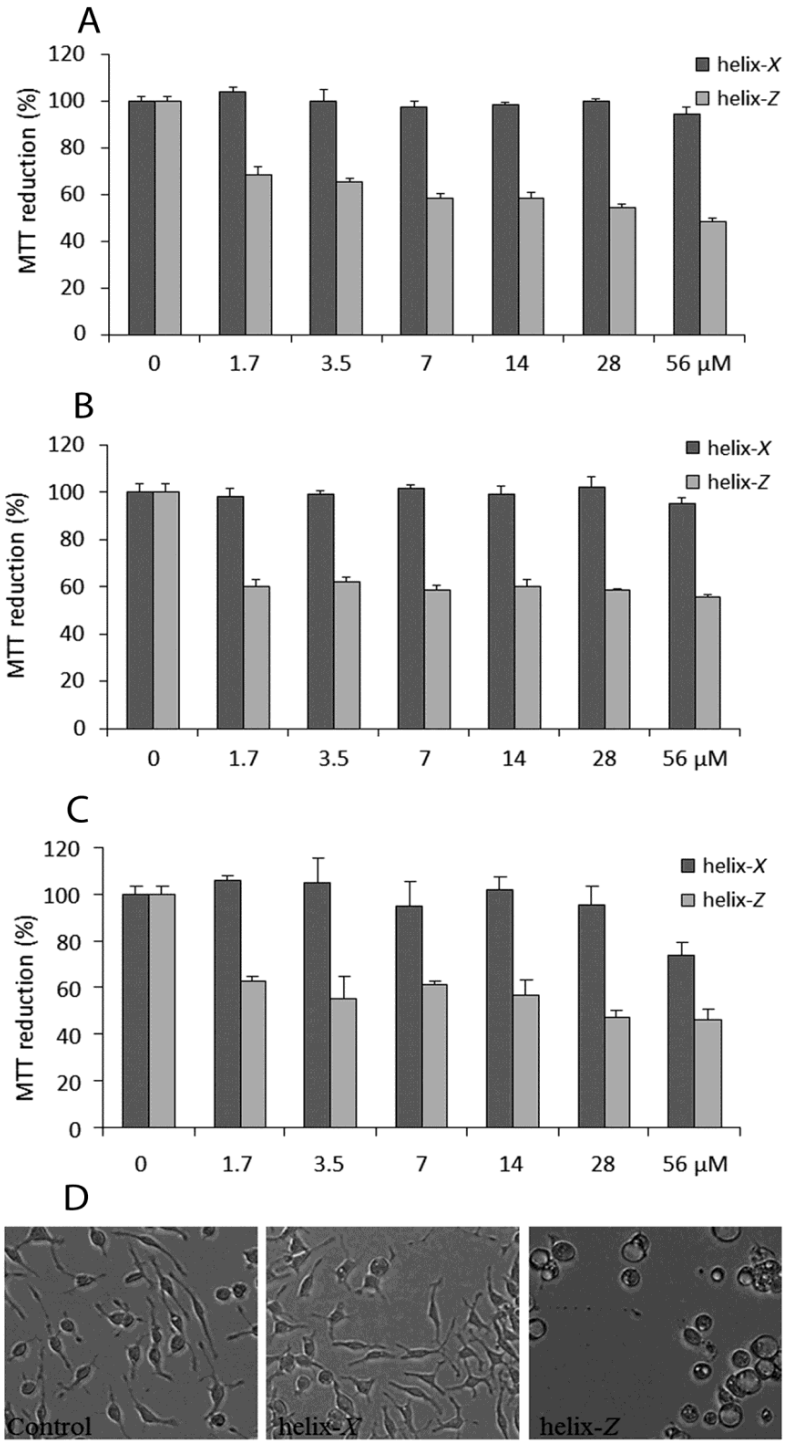

Figura 8. Efectos citotóxicos en células de microglia asociados a la exposición de la hélice-*X* y hélice-*Z*. (**A**) Viabilidad celular determinada a través de MTT en células tratadas con péptidos previamente incubados durante 0.5 h a 37 °C; (**B**) Células expuestas a los péptidos previamente incubados 6 h a 37 °C; (**C**) Células tratadas con péptidos previamente incubados 120 h a 37 °C; (**D**) Microscopía óptica de células de microglia tratadas con ambos péptidos (56 µM), previamente incubados 120 h a 37 °C.

De hecho, algunos autores han propuesto que la fibrilogénesis puede funcionar como un mecanismo de defensa para disminuir los fenómenos de toxicidad relacionados con la presencia de oligómeros [50,51].

Es interesante mencionar que mientras los oligómeros de la hélice-*Z* que se forman en un pH de 7.2 son citotóxicos, agregados amorfos del péptido β-amiloide obtenidos en el mismo pH, no presentaron la capacidad de inducir un daño a las células de microglia en cultivo. Los cambios encontrados en la morfología celular bajo el tratamiento con la hélice-*Z* están posiblemente relacionados con la presencia de una condición de estrés oxidativo, generado en gran medida por la formación de especies reactivas de oxígeno (ERO), condición que si se mantiene de forma extensiva puede desencadenar la aparición de fenómenos como la apoptosis. Esto ha sido descrito por nuestro grupo de trabajo en el estudio de moléculas como el péptido β-amiloide [22] (Figura 8D), y la proteína paramiosina [52]. Cabe destacar que el ensayo con MTT se ha empleado como indicador de estrés oxidativo y también de cambios que ocurren en el tráfico vesicular de las células [53,54].

Previamente, en nuestro grupo de trabajo se ha encontrado que la proteína adaptadora β-adaptina tiene un papel clave en la internalización del péptido β-amiloide en células de microglia, ya que durante un estado de estrés oxidativo la expresión de la β-adaptina se encuentra suprimida [49]. De tal forma, evaluamos si esta condición de citotoxicidad puede extenderse a otras estructuras fibrilares que no están relacionadas de forma directa con una condición patológica como es el caso de la hélice-*Z*.

3.4 Expresión de proteínas endocíticas

Después de un período de incubación por 120 h a 37 °C de manera previa al tratamiento, condición en la cual la hélice-*Z* forma estructuras fibrilares maduras,

células de microglia fueron expuestas por 20 h a concentraciones graduales de los péptidos. El experimento estuvo enfocado en evaluar los niveles de expresión de proteínas que participan en el proceso de endocitosis mediada por receptor, tales como β-adaptina, eps 15 y CALM (clathrin assembly lymphoid myeloid leukemia). Las células expuestas a la hélice-*Z* mostraron una expresión diferencial en algunas de estas proteínas endocíticas. No obstante, en los experimentos realizados con la hélice-*X* no se encontraron cambios. Si bien la expresión de proteínas tales como eps15 se mantuvo constante, la expresión de la proteína β-adaptina disminuyó con respecto al tratamiento con concentraciones crecientes de hélice-*Z*, incluso registrándose una señal mínima en la concentración de 112 μM (Figura 9A). En contraste, la expresión de la proteína CALM se vio aumentada con respecto a la concentración de hélice-*Z* (Figura 9B). De manera general estos resultados son similares a los que se obtuvieron con el péptido β-amiloide (βA_{25-35}), los cuales se muestran en el siguiente capítulo.

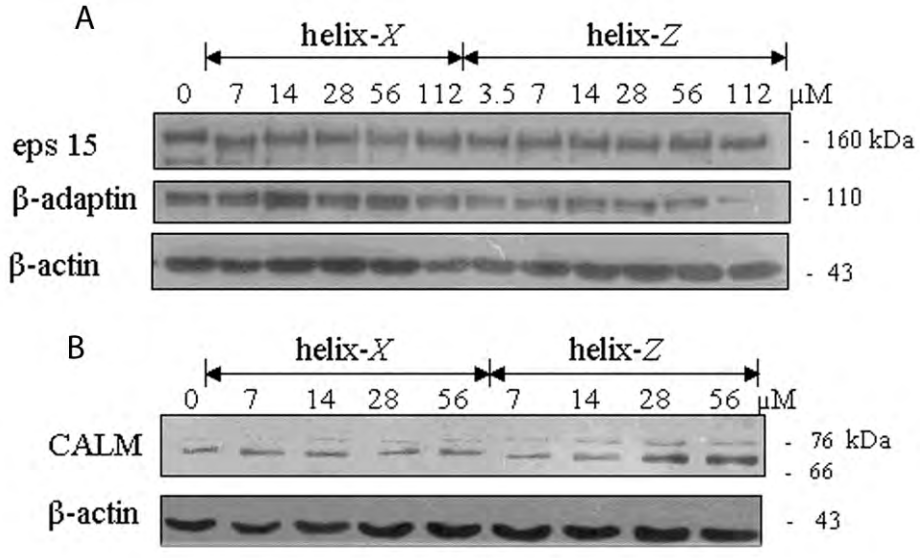

Figura 9. Expresión de proteínas endocíticas en células de microglia tratadas con la hélice-*X* y hélice-Z. Ambos péptidos se incubaron previamente 120 h a 37 °C. (**A**) Análisis por western-blot de eps15 y β-adaptina; (**B**) Western-blot de la proteína CALM. La β-actina fue usada como control de carga.

3.5 Efecto del péptido-βA_{25-35} bajo condiciones de agregación desordenada

Debido a que las características fisicoquímicas del medio son clave en la formación de estructuras amiloides, se evaluaron diferentes condiciones en las cuales se interrumpe la formación de fibras amiloides bien definidas en el péptido-βA_{25-35}. De tal forma que cuando el péptido βA_{25-35} es incubado en un pH cercano a la neutralidad (pH 7.2) tiende a formar agregados desordenados con características amorfas (Figura 10A). En muestras analizadas por MET no se identificaron las características morfológicas y de tamaño en las fibras de tipo amiloide (7-13 nm de ancho). Así mismo, cuando células de microglia fueron tratadas con estas muestras no se observó la disminución en la expresión de la proteína β-adaptina, ni cambios en la expresión de CALM (Figura 10B). Incluso al usar junto con altas concentraciones de βA_{25-35} (400 μg/ml) una dosis muy baja de terbutil hidroperóxido (1μM), agente que induce la producción de ERO, no se vio modificada la respuesta en la expresión de las proteínas β-adaptina y CALM (datos no mostrados).

Sin embargo, cuando el péptido βA_{25-35} se incubo en H_2O pH 5.5 por 72 h a 37 °C de manera previa al tratamiento celular, se registró la formación de fibras amiloides en muestra procesadas por MET (Figura 10C). Bajo estas condiciones, en células de microglia expuestas a estas fibras amiloides se encontraron cambios en la expresión de las proteínas endocíticas (Figura 10D), lo cual está asociado con la presencia de un estado de estrés oxidativo y una disminución en la viabilidad celular evaluada a través del ensayo con MTT (Figura 10E). Los resultados confirman que las propiedades del medio circundante son un factor clave en el desplazamiento hacia la formación ordenada de estructuras fibrilares. De hecho, algunos autores han planteado que la agregación inespecífica y la formación ordenada de fibras son dos fenómenos competitivos que pueden aparecer simultáneamente [55], de manera que cambios sutiles en el medio circundante podrían favorecer la formación de uno u otro estado.

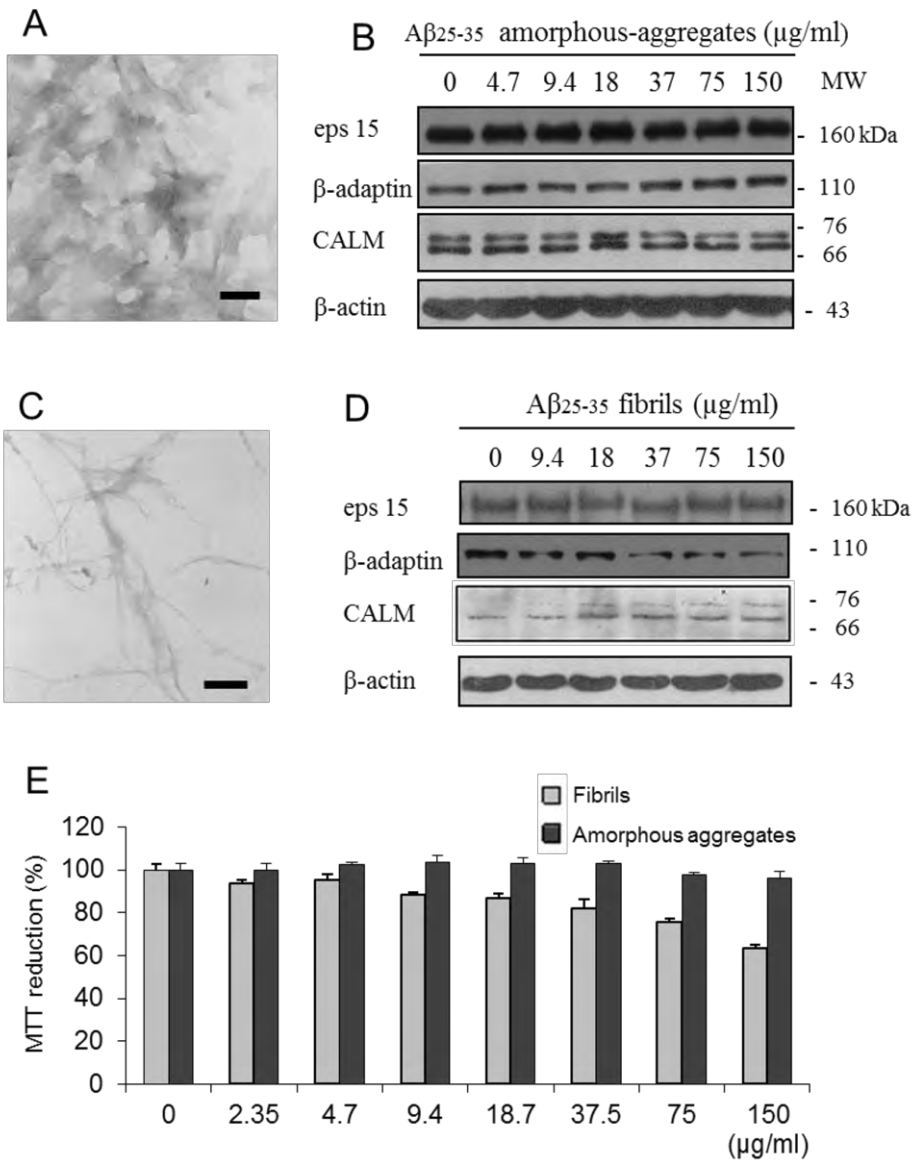

Figura 10. Efecto del pH sobre la formación de fibras en el péptido $\beta A_{25\text{-}35}$. (**A**) El péptido $\beta A_{25\text{-}35}$ incubado por 72h a pH 7.2 favorece la formación de agregados amorfos; (**B**) En célula de microglia tratadas con estos agregados amorfos no se producen cambios en la expresión de proteínas endocíticas; (**C**) La incubación del péptido $\beta A_{25\text{-}35}$ por 72 h a un pH de 5.5 induce la formación de fibras amiloides bien definidas; (**D**) Células tratadas con fibras del $\beta A_{25\text{-}35}$ muestran cambios en la expresión de β-adaptina y CALM; (**E**) El tratamiento con fibras bien definidas del péptido $\beta A_{25\text{-}35}$ inducen una disminución gradual en la viabilidad celular de microglia. Las imágenes de MET se obtuvieron con una concentración 60 μg/mL de péptido. Las barras corresponden a 200 nm.

3.6 El grado de solvatación sobre la superficie es una condición clave para mantener la estructura hélice-α

Los resultados hasta ahora mostrados indican que el péptido hélice-*Z* forma una estructura secundaria de tipo-β dependiente del pH, fenómeno que se extiende hasta la formación de fibras amiloides. De manera que en esta última etapa del trabajo se evaluó el efecto de varios arreglos de lípidos sobre la estructura de la hélice-*Z* a un pH de 7.2, condición en la cual se presentaron los niveles más altos de estructura-β. Específicamente, se realizó una serie de experimentos estudiando algunas de las propiedades estructurales de los lípidos, tales como el tamaño de la cabeza polar, la longitud de la cadena acilo, la carga electrostática y el grado de solvatación, condiciones que pueden modificar la estructura secundaria de la hélice-*Z*.

El tratamiento con concentraciones crecientes de lisofosfatidilcolina-C_{12} (lyso-C_{12}PC) de 0.01 a 40 mM mostró que concentraciones de lípido por debajo de 5 mM permiten a la hélice-*Z* mantener la conformación en hoja-β (Figura 11A). La incubación con 1 mM de lyso-C_{12}PC, una concentración cercana a la concentración micelar crítica (cmc) de este lípido (0.9 mM), indujo un aumento en los valores de elipticidad que corresponden todavía a la presencia de una estructura-β (Figura 11A, 11B). Bajo esta condición, las interacciones de la hélice-*Z* con la lyso-C_{12}PC en un ambiente acuoso deben llevarse a cabo en un equilibrio dinámico, por un lado entre el péptido con los monómeros de lípido, así como el péptido con las micelas de lípido formadas. En este respecto, se ha reportado que moléculas con una estructura similar a la lyso-C_{12}PC disparan el fenómeno de agregación en proteínas amiloidogénicas bajo concentraciones equivalentes a las usadas en este estudio [56].

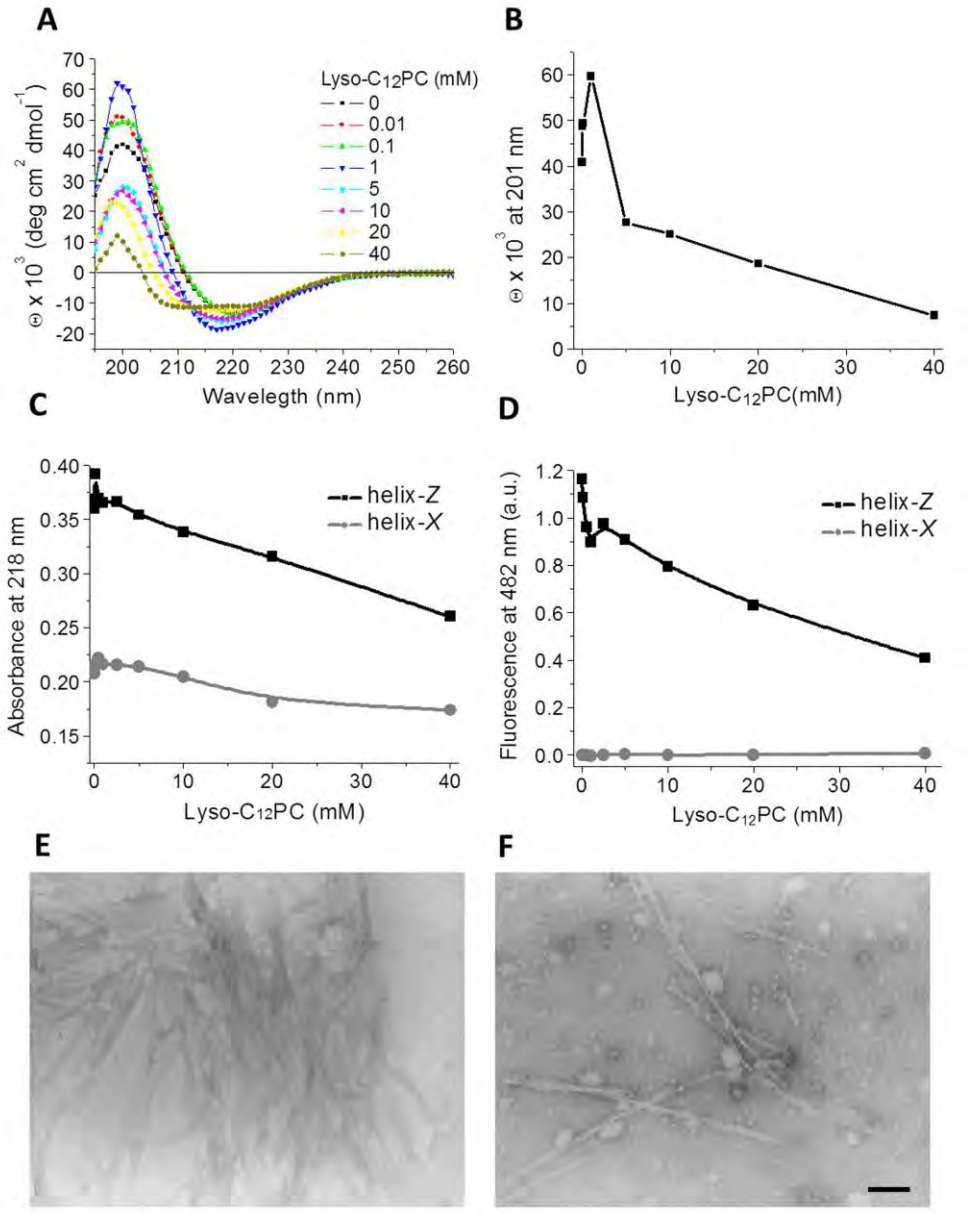

Figura 11. Efecto de la lyso-C_{12}PC sobre la estructura de la hélice-*Z*. (**A**) Espectros de DC obtenidos bajo el tratamiento con concentraciones crecientes de lyso-C_{12}PC; (**B**) Valores de elipticidad molar media a 201 nm; (**C**) Bajo las mismas condiciones, se evaluó la absorbancia a 218 nm; (**D**) Valores de fluorescencia a 482 nm; (**E**) Fibras amiloides en la hélice-*Z*; (**F**) Muestras de la hélice-*Z* incubadas con lyso-C_{12}PC (10 mM). La barra corresponde a 100 nm.

Sin embargo, cuando se usaron concentraciones de lyso-C_{12}PC cercanas a 10 mM, se observó un punto de transición entre la estructura de tipo-β y la formación de una estructura α-helicoidal. Así mismo, este cambio fue seguido a través de evaluar el pico de elipticidad a 201 nm (Θ_{201nm}), característico de la presencia de una estructura en hoja-β (Figura 11B). Este fenómeno fue también estudiado siguiendo los cambios en la absorbancia del enlace peptídico a 218 nm (Figura 11C) y por medio de la fluorescencia acoplada a ThT (Figura 11D). Bajo el tratamiento con lyso-C_{12}PC (10 mM) aún se identificaron estructuras fibrilares, en cantidades reducidas pero más extendidas con respecto a muestras de la hélice-*Z* que no se incubaron con lípidos (Figura 11E, 11F). En las concentraciones más altas de lyso-C_{12}PC (20 y 40 mM), una señal residual de estructura-β fue detectada siguiendo la absorbancia del enlace peptídico y por medio de fluorescencia acoplada a ThT, sin embargo los espectros de DC muestran la formación de una estructura α-helicoidal bien definida.

Considerando que las características hidrofóbicas del microambiente circundante son condiciones clave que favorecen cambios estructurales en dominios específicos de proteínas de unión a lípidos, en otra serie de experimentos se evaluaron varias moléculas de lípido con estructuras similares a la lyso-C_{12}PC, molécula que en estudios previos de nuestro laboratorio mostró la capacidad de modular la estructura secundaria del dominio C-terminal de la apolipoproteína-CI [7].

En un rango de concentración de 0.1 a 10 mM de ácido lisofosfatídico (LPA), lípido con una pequeña cabeza polar cercana a la cadena acilo y un grupo hidroxilo libre en el esqueleto de glicerol, se llevaron a cabo una serie de experimentos en los cuales se estudiaron posibles cambios conformacionales de estructuras-β hacia hélices-α. Los espectros obtenidos mostraron un punto isodicroíco cercano a 215 nm asociado a la presencia de sólo dos estados conformacionales (Figura 12A).

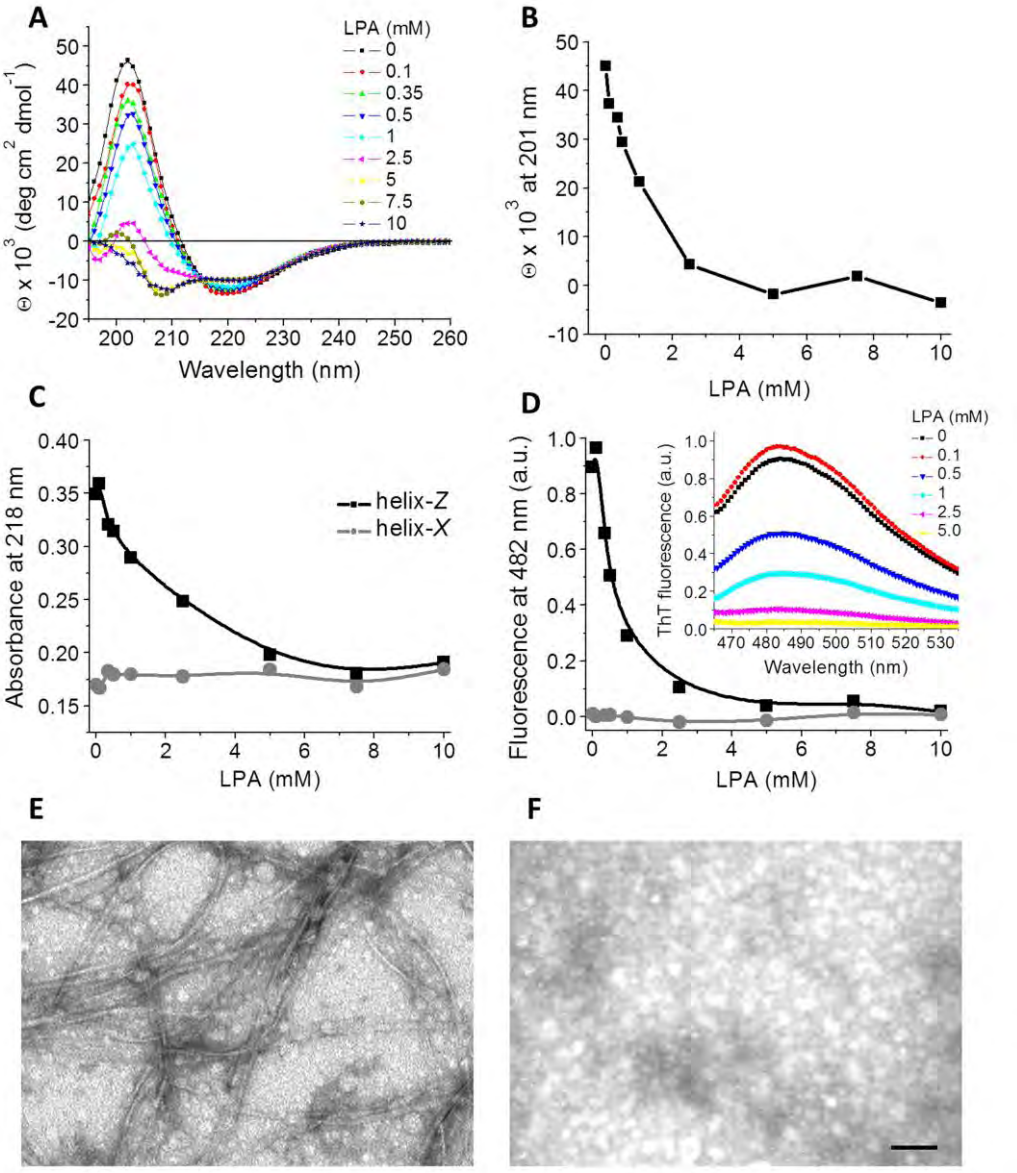

Figura 12. El LPA modula la formación de fibras amiloides en la hélice-*Z*. (**A**) Espectros de DC de la hélice-*Z*, incubada con concentraciones crecientes de LPA; (**B**) Valores de elipticidad molar media a 201 nm del péptido en las mismas condiciones experimentales; (**C**) Valores de absorbancia de los péptidos a 218 nm; (**D**) Registros de fluorescencia-ThT a 482 nm; (**E**) Fibras amiloides en la hélice-*Z*; (**F**) Efecto del tratamiento con LPA en la formación de fibras, cuatro muestras fueron procesadas en diferentes días. La barra corresponde a 100 nm.

Los experimentos de DC muestran que esta transición de β- hacia α- también fue identificada a través del cambio en la señal de Θ_{201nm}, en donde se observó que la incubación con concentraciones de LPA por arriba de 1 mM induce una disminución drástica en los valores de DC asociados con la pérdida de estructura-β (Figura 12B). De forma paralela, los cambios conformacionales fueron seguidos a través del registro de la absorbancia del enlace peptídico a 218 nm (Figura 12C) y por medio de la fluorescencia acoplada a ThT (Figura 12D).

Los resultados indican que en concentraciones por arriba de la cmc, el LPA induce una transición bien definida en la estructura secundaria de la hélice-*Z*, de una hoja-β hacia una hélice-α. De hecho, después del tratamiento con 2.5 mM de LPA, la fluorescencia asociada a ThT fue suprimida (Figura 12D inserto), indicando una pérdida completa del contenido de estructura-β. En este sentido, no se encontraron estructuras fibrilares en las muestras analizadas de LPA por debajo de 10 mM, cuando fueron procesadas a través de MET (Figura 12F). Nuestros resultados sugieren que los cambios conformacionales en la estructura secundaria dependientes de LPA están asociados con un proceso cooperativo, en donde la hélice-Z recupera los niveles de estructura α-helicoidal de manera similar a los que se encontraron cuando el péptido nativo es estudiado (Figura 13). Sin embargo, esto no se puede considerar como un fenómeno general a los lípidos con grupos hidroxilos libres en la cabeza polar, ya que en el panel de experimentos en donde se evaluó el efecto de la lyso-C_{12}PC, en las concentraciones más altas (20 y 40 mM) la señal de fluorescencia acoplada a ThT no fue completamente suprimida; de manera que la incubación con lyso-C_{12}PC puede estar asociada con una transición parcial hacia la formación de hélices-α.

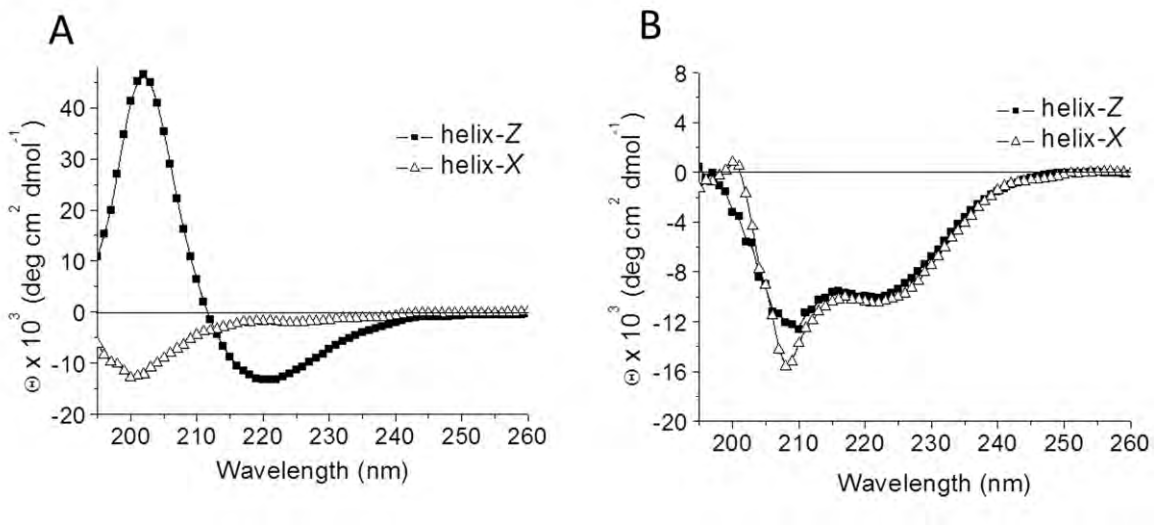

Figura 13. Espectros de DC de la hélice-*Z* y del péptido nativo hélice-*X* en la ausencia de lípidos (**A**), y en presencia de 10 mM de LPA (**B**).

El tamaño de la cabeza polar y la presencia de un grupo hidroxilo libre en la posición sn2 del esqueleto de glicerol, propiedades que pueden modificar el grado de solvatación en la superficie de las interfaces [7], deben jugar un papel clave en los mecanismos que modulan la formación de fibras amiloides dependiente de lípidos [4,7]. En este caso, los componentes hidrofílicos de los fosfolípidos tales como el grupo hidroxilo libre del LPA, pueden afectar la posición y el arreglo de los ensamblajes hidrofóbicos en relación con las interfaces [57,58]. De manera que hemos evaluado esta posibilidad a través del tratamiento con concentraciones crecientes de ácido fosfatídico (PA); una molécula de lípido con dos cadenas acilo unidas al esqueleto de glicerol, condiciones que no deben favorecer el cambio conformacional de la estructura en hoja-β hacia la hélice-α. Esta tesis fue corroborada cuando se estudió al péptido hélice-*Z*. Empleando las mismas técnicas espectroscópicas, se incubó al péptido hélice-*Z* bajo un rango de concentración 0.1-5 mM de PA. La estructura en hoja-β se mantuvo junto con la capacidad de formación de fibras amiloides (Figura 14).

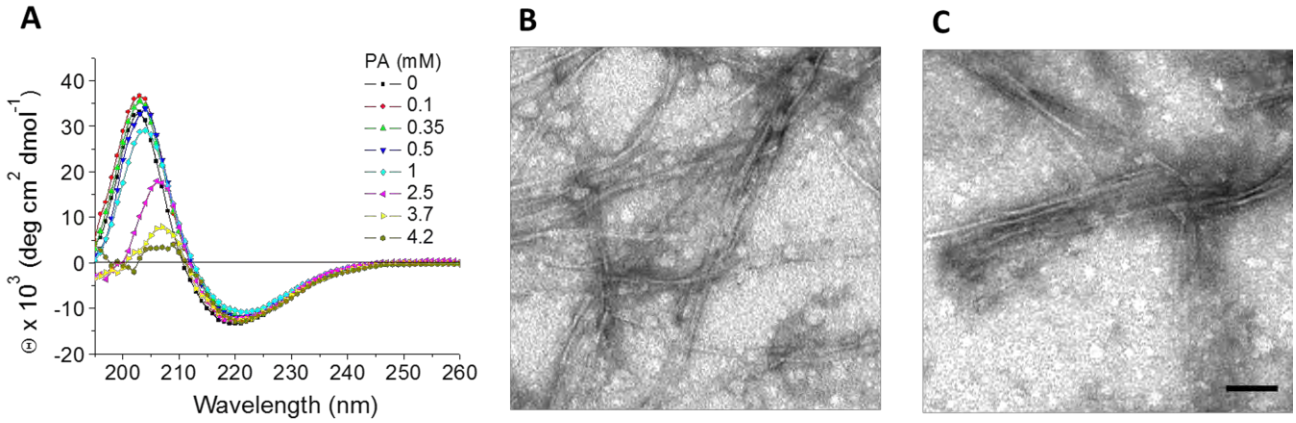

Figura 14. El tratamiento con ácido fosfatídico (PA) no induce un cambio estructural en la hélice-*Z*. (**A**) Espectros de DC de la hélice-*Z* en diferentes concentraciones de PA; (**B**) Imagen de la hélice-*Z* sin la incubación con PA obtenida con MET; (**C**) Efecto del tratamiento con 2.5 mM de PA. La barra corresponde a 100 nm.

Considerando que la carga electrostática sobre la superficie de los lípidos es un factor que podría modular la estructura secundaria de la hélice-Z, se estudió el efecto de una serie de mezclas de fosfolípidos con LPA (76%/24%) (Figura 15). El tratamiento de los péptidos con micelas con carga negativa formadas por POPC/POPG y LPA no modificó el perfil de la estructura secundaria-β evaluada a través de DC y fluorescencia acoplada a ThT (Figura 15A, 15B). Esta condición se mantuvo durante todo el intervalo de concentración de 0.1-2.4 mM de estas mezclas (datos no mostrados).

Cuando la hélice-Z se incubó con micelas neutras compuestas de POPC (1.23 mM) y LPA (0.37 mM), los espectros de DC y los valores de emisión de fluorescencia fueron similares a los valores del control, sin la adición de lípidos (Figura 15A, 15B). Una respuesta similar se obtuvo cuando micelas neutras con fosfatidilcolina (PC) fueron estudiadas, una condición en la que se mantiene la formación de fibras amiloides bien definidas (Figura 15C, 15D). Debido a que se

utilizó un tiempo de incubación prolongado (24 h) durante los experimentos, la presencia de estructuras oligoméricas es reducida [38]. Sin embargo, en estas muestras fue posible identificar fibras amiloides localizadas cerca de la superficie de las micelas de lípidos (Figura 15D inserto), una condición que sugiere la posibilidad de interacciones sobre la superficie de las micelas sin la presencia de un cambio estructural en la hélice-*Z*.

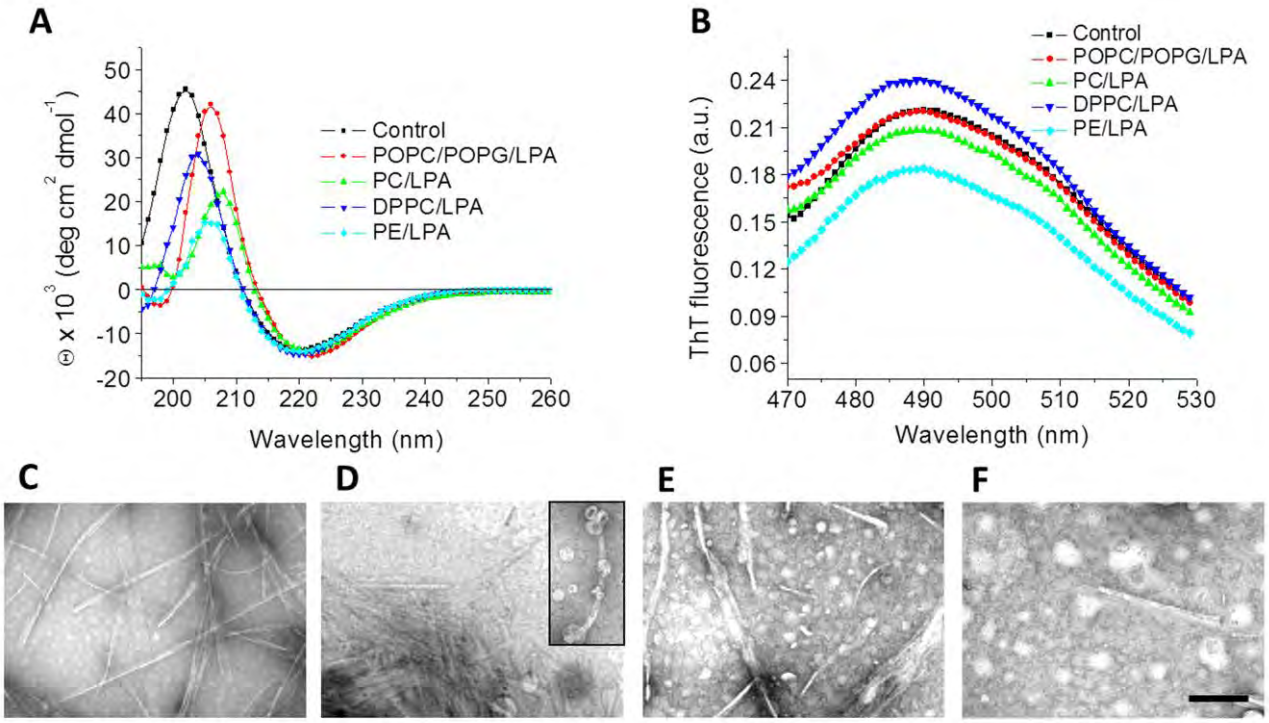

Figura 15. Efecto de la carga electrostática de los lípidos sobre la estructura de la hélice-*Z*. (**A**) Espectros de DC de la hélice-*Z* bajo diferentes tratamientos de lípidos; (**B**) Espectros de emisión de fluorescencia acoplada a ThT. Imágenes obtenidas a través de MET de muestras de la hélice-*Z* sin tratamiento con lípidos (**C**); bajo la incubación con vesículas compuestas de PC/LPA (**D**); DPPC/LPA (**E**) y PE/LPA (**F**). La barra corresponde a 200 nm

Bajo las mismas condiciones, la incubación con micelas neutras formadas por DPPC y LPA mantiene la conformación-β en la hélice-*Z*. Sin embargo, en este caso fue registrado un aumento en el espectro de fluorescencia acoplada a ThT, condición que está relacionada con la presencia de altas concentraciones de fibras encontradas en muestras procesadas a través de MET. De igual forma, varias características relacionadas con la morfología de estas fibras, como un patrón altamente heterogéneo fueron registradas (Figura 15E).

El tratamiento con micelas compuestas de fosfatidiletanolamina (PE) y LPA con una carga positiva sobre la superficie y un grupo de cabeza polar pequeño, indujo una disminución moderada en el contenido de estructura-β de la hélice-*Z* (Figura 15A, 15B). Así mismo, se registraron bajas cantidades de fibras amiloides con respecto a los tratamientos anteriores de lípidos (Figura 15F). Bajo las condiciones experimentales evaluadas, en un pH neutro la hélice-*Z* mantiene una carga neta negativa (-1), de manera que estos resultados pueden estar asociados con una baja capacidad de unión electrostática sobre la superficie de las micelas con carga positiva. De forma interesante, cuando la hélice-*X,* en un estado desordenado fue evaluada con la incubación de micelas de PE/LPA, los niveles más altos de estructura hélice-α fueron promovidos (Figura 16).

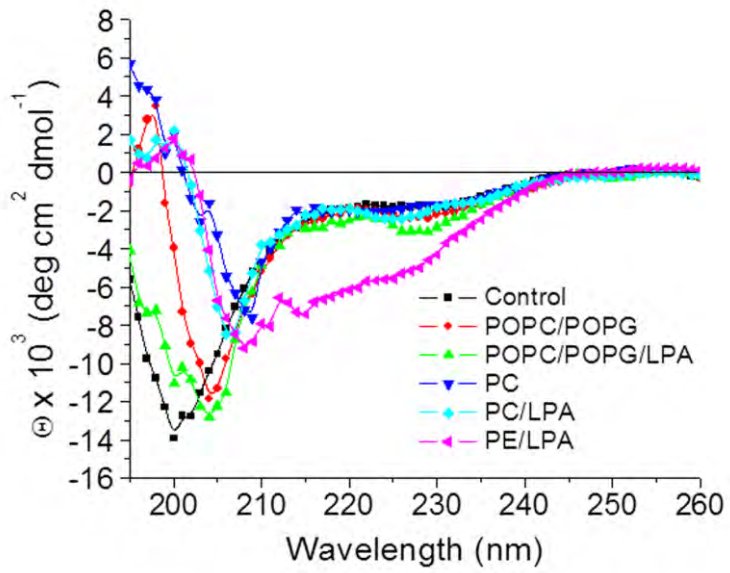

Figura 16. Efecto de la carga electrostática de los lípidos sobre la estructura secundaria del péptido nativo hélice-*X*. Espectros de DC de la hélice-*X* bajo la incubación con micelas de diferente composición lipídica.

4. Discusión

En la búsqueda de los factores que pueden explicar la formación de la estructura-β en la hélice-*Z*, se propone que esta característica estructural no está determinada por parámetros como el momento hidrofóbico (μH) o la hidrofobicidad promedio en la secuencia, ya que las diferencias en estos valores con respecto a la secuencia nativa hélice-*X* son mínimos (Tabla 1). Sin embargo, hemos encontrado que la hélice-*Z* presenta una estructura de tipo-β, solamente cuando la secuencia de aminoácidos mantiene una carga neta cercana a -1 dentro de un rango de pH de 7-8, en donde la cadena lateral de la H_{466} debe proporcionar un poder amortiguador significativo en este intervalo. En contraste, la hélice-*X* con una carga neta cercana a -2 permanece en un estado desordenado (Tabla 2).

Tabla 1. Parámetros fisicoquímicos de los péptidos.

Parámetro	hélice-*X*	hélice-*Z*	βA_{1-42}	βA_{25-35}
PM (Da)	1 399.8	1 399.6	4 514	1 060.3
Punto isoeléctrico	4.17	5.13	5.21	8.75
Hidrofobicidad (kcal/mol)	0.27	0.28	0.21	0.37
μH (kcal/mol)	0.41	0.41	0.08	0.03

Tabla 2. Distribución de la carga neta de los péptidos en función del pH.

pH	hélice-*X*	hélice-*Z*	βA_{1-42}	βA_{25-35}
4	0.07	0.65	3.17	1.02
4.5	-0.47	0.34	1.55	1.01
5	-0.87	0.06	0.38	1.00
5.5	-1.16	-0.18	-0.49	1.00
6	-1.47	-0.48	-1.42	0.99
6.5	-1.75	-0.75	-2.25	0.99
7	-1.91	-0.91	-2.72	0.99
7.5	-1.97	-0.97	-2.92	0.99
8	-2.00	-1.01	-3.01	0.97
8.5	-2.06	-1.06	-3.1	0.93
9	-2.16	-1.17	-3.32	0.79
9.5	-2.39	-1.39	-3.81	0.52

Los datos fueron obtenidos de la plataforma Biology Workbench, para el cálculo usa los datos disponibles del libro Bioquímica de Lehninger.

En este sentido, hay reportes que muestran una mayor propensión para formar una estructura secundaria de tipo-β cuando se combina la presencia de una carga neta baja y una hidrofobicidad alta en secuencias de péptidos modelo, condiciones que son óptimas para promover la formación de fibras de tipo amiloide [59-61]. Considerando estos factores, López de la Paz *et al*. [62] han reportado que secuencias específicas de péptidos son capaces de formar fibras sólo cuando presentan una carga neta de +1 o -1, ya que las distancias entre las cargas electrostáticas de las cadenas laterales están maximizadas, permitiendo la

fibrilogénesis de manera ordenada como puede observarse en la región 25-35 del péptido β-amiloide (Tabla 2). De hecho, existe una fuerte evidencia de que las proteínas intrínsecamente desordenadas mantienen una carga neta elevada en la secuencia como una estrategia para prevenir la agregación [63]. Incluso, este fenómeno se ha propuesto como una característica clave en la evolución molecular que previene la aparición de eventos como el plegamiento anómalo [64].

De tal forma que la carga neta en la secuencia de aminoácidos puede ser uno de los factores clave que desencadenan la formación ordenada de fibras, como se ha mostrado en la hélice-*Z*, lo cual posiblemente acarrea la formación de nuevas interacciones, como un mayor número de puentes de hidrógeno en la cadena principal y entre las cadenas laterales de los residuos, únicamente cuando el péptido se encuentra en un rango de pH entre 7-8. En algunos casos se ha identificado a la reducción de la carga neta como una condición determinante en varios tipos de enfermedades asociadas con la formación de fibras amiloides [65]. En este sentido, la formación de fibras se ha considerado como un proceso de dos etapas, con un período de retraso asociado con la formación de agregados y centros de nucleación, y una segunda etapa relacionada con una propagación rápida [66].

Tomando como base los resultados espectrofotométricos, la evidencia de estructuras fibrilares y las propiedades fisicoquímicas de la hélice-*Z*, tales como el μH, la hidrofobicidad, el pKa de las cadenas laterales de los residuos y una carga neta de -0.96 bajo un pH de 7.2, se presenta un modelo de la posible disposición de los residuos de la hélice-*Z* dentro de una cadena-β (Figura 17A). Considerando que la mutación $D_{470}N$ representa la pérdida de una carga negativa, en el clúster hidrofóbico que se forma en la nueva secuencia (^{467}LLVNFLQ^{473}) se mantiene la estructura-β a través de interacciones hidrofóbicas. También es importante tomar en cuenta que dentro de la secuencia hay residuos de asparagina y glutamina que son considerados inductores de estructuras-β, ya que favorecen fenómenos como el

apilamiento entre las cadenas polipeptídicas [67]. En la hélice-*X* no se presentan estos fenómenos, en gran parte debido a la repulsión electrostática por la carga negativa del D470 que previene la formación del clúster hidrofóbico, y mantiene al péptido en un estado desordenado (Figura 17B).

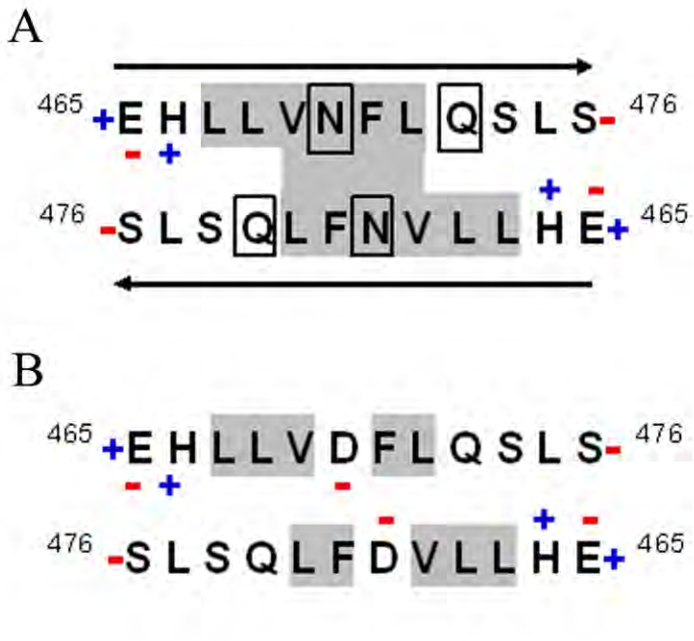

Figura 17. Modelo de una cadena-β antiparalela en la hélice-*Z*. (**A**) La carga de cada residuo se determinó considerando un pH de 7.2. Los grupos N- y C-terminal se mantienen cargados permitiendo una atracción electrostática entre las cadenas peptídicas. Las regiones sombreadas identifican al clúster hidrofóbico ^{467}LLVNFLQ^{473}, así como a los residuos N y Q; (**B**) La hélice-*X* no presenta la estructura secundaria-β debido a la repulsión electrostática entre los residuos D470.

Los datos cristalográficos de CETP muestran que la hélice-*X* se mantiene con una estructura hélice-α, sin embargo debido a su valor de μH de 0.41 kcal/mol, un factor-*B* alto, y que es una región que se encuentra alejada del cuerpo principal de la proteína, estas características sugieren que puede presentar una estructura desordenada. A este respecto, secuencias de péptidos que muestran el potencial para el desorden intrínseco y dominios con valores altos de factor-*B* están asociados con

una elevada vibración térmica de los átomos individuales y por lo tanto presentan una alta flexibilidad intramolecular, como es el caso del C-terminal de CETP [68]. Aunque la hélice-*X* presenta un perfil de hélice-α en la estructura cristalográfica de CETP, cuando se mantiene fuera de un ambiente de lípidos podría adquirir una estructura desordenada con la posibilidad de que esta región presente transiciones conformacionales orden-al-desorden y/o desorden-al-orden. Dominios similares a la hélice-*X* se han documentado en otras proteínas de unión a lípidos como la apolipoproteína A-1, siendo regiones ligeramente apartadas del cuerpo global de la proteína y que son sitios clave para la interacción con lípidos [69,70].

El tipo de transiciones descritas previamente, podrían presentar un equilibrio diferente cuando cambios como el que se encuentra en la hélice-Z se introducen en esta región, en donde la formación de la cadena-β puede ser reversible, requiriéndose de condiciones específicas para modular la estructura secundaria. De forma interesante, estudios recientes del laboratorio sugieren un posible mecanismo para la transferencia de lípidos llevado a cabo por CETP, asignando al dominio C-terminal la propiedad de facilitar por medio de transiciones de estructura secundaria desorden-al-orden, la desorción de lípidos a través de un ambiente acuoso en la forma de micelas de lípido [58].

Los resultados obtenidos con micelas de SDS sugieren que la interacción dentro de una interfase hidrofílica/hidrofóbica es clave para mantener la estructura secundaria α-helicoidal, y en el caso de la hélice-*Z* para evitar la formación de la estructura-β y la posterior formación de fibras amiloides, lo cual pudiera ser extrapolado a la interacción del dominio C-terminal de CETP con la superficie de lípidos. Este análisis se ha extendido a una serie más amplia de arreglos de lípidos.

En este sentido, las interfaces hidrofóbicas-hidrofílicas presentan la capacidad de promover la estabilización de la estructura secundaria de los péptidos. De hecho,

se ha propuesto que dicha propiedad está relacionada con cambios en los puentes de hidrógeno entre el péptido y la superficie hidrofóbica, así como a una reducción en el costo energético de partición cuando se lleva a cabo la unión [71]. Como se ha sugerido previamente para el péptido melitina derivado del veneno de abejas, la cual es una secuencia en gran parte desordenada en solución, no obstante se estructura en hélice-α cuando se particiona sobre vesículas unilamelares de fosfolípidos [72]. Se ha encontrado que mientras la reducción de energía libre por residuo observada para el plegamiento de la melitina en una interface de membrana es casi 0.4 kcal/mol consistente con la formación de puentes de hidrógeno, valores cercanos a 0.6 kcal/mol han sido reportados en péptidos formadores de cadenas-β [72].

Por otra parte, estudios realizados por nuestro grupo de trabajo utilizando fibras del péptido β-amiloide como un ligando natural para los receptores scavenger (RS), una asociación directamente conectada con el desarrollo de estrés oxidativo, han mostrado cambios en la expresión de varias proteínas adaptadoras que participan en la maquinaria de endocitosis de macrófagos y microglia [49,73]. De acuerdo a la dosis, el tratamiento con el péptido βA afecta de forma importante la disponibilidad de la β-adaptina, una proteína que es clave para su internalización, lo que origina la acumulación del βA en el espacio extracelular de las células [49].

Los resultados obtenidos en el presente trabajo muestran que cuando las células de microglia son expuestas a la hélice-*Z*, los oligómeros del péptido en primera instancia, y posteriormente las fibras de tipo amiloide, representan la principal causa de los fenómenos citotóxicos registrados. En este sentido, consideradas como especies precursoras a las fibras maduras que aparecen en tiempos cortos de incubación, en varias de las proteínas amiloidogénicas que se han estudiado, los agregados oligoméricos son las especies moleculares que inducen los principales efectos citotóxicos [74,75], como ya se ha mencionado previamente.

En nuestras condiciones experimentales, el tratamiento con fibras de la hélice-*Z* en concentraciones elevadas inhibe la expresión de la proteína β-adaptina, molécula que forma parte del complejo adaptador AP2, además de que su interacción con el arreglo de clatrina es clave durante la selección del ligando que va a ser internalizado [76,77]. La disminución de β-adaptina, de forma concomitante al incremento observado en la expresión de CALM podría funcionar como un mecanismo compensatorio para mantener la función celular de endocitosis. En este sentido, el dominio ANTH (AP180 N-Terminal Homology) que comprende los primeros 300 residuos del N-terminal de CALM permite la interacción con el lípido de membrana fosfatidilinositol 4,5-bifosfato [78], lo cual funciona como un puente entre los pozos recubiertos de clatrina en la membrana plasmática y otras proteínas adaptadoras [79]. Así mismo, CALM desarrolla una función importante en la regulación y en el orden progresivo de la formación de los pozos cubiertos de clatrina [80]. Estas funciones la identifican como una proteína con una capacidad compensatoria, que pudiera coadyuvar en la función de otras proteínas adaptadoras. Tomando en cuenta que una respuesta similar en β-adaptina y CALM fue encontrada cuando las células de microglia fueron expuestas a estructuras fibrilares derivadas de la hélice-*Z*, estructura no asociada a una condición clínica, posiblemente esta respuesta puede estar relacionada con un fenómeno general de citotoxicidad producido en las células bajo el tratamiento con las fibras amiloides.

Resultados recientes obtenidos por nuestro grupo de trabajo sugieren que la proteína β-adaptina no sólo tiene una función como estructura adaptadora en los mecanismos de endocitosis, sino que podría tener una función alterna relacionada con la regulación de mecanismos como el ciclo celular a través de la interacción con el factor c-myc en el núcleo [Manuscrito en preparación].

Por otra parte, el clúster hidrofóbico originado por la mutación $D_{470}N$ en el dominio C-terminal de CETP [^{467}LLVNFLQ^{473}] comparte características similares

con los motivos estructurales hidrofóbicos denominados *steric zippers*, que se han descrito forman la estructura molecular de las fibras amiloides [81,82]. En este sentido, la mutación $D_{470}N$ minimiza la repulsión electrostática entre monómeros de péptidos, lo cual promueve la formación de puentes de hidrógeno en la cadena principal, disparando la estructura en hoja-β y la formación de fibras amiloides en la hélice-Z [38]. Estos fenómenos están restringidos a los últimos 12 residuos del extremo C-terminal (residuos 465-476), ya que la secuencia del péptido ^{460}DFGFPEHL^{467} que antecede al clúster hidrofóbico no muestra la formación de estructura-β y permanece en un estado desordenado, incluso en la presencia de lípidos (datos no mostrados).

La inhibición en la formación de fibras amiloides y la estabilización de la estructura α-helicoidal en la hélice-*Z*, son condiciones que pueden estar directamente asociadas con las propiedades fisicoquímicas específicas del LPA. La presencia de un grupo hidroxilo libre y una cabeza polar pequeña pueden facilitar el reconocimiento molecular en la hélice-*Z*, lo que facilita la interacción de los péptidos monoméricos sobre la superficie de las micelas. De manera que la nucleación y el apilamiento de los péptidos, fenómenos que conducen a la agregación y finalmente a la formación de fibrillas son suprimidos. En este sentido, se ha reportado que la estabilidad del plegamiento nativo está determinada principalmente por interacciones hidrofóbicas entre las cadenas laterales, mientras que la estabilidad de las fibras amiloides es en mayor medida dependiente de los puentes de hidrogeno en el esqueleto [83].

5. Conclusiones

La mutación $D_{470}N$ en el dominio C-terminal de CETP ejemplifica el delicado equilibrio en los cambios conformacionales a nivel de estructura secundaria modulados por el pH y la modificación de la carga electrostática en los aminoácidos. La disrupción de este equilibrio dinámico puede conducir a la formación de nuevas interacciones como puentes de hidrógeno dentro de la cadena principal y entre las cadenas laterales, que promueven la agregación y finalmente la formación ordenada de estructuras fibrilares [83]. Aunque la mutación $D_{470}N$ (hélice-*Z*) que se describe en este trabajo no se ha encontrado en la naturaleza, la hélice-*X*, el segmento natural de 12 residuos del dominio C-terminal de CETP, cuando se particiona en agua o en interfaces hidrofilicas/hidrofóbicas podría presentar potenciales transiciones orden-al-desorden y/o desorden-al-orden que normalmente son difíciles de identificar. De manera que hemos utilizado a la hélice-*Z* para mimetizar posibles cambios en la estructura secundaria de la hélice-*X* a través de la simple modificación de un puente de hidrógeno, que a su vez podría explicar cambios en la función general de la CETP nativa cuando es estudiada *in vivo*.

Un gran número de eventos que ocurren en estrecha asociación con los lípidos están determinados por los puentes de hidrógeno [84], de manera que la unión hélice-Z/lípido sobre la superficie de las micelas o lipoproteínas puede implicar la liberación de moléculas de agua altamente ordenadas localizadas en las primeras capas de hidratación, con la consiguiente reorganización de puentes de hidrógeno e interacciones hidrofóbicas. Por lo tanto, los cambios conformacionales y la modulación de la estructura secundaria de los péptidos que hemos estudiado requieren condiciones específicas asociadas al microambiente circundante de lípidos, siendo componentes clave el grado de solvatación y el tamaño de la cabeza

polar de los lípidos. De manera que nuestros resultados sugieren un papel regulador para el LPA a través de la modulación de los mecanismos que mantienen al dominio C-terminal de CETP en la conformación funcional hélice-α.

Experimentos en curso empleando CETPI, una nueva isoforma de CETP que carece del dominio C-terminal nativo y en su lugar puede presentar un nuevo carboxilo-terminal estructurado como una hoja-β [85], apoyan la propuesta de que pequeñas transiciones orden-al-desorden y/o desorden-al-orden sustentadas por cambios en los puentes de hidrógeno pueden dar a las proteínas una función fisiológica completamente nueva [4].

A través de una amplia evidencia experimental se ha demostrado que un número determinado de polipéptidos que no están relacionados de manera directa con alguna enfermedad pueden formar estructuras amiloides; incluso se ha propuesto que la agregación amiloide puede ser una propiedad común a las cadenas polipeptídicas [86]. Tomando en consideración que varias estructuras funcionales de los amiloides han sido caracterizadas en bacterias [87,88], hongos [89-91], insectos [92,93] y mamíferos [94,95] existe un consenso de que la formación de fibras amiloides podría representar una vía evolutiva bien conservada en la estructura de proteínas [96]. De manera que la diferencia entre amiloides funcionales y los que están asociados con enfermedad se podría explicar en términos de los mecanismos regulatorios que las células han desarrollado para controlar su formación. En la actualidad, muchas enfermedades con mecanismos moleculares poco entendidos, encontrarán su explicación en la forma en que el fenómeno del plegamiento de las proteínas es regulado [39], así mismo este conocimiento que se ha generado permitirá el desarrollo de estrategias terapéuticas óptimas para controlar a estas patologías asociadas al plegamiento de proteínas.

6. Perspectivas

Las transiciones en la estructura secundaria del dominio C-terminal de CETP pueden ser claves en la función fisiológica de la proteína. De tal forma que en el doctorado nos hemos centrado en el estudio de la función de la isoforma CETPI descubierta por nuestro grupo de trabajo, la cual es expresada solamente en intestino delgado y se encuentra en plasma. Resultados experimentales sugieren que su función está asociada con la unión a lipopolisacáridos (LPS), componente de la membrana externa de bacterias Gram-negativas [97]. La diferencia entre CETP y CETPI está restringida al dominio C-terminal, mientras en CETP es clave la conservación de la estructura hélice-α, la estructura secundaria primordialmente de tipo-β en CETPI podría favorecer la unión a LPS. De tal forma que el cambio en la función puede estar determinado por cambios sutiles a nivel de estructura secundaria.

En el presente trabajo ha quedado pendiente determinar de manera concreta si las estructuras oligómericas son las especies moleculares que ejercen los principales efectos citotóxicos registrados en células de microglia, de manera que se tiene proyectado el desarrollo de una metodología para que a partir de la hélice-*Z* se tenga una población primordialmente de oligómeros, y evaluar su efecto citotóxico a través de las metodologías que se han usado en este estudio. De manera paralela se tiene planeado explorar los mecanismos específicos de toxicidad celular que desarrollan estas especies moleculares.

Agradecimientos

Le agradezco a Blanca Delgado por su excelente asistencia técnica, y a Rodolfo Paredes por el apoyo técnico en el procesamiento de las muestras a través de MET. Este trabajo fue apoyado por los proyectos del Consejo Nacional de Ciencia y Tecnología de México (CONACyT 083.673) y de la Universidad Nacional Autónoma de México/ DGAPA(IN228607).

7. Referencias

1. Uversky, V.N.; Oldfield, C.J.; Midic, U.; Xie, H.; Xue, B.; Vucetic, S.; Iakoucheva, L.M.; Obradovic, Z.; Dunker, A.K. Unfoldomics of human diseases: linking protein intrinsic disorder with diseases. *BMC Genomics* 2009, *10*, S7.

2. Berson, J.F.; Theos, A.C.; Harper, D.C.; Tenza, D.; Raposo, G.; Marks, M.S. Proprotein convertase cleavage liberates a fibrillogenic fragment of a resident glycoprotein to initiate melanosome biogenesis. *J. Cell. Biol.* 2003, *161*, 521–533.

3. Dobson, C.M. Protein folding and misfolding. *Nature* 2003, *426*, 884–890.

4. Mendoza-Espinosa, P.; García-González, V.; Moreno, A.; Castillo, R.; Mas-Oliva, J. Disorder-to-order conformational transitions in protein structure and its relationship to disease. *Mol. Cell. Biochem.* 2009, *330*, 105–120.

5. Xicohtencatl-Cortes, J.; Castillo, R.; Mas-Oliva, J. In search of new structural states of exchangeable apolipoproteins. *Biochem. Biophys. Res. Commun.* 2004, *324*, 467–470.

6. Ramos, S.; Campos-Terán, J.; Mas-Oliva, J.; Nylander, T.; Castillo, R. Forces between hydrophilic surfaces adsorbed with apolipoprotein AII alpha helices. *Langmuir* 2008, *24*, 8568–8575.

7. Mendoza-Espinosa, P.; Moreno, A.; Castillo, R.; Mas-Oliva, J. Lipid dependant disorder-to-order conformational transitions in apolipoprotein CI derived peptides. *Biochem. Biophys. Res. Commun.* 2008, *365*, 8–15.

8. Rye, K.A., Hime, N.J.; Barter, P.J. The influence of cholesteryl ester transfer protein on the composition, size, and structure of spherical, reconstituted high density lipoproteins. *J. Biol. Chem.* 1995, 270, 189-196.

9. Klerkx, A.H.; El Harchaoui, K.; van der Steeg, W.A.; Boekholdt, S.M.; Stroes, E.S.; Kastelein, J.J.; Kuivenhoven, J.A. Cholesteryl ester transfer protein (CETP) inhibition beyond raising high-density lipoprotein cholesterol levels: pathways by which modulation of CETP activity may alter atherogenesis. *Arterioscler. Thromb. Vasc. Biol.* 2006, *26*, 706–715.

10. Bolaños-García, V.M.; Soriano-García, M.; Mas-Oliva, J. Stability of the C-terminal peptide of CETP mediated through an (*i*, *i* + 4) array. *Biochim. Biophys. Acta* 1998, *1384*, 7–15.

11. Wang, S.; Wang, X.; Deng, L.; Rassart, E.; Milne, R.S.; Tall, A.R. Point mutagenesis of carboxyl-terminal amino acids of cholesteryl ester transfer protein. *J. Biol. Chem.* 1993, *66*, 1955–1959.

12. Wang, S.; Kussie, P.; Deng, L.; Tall, A. Defective binding of neutral lipids by a carboxyl-terminal deletion mutant of cholesteryl ester transfer protein. Evidence for a carboxyl-terminal cholesteryl ester binding site essential for neutral lipid transfer activity. *J. Biol. Chem.* 1995, *270*, 612–618.

13. Qiu, X.; Mistry, A.; Ammirati, M.J.; Chrunyk, B.A.; Clark, R.W.; Cong, Y.; Culp, J.S.; Danley, D.E.; Freeman, T.B.; Geoghegan, K.F.; Griffor, M.C.; Hawrylik, S.J.; Hayward, C.M.; Hensley, P.; Hoth, L.R.; Karam, G.A.; Lira, M.E.; Lloyd, D.B.; McGrath, K.M.; Stutzman-Engwall, K.J.; Subashi, A.K.; Subashi, T.A.; Thompson, J.F.; Wang, I.K.; Zhao, H.; Seddon, A.P. Crystal structure of cholesteryl ester transfer protein reveals a long tunnel and four bound lipid molecules. *Nat. Struct. Mol. Biol.* 2007, 14, 106–113.

14. Beamer, L.J. Structure of human BPI (bactericidal/permeability-increasing protein) and implications for related proteins. *Biochem. Soc. Trans.* 2003, 31, 791-794.

15. García-González, V.; Mas-Oliva, J. Structural Arrangement that Supports Lipid Transfer in the cholesteryl-ester transfer protein (CETP). USA-México Workshop in Biological Chemistry: Multidisciplinary Approaches to Protein Folding, Mexico City, Mexico, 25–27 March 2009.

16. Bolaños-García, V.M.; Mas-Oliva, J.; Ramos, S.; Castillo R. Phase transitions in monolayers of human apolipoprotein C-I. *J. Phys. Chem. B* 1999,103, 6236-6242.

17. Bolaños-García V.M.; Ramos, S.; Xicohtencatl-Cortés, J.; Castillo, R.; Mas-Oliva, J. Monolayers of apolipoproteins at the air/water interface. *J. Phys. Chem. B*. 2001, 105, 5757-5765.

18. Mas-Oliva, J.; Moreno, A.; Ramos, S.; Xicohtencatl-Cortés, J.; Campos, J.; Castillo, R. Frontiers in cardiovascular health. Dhalla NS, et al (editors). Monolayers of apolipoprotein AII at the air/water interface, Kluwer Academic Publishers, Boston USA 2003, 341-352.

19. Xicohtencatl-Cortés, J.; Mas-Oliva, J.; Castillo, R. Phase transitions of phospholipid monolayers penetrated by apolipoproteins. *J. Phys. Chem. B* 2004, 108, 7307-7315.

20. Ruíz-García, J.; Moreno, A.; Brezesinski, G.; Möhwald, H.; Mas-Oliva, J.; Castillo, R. Phase transitions, conformational changes in monolayers of human apolipoprotein CI and AII. *J. Phys. Chem. B* 2003, 107, 11117-11124.

21. Campos-Terán, J.; Mas-Oliva, J.; Castillo, R. Interactions and conformations of a-helical human apolipoprotein CI on hydrophilic and on hydrophobic substrates. *J. Phys. Chem. B* 2004,108, 20442-20450.

22. Bustos, D.M.; Iglesias, A.A. Intrinsic disorder is a key characteristic in partners that bind 14-3-3 proteins. *Proteins* 2006, 63, 35-42.

23. Kriwacki, R.W.; Hengst, L.; Tennant, L.; Reed, S.I.; Wright, P.E. Structural studies of p21Waf1/Cip1/Sdi1 in the free and Cdk2-bound state: conformational disorder mediates binding diversity. *Proc. Natl. Acad. Sci.* U S A 1996, 93, 11504-11509.

24. Dalal, S.; Regan, L. Understanding the sequence determinants of conformational switching using protein design. *Protein Sci.* 2000, 9, 1651-1659.

25. Mendoza-Espinosa, P.; García-González, V.; Moreno, A.; Castillo, R.; Mas-Oliva J. Amyloid like fibril structure developed by apolipoprotein A1 derived peptides (En revisión).

26. Andreola, A.; Bellotti, V.; Giorgetti, S.; Mangione, P.; Obici, L.; Stoppini, M.; Torres, J.; Monzani, E.; Merlini, G.; Sunde, M. Conformational switching and fibrillogenesis in the amyloidogenic fragment of apolipoprotein a-I. *J. Biol. Chem.* 2003, 278, 2444-2451.

27. Ban, T.; Hoshino, M.; Takahashi, S.; Hamada, D.; Hasegawa, K.; Naiki, H.; Goto, Y. Direct observation of Abeta amyloid fibril growth and inhibition. *J. Mol. Biol.* 2004, 344, 757-767.

28. Collinge, J**.** Prion diseases of humans and animals: their causes and molecular basis. *Annu. Rev. Neurosci.* 2001, 24, 519-550.

29. Manzano-León, N.; Mas-Oliva, J. Estrés oxidativo, péptido β-amiloide y enfermedad de Alzheimer. *Gac. Med. Mex.* 2006, 142, 229-238.

30. Zhu, X.; Smith, M.A.; Honda, K.; Aliev, G.; Moreira, P.I.; Nunomura, A.; Casadesus, G.; Harris, P.L.; Siedlak, S.L.; Perry, G. Vascular oxidative stress in Alzheimer disease. *J. Neurol. Sci.* 2007, 257, 240-246.

31. Lazar, K.L.; Miller-Auer, H.; Getz, G.S.; Orgel, J.P., Meredith, S.C. Helix-turn-helix peptides that form alpha-helical fibrils: turn sequences drive fibril structure. *Biochemistry* 2005, 44, 12681-12689.

32. Ungewickell, E. J.; Hinrichsen, L. Endocytosis: clathrin-mediated membrane budding. *Current Opinion in Cell Biology* 2007, 19, 417–425.

33. McMahon, H.T.; Boucrot, E. Molecular mechanism and physiological functions of clathrin-mediated endocytosis. *Nat Rev Mol Cell Biol*. 2011, 12, 517-533.

34. Schmid, S.L. Clathrin-coated vesicle formation and protein sorting: an integrated process. *Annu Rev Biochem.* 1997, 66, 511-548.

35. Mousavi, S.A.; Malerød, L.; Berg, T.; Kjeken, R. Clathrin-dependent endocytosis. *Biochem. J.* 2004, *377*, 1–16.

36. Sheikh, A.M.; Nagai, A. Lysophosphatidylcholine modulates fibril formation of amyloid beta peptide, *FEBS J*. 2011, 278, 634-642.

37. Evangelisti, E.; Cecchi, C.; Cascella, R.; Sgromo, C.; Becatti, M.; Dobson, C.M.; Chiti, F.; Stefani, M. Membrane lipid composition and its physicochemical properties define cell vulnerability to aberrant protein oligomers. *J. Cell Sci.* 2012, 125, 2416-2427.

38. García-González, V.; Mas-Oliva, J. Amyloidogenic Properties of a D/N Mutated 12 Amino Acid Fragment of the C-Terminal Domain of the Cholesteryl-Ester Transfer Protein (CETP). *Int. J. Mol. Sci.* 2011, 12, 2019-2035.

39. García-González, V.; Mas-Oliva, J. El concepto de enfermedad asociado a la conformación de proteínas. México: UNAM, Programa Universitario de Investigación en Salud, Editorial El Manual Moderno, 2012. ISBN 978-607-02-3363-0 (UNAM), ISBN 978-607-448-224-9 (El Manual Moderno).

40. Ookoshi, T.; Hasegawa, K.; Ohhashi, Y.; Kimura, H.; Takahashi, N.; Yoshida, H.; Miyazaki, R.; Goto, Y.; Naiki, H. Lysophospholipids induce the nucleation and

extension of beta2-microglobulin-related amyloid fibrils at a neutral pH. *Nephrol. Dial. Transplant.* 2008, 23, 3247-3255.

41. Pál-Gábor, H.; Gombos, L.; Micsonai, A.; Kovács, E.; Petrik, E.; Kovács, J.; Gráf, L.; Fidy, J.; Naiki, H.; Goto, Y.; Liliom, K.; Kardos, J. Mechanism of lysophosphatidic acid-induced amyloid fibril formation of beta(2)-microglobulin in vitro under physiological conditions. *Biochemistry* 2009, 48, 5689-5699.

42. Nakanaga, K.; Hama, K.; Aoki, J. Autotaxin an LPA producing enzyme with diverse functions. *J. Biochem.* 2010, 148, 13-24.

43. Okudaira, S.; Yukiura, H.; Aoki, J. Biological roles of lysophosphatidic acid signaling through its production by autotaxin. *Biochimie* 2010, 92, 698-706.

44. Klunk, W.E.; Jacob, R.F.; Mason, R.P. Quantifying amyloid beta-peptide (Abeta) aggregation using the Congo red-Abeta (CR-abeta) spectrophotometric assay. *Anal. Biochem*. 1999, *266*, 66–76.

45. García-González, V.; Mas-Oliva, J. Amyloid fibril formation modulated by lipids at the C-terminus of CETP. En prensa. *Biochem. Biophys. Res. Commun*. (2013).

46. Blancas-Mejía, L.M.; Ramirez-Alvarado, M. Systemic Amyloidoses. *Annu. Rev. Biochem*. 2013. En prensa.

47. El Khoury, J.; Luster, A.D. Mechanisms of microglia accumulation in Alzheimer's disease: therapeutic implications. *Trends. Pharmacol. Sci.* 2008, *29*, 626–632.

48. Hickman, S.E.; Allison, E.K.; El Khoury, J. Microglial dysfunction and defective beta-amyloid clearance pathways in aging Alzheimer's disease mice. *J. Neurosci.* 2008, *28*, 8354–8360.

49. Manzano-León, N.; Delgado-Coello, N.B.; Guaderrama-Díaz, M.; Mas-Oliva, J. Beta-adaptin: Key molecule for microglial scavenger receptor function under oxidative stress. *Biochem. Biophys. Res. Commun*. 2006, 351, 588–594.

50. Fowler, D.M.; Koulov, A.V.; Alory-Jost, C.; Marks, M.S.; Balch, W.E.; Kelly, J.W. Functional amyloid formation within mammalian tissue. *PLoS Biol*. 2006, 4:e6.

51. Mannini, B.; Cascella, R.; Zampagni, M.; van Waarde-Verhagen, M.; Meehan, S.; Roodveldt, C.; Campioni, S.; Boninsegna, M.; Penco, A.; Relini, A.; Kampinga, H.H.; Dobson, C.M.; Wilson, M.R.; Cecchi, C.; Chiti, F. Molecular mechanisms used by chaperones to reduce the toxicity of aberrant protein oligomers. *Proc Natl Acad Sci U S A*. 2012, 109, 12479-12484.

52. Guaderrama-Díaz, M.; Solís, C.F.; Velasco-Loyden, G.; Laclette, J.P.; Mas-Oliva**,** J. Control of scavenger receptor-mediated endocytosis by novel ligands of different length. *Mol. Cell. Biochem.* 2005, 271, 123-32.

53. Abe, K.; Saito, H. Both oxidative stress-dependent and independent effects of amyloid beta protein are detected by 3-(4,5-dimethylthiazol-2-yl)-2,5-diphenyltetrazolium bromide (MTT) reduction assay. *Brain Res.* 1999, *830*, 146–154.

54. Liu, Y.; Peterson, D.A.; Schubert, D. Amyloid beta peptide alters intracellular vesicle trafficking and cholesterol homeostasis. *Proc. Natl. Acad. Sci. USA* 1998, *95*, 13266–13271.

55. Zurdo, J.; Guijarro, J.I.; Jiménez, J.L.; Saibil, H.R.; Dobson, C.M. Dependence on solution conditions of aggregation and amyloid formation by an SH3 domain. *J Mol Biol* 2001, 311, 325-340.

56. Yamamoto, S.; Hasegawa, K.; Yamaguchi, I.; Tsutsumi, S.; Kardos, J.; Goto, Y.; Gejyo, F.; Naiki, H. Low concentrations of sodium dodecyl sulfate induce the

extension of beta 2-microglobulin-related amyloid fibrils at a neutral pH, *Biochemistry* 2004, 43, 11075-11082.

57. Chandler, D. Interfaces and the driving force of hydrophobic assembly. *Nature* 2005, 437, 640-647.

58. García-González, V.; Gutiérrez-Quintanar, N.; Mendoza-Espinosa, P.; Brocos, P.; Piñeiro, Á.; Castillo, R.; Mas-Oliva, J. Key Structural Arrangements at the C-terminus Domain of CETP Promote a Mechanism for Lipid-transfer Activity. 2013. Envíado a revisión

59. Broome, B.M.; Hecht, M.H. Nature disfavors sequences of alternating polar and non-polar amino acids: implications for amyloidogenesis. *J. Mol. Biol.* 2000, *296*, 961–968.

60. Schwartz, R.; Istrail, S.; King, J. Frequencies of amino acid strings in globular protein sequences indicate suppression of blocks of consecutive hydrophobic residues. *Protein Sci.* 2001, *10*, 1023–1031.

61. Chiti, F.; Calamai, M.; Taddei, N.; Stefani, M.; Ramponi, G.; Dobson, C.M. Studies of the aggregation of mutant proteins *in vitro* provide insights into the genetics of amyloid diseases. *Proc. Natl. Acad. Sci. USA* 2002, *99*, 16419–16426.

62. López De La Paz, M.; Goldie, K.; Zurdo, J.; Lacroix, E.; Dobson, C.M.; Hoenger, A.; Serrano, L. *De novo* designed peptide-based amyloid fibrils. *Proc. Natl. Acad. Sci. USA* 2002, 99, 16052–16057.

63. Uversky, V.N. Natively unfolded proteins: A point where biology waits for physics. *Protein Sci.* 2002, *11*, 739–756.

64. Monsellier, E.; Chiti, F. Prevention of amyloid-like aggregation as a driving force of protein evolution. *EMBO Rep.* 2007, *8*, 737–742.

65. Chiti F., Calamai M., Taddei N., Stefani M., Ramponi G., Dobson CM. Studies of the aggregation of mutant proteins in vitro provide insights into the genetics of amyloid diseases *PNAS* 2002, 99, 16419-16426.

66. Wetzel, R. Kinetics and thermodynamics of amyloid fibril assembly. *Acc. Chem. Res.* 2006, *39*, 671–679.

67. Nelson, R.; Sawaya, M.R.; Balbirnie, M.; Madsen, A.Ø.; Riekel, C.; Grothe, R.; Eisenberg, D. Structure of the cross-beta spine of amyloid-like fibrils. *Nature* 2005, *435*, 773–778.

68. Radivojac, P.; Obradovic, Z.; Smith, D.K.; Zhu, G.; Vucetic, S.; Brown, C.J.; Lawson, J.D.; Dunker, A.K. Protein flexibility and intrinsic disorder. *Protein Sci.* 2004, *13*, 71–80.

69. Oda, M.N.; Forte, T.M.; Ryan, R.O.; Voss, J.C. The C-terminal domain of apolipoprotein A-I contains a lipid-sensitive conformational trigger. *Nat. Struct. Biol.* 2003*,* 10, 455-460.

70. Kono, M.; Okumura, Y.; Tanaka, M.; Nguyen, D.; Dhanasekaran, P.; Lund-Katz, S.; Phillips, M.C.; Saito, H. Conformational flexibility of the N-terminal domain of apolipoprotein a-I bound to spherical lipid particles. *Biochemistry* 2008**,** 47, 11340-11347.

71. Ladokhin, A.S.; White, S.H. Folding of amphipathic alpha-helices on membranes: energetics of helix formation by melittin. *J. Mol. Biol.* 1999, *285*, 1363–1369.

72. White, S.H.; Wimley, W.C. Hydrophobic interactions of peptides with membrane interfaces. *Biochim. Biophys. Acta* 1998, *1376*, 339–352.

73. Aguilar-Gaytan, R.; Mas-Oliva, J. Oxidative stress impairs endocytosis of the scavenger receptor class A. *Biochem. Biophys. Res. Commun.* 2003, *305*, 510–517.

74. Bucciantini, M.; Giannoni, E.; Chiti, F.; Baroni, F.; Formigli, L.; Zurdo, J.; Taddei, N.; Ramponi, G.; Dobson, C.M.; Stefani, M. Inherent toxicity of aggregates implies a common mechanism for protein misfolding diseases. *Nature* 2002, 416, 507-511.

75. Chiti, F.; Dobson, C.M. Protein misfolding, functional amyloid, and human disease. *Annu. Rev. Biochem.* 2006, 75, 333–366.

76. Owen, D.J.; Vallis, Y.; Pearse, B.M.; McMahon, H.T. The structure and function of the beta 2-adaptin appendage domain. *EMBO J.* 2000, 19, 4216-4227.

77. Rapoport, I.; Chen, Y.C.; Cupers, P.; Shoelson, S.E.; Kirchhausen, T. Dileucine-based sorting signals bind to the beta chain of AP-1 at a site distinct and regulated differently from the tyrosine-bassed motif-binding site. *EMBO J.* 1998, 19, 2148-2155.

78. Ford, M.G.; Pearse, B.M.; Higgins, M.K.; Vallis, Y.; Owen, D.J.; Gibson, A.; Hopkins, C.R.; Evans, P.R.; McMahon, H.T. Simultaneous binding of PtdIns(4,5)P2 and clathrin by AP180 in the nucleation of clathrin lattices on membranes. *Science* 2001, 291, 1051–1055.

79. Legandre-Guillemin, V.; Wasiak, S.; Hussain, N.K.; Angers, A.; McPherson, P.S. ENTH/ANTH proteins and clatrin-mediated membrane budding. *J. Cell. Sci.* 2004, 117, 9–18.

80. Meyerholz, A.; Hinrichsen, L.; Groos, S.; Esk, P.C.; Brandes, G.; Ungewickell, E.J. Effect of Clathrin Assembly Lymphoid Myeloid Leukaemia Protein Depletion on Clathrin Coat Formation. *Traffic* 2005, 6, 1225-1234.

81. Sawaya, M.R.; Sambashivan, S.; Nelson, R.; Ivanova, M.I.; Sievers, S.A. Apostol, M.I.; Thompson, M.J.; Balbirnie, M.; Wiltzius, J.J.; McFarlane, H.T.; Madsen, A.Ø.; Riekel, C.; Eisenberg, D. Atomic structures of amyloid cross-beta spines reveal varied steric zippers. *Nature* 2007, 447, 453-457.

82. Sievers, S.A.; Karanicolas, J.; Chang, H.W.; Zhao, A.; Jiang, L.; Zirafi, O.; Stevens, J.T.; Münch, J.; Baker, D.; Eisenberg, D. Structure-based design of non-natural amino-acid inhibitors of amyloid fibril formation. *Nature* 2011, 475, 96-100.

83. Knowles, T.P.; Fitzpatrick, A.W.; Meehan, S.; Mott, H.R.; Vendruscolo, M.; Dobson, C.M.; Welland, M.E. Role of intermolecular forces in defining material properties of protein nanofibrils. *Science* 2007, *318*, 1900–1903.

84. Fitzpatrick, A.W.; Knowles, T.P.; Waudby, C.A.; Vendruscolo, M.; Dobson, C.M. Inversion of the balance between hydrophobic and hydrogen bonding interactions in protein folding and aggregation. *PLoS Comput. Biol.* 2011, 7, e1002169.

85. Alonso, A.L.; Zentella-Dehesa, A.; Mas-Oliva, J. Characterization of a naturally occurring new version of the cholesterol ester transfer protein (CETP) from small intestine. *Mol. Cell. Biochem.* 2003, *245*, 173–182.

86. Dobson, C.M. Protein chemistry. In the footsteps of alchemists. *Science* 2004, 304, 1259-1262.

87. Chapman, M.R.; Robinson, L.S.; Pinkner, J.S.; Roth, R.; Heuser, J.; Hammar, M.; Normark, S.; Hultgren, S.J. Role of *Escherichia coli* curli operons in directing amyloid fiber formation. *Science* 2002, 295, 851-855.

88. Claessen, D.; Rink, R.; de Jong, W.; Siebring, J.; de Vreugd, P.; Boersma, F.G.; Dijkhuizen, L.; Wosten, H.A. A novel class of secreted hydrophobic proteins is involved in aerial hyphae formation in *Streptomyces coelicolor* by forming amyloid-like fibrils. *Genes Dev* 2003, 17, 1714-1726.

89. Mackay, J.P.; Matthews, J.M.; Winefield, R.D.; Mackay, L.G.; Haverkamp, R.G.; Templeton MD: The hydrophobin EAS is largely unstructured in solution and functions by forming amyloid-like structures. *Structure* 2001, 9, 83-91.

90. Coustou, V.; Deleu, C.; Saupe, S.; Begueret, J. The protein product of the het-s heterokaryon incompatibility gene of the fungus Podospora anserina behaves as a prion analog. *Proc Natl Acad Sci USA* 1997, 94, 9773-9778.

91. King, C.Y.; Tittmann, P.; Gross, H.; Gebert, R.; Aebi, M.; Wüthrich, K. Prion-inducing domain 2-114 of yeast Sup35 protein transforms *in vitro* into amyloid-like filaments. *Proc Natl Acad Sci USA* 1997, 94, 6618-6622.

92. Iconomidou, V.A.; Vriend, G.; Hamodrakas, S.J. Amyloids protect the silkmoth oocyte and embryo. *FEBS Lett* 2000, 479, 141-145.

93. Iconomidou, V.A.; Chryssikos, G.D.; Gionis, V.; Galanis, A.S.; Cordopatis, P.; Hoenger, A.; Hamodrakas, S.J. Amyloid fibril formation propensity is inherent into the hexapeptide tandemly repeating sequence of the central domain of silkmoth chorion proteins of the A-family. *J Struct Biol* 2006, 156, 480-488.

94. Watt, B.; van Niel, G.; Fowler, D.M.; Hurbain, I.; Luk, K.C.; Stayrook, S.E.; Lemmon, M.A.; Raposo, G.; Shorter, J.; Kelly, J.W.; Marks, M.S. N-terminal domains elicit formation of functional Pmel17 amyloid fibrils. *J Biol Chem* 2009, 284, 35543-35555.

95. Kobayashi, T.; Urabe, K.; Orlow, S.J.; Higashi, K.; Imokawa, G.; Kwon, B.S.; Potterf, B.; Hearing, V.J. The Pmel 17/silver locus protein. Characterization and investigation of its melanogenic function. *J Biol Chem* 1994, 269, 29198-29205.

96. Fowler, D.M.; Koulov, A.V.; Balch, W.E.; Kelly, J.W. Functional amyloid from bacteria to humans. *Trends Biochem Sci* 2007, 32, 217-224.

97. García-González, V.; Mas-Oliva, J. Novedosa Función de CETPI (Isoforma de la Proteína Transferidora de Ésteres de Colesterol). Reunión Ciencia y Humanismo 2012. Academia Mexicana de Ciencias, Ciudad de México, México. 18-20 de Enero de 2012

Abreviaturas

ApoC-I: Apolipoproteína C-I

ANTH: AP180 N-Terminal Homology

BPI: Bactericidal/permeability-increasin protein

CALM: Clathrin Assembly Lymphoid Myeloid leukemia

CETP: Proteína transferidora de ésteres de colesterol

CETPI: Isoforma I de la proteína transferidora de ésteres de colesterol

CMR: Concentración media por residuo

D: Aminoácido aspartato

DC: Dicroísmo circular

DPPC: Dipalmitoil fosfatidilcolina

ERO: Especies reactivas de oxígeno

HDL: Lipoproteínas de alta densidad

LDL: Lipoproteínas de baja densidad

LPA: Ácido lisofosfatídico

LPS: Lipopolisacáridos

Lyso-C_{12}PC: lisofosfatidilcolina C-12

MET: Microscopía Electrónica de Transmisión

N: Aminoácido asparagina

μH: Momento hidrofóbico

MTT: 3-(4,5-dimetiltiazol-2-ilo) 2,5 bromuro difeniltetrazolio

PA: Ácido fosfatídico

PC: Fosfatidilcolina

PE: Fosfatidiletanolamina

PDB: Protein Data Bank

Péptido βA: Péptido β-amiloide

POPC: 1-palmitoil-2-oleoil-sn-glicero-3-fosfocolina

POPG: 1-palmitoil-2-oleoil-sn-glicero-3-fosfoglicerol

RS: Receptores scavenger

SDS: Dodecil sulfato de sodio

TBH: Terbutil hidroperóxido

TBS: Solución salina amortiguada con Tris

ThT: Tioflavina-T

UV/Vis: Ultravioleta/visible

VLDL: Lipoproteínas de muy baja densidad

Publicaciones

Biochemical and Biophysical Research Communications 434 (2013) 54–59

Contents lists available at SciVerse ScienceDirect

Biochemical and Biophysical Research Communications

journal homepage: www.elsevier.com/locate/ybbrc

Amyloid fibril formation of peptides derived from the C-terminus of CETP modulated by lipids

Victor García-González [a], Jaime Mas-Oliva [a,b,*]

[a] Instituto de Fisiología Celular, Universidad Nacional Autónoma de México, 04510 México, DF, Mexico
[b] División de Investigación, Facultad de Medicina, Universidad Nacional Autónoma de México, 04510 México, DF, Mexico

ARTICLE INFO

Article history:
Received 8 March 2013
Available online 29 March 2013

Keywords:
CETP
Peptide conformational change
β-Sheet to α-helix transition
Amyloid fibrils
Lysophosphatidic acid

ABSTRACT

Cholesteryl-ester transfer protein (CETP) is a plasmatic protein involved in neutral lipid transfer between lipoproteins. Focusing on the last 12 C-terminus residues we have previously shown that mutation $D_{470}N$ promotes a conformational change towards a β-secondary structure. In turn, this modification leads to the formation of oligomers and fibrillar structures, which cause cytotoxic effects similar to the ones provoked by amyloid peptides. In this study, we evaluated the role of specific lipid arrangements on the structure of peptide helix-*Z* ($D_{470}N$) through the use of thioflavin T fluorescence, peptide bond absorbance, circular dichroism and electron microscopy. The results indicate that the use of micelles formed with lysophosphatidylcholine and lysophosphatidic acid (LPA) under neutral pH induce a conformational transition of peptide helix-*Z* containing a β-sheet conformation to a native α-helix structure, therefore avoiding the formation of amyloid fibrils. In contrast, incubation with phosphatidic acid does not change the profile for the β-sheet conformation. When the electrostatic charge at the surface of micelles or vesicles is regulated through the use of lipids such as phospholipid and LPA, minimal changes and the presence of β-structures were recorded. Mixtures with a positive net charge diminished the percentage of β-structure and the amount of amyloid fibrils. Our results suggest that the degree of solvation determined by the presence of a free hydroxyl group on lipids such as LPA is a key condition that can modulate the secondary structure and the consequent formation of amyloid fibrils in the highly flexible C-terminus domain of CETP.

1. Introduction

CETP facilitates the transfer of neutral lipids between lipoproteins, and plays an important role in reverse cholesterol transport. The tridimensional view of the C-terminus region of CETP (aa 453–476) is composed of a β-sheet (aa 453–462) and the native amphipathic α-helix (aa 465–476) named helix-*X* (Fig. 1). Several studies have demonstrated that a critical site for the transfer process is restricted specifically to the 12 residue C-terminus domain structured as an amphipathic α-helix [1–3]. Notwithstanding, our group has reported that this domain shows conformational changes in a non-lipid microenvironment when mutation $D_{470}N$ is introduced through the use of peptide denominated helix-*Z* [4,5]. These conditions give origin to a hydrophobic cluster (^{467}LLVNFLQ^{473}) which favors the presence of a β-secondary structure, a mechanism coupled with the formation of oligomers and amyloid fibrils [5]. Employing helix-*Z* as a model peptide, we have studied the role of several lipid arrangements as potential modulators of secondary structure and potentially upon amyloid fibril formation.

It has been reported that under specific conditions, lipid molecules induce conformational changes in various amyloid precursor proteins, in addition to the key role in the formation and stabilization of amyloid fibrils [6–8]. Likewise, the interaction between oligomeric precursor species on specific domains of the cell membrane is a primary event that results in the appearance of early cytotoxic effects associated with disease [9,10]. In this case, the role of specific lipid compositions on the hydrophilic/hydrophobic interface must be critical as a recognition site that can modulate possible conformational changes in secondary structure, which in turn could modify the formation of structures controlled by order-to-disorder and disorder-to-order transitions [5–7,9,11]. In this respect, it has been described that molecules such as lysophosphatidic acid (LPA), a phospholipid derived from the enzymatic action of several extracellular phospholipases from precursor molecules such as lysophosphatidylcholine or phosphatidic acid (PA), can promote in the protein β_2-microglobulin the formation *in vitro* of amyloid fibrils [12,13]. Nevertheless, the route by which the autotaxin enzyme particularly produces a high amount of LPA from lysophosphatidylcholine, is still not well understood [14,15].

* Corresponding author at: Instituto de Fisiología Celular, Universidad Nacional Autónoma de México, 04510 México, DF, Mexico. Fax: +52 55 5622 5611.
E-mail address: jmas@ifc.unam.mx (J. Mas-Oliva).

0006-291X/$ - see front matter © 2013 Elsevier Inc. All rights reserved.
http://dx.doi.org/10.1016/j.bbrc.2013.03.067

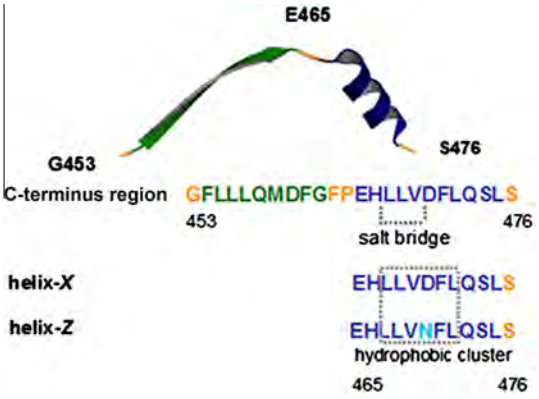

Fig. 1. Structural representation of the C-terminus region of CETP showing sequences of peptides helix-*X* and helix-*Z*. The H466-D470 salt bridge and the hydrophobic cluster are shown. The structure was obtained from the Protein Data Bank, access code: 2obd.

In this study, we present a series of experiments which demonstrate that treatment of helix-*Z* with LPA and lysophosphatidylcholine (lyso-C_{12}PC), lipids that can be found on the surface of lipoproteins, promote a structural change from a β-chain to a native α-helix structure. Incubation of helix-*Z* with LPA concentrations above 2.5 mM completely inhibits the formation of amyloid fibrils, in a manner that interactions of peptide with specific hydrophilic/hydrophobic interfaces formed by this lipid, should retain peptide monomers at the surface and consequently prevent peptide self-assembly. These conditions might allow helix-*Z* to recover and maintain the functional α-helix conformation of the C-terminus domain of CETP and therefore warranty protein function.

2. Materials and methods

Cholesterol, cholesteryl-ester, L-α phosphatidic acid dipalmitoyl (PA), L-α-phosphatidylethanolamine dipalmitoyl (PE), L-α-phosphatidylcholine dipalmitoyl (DPPC) and thioflavin T (ThT) were obtained from Sigma–Aldrich (St. Louis, MO). L-α-Phosphatidylcholine (PC), 1-palmitoyl-2-oleoyl-sn-glycero-3-phosphocholine (POPC), 1-palmitoyl-2-oleoyl-sn-glycero-3-phospho-1-glycerol (POPG), 1-lauroyl-2-hydroxy-sn-glycero-3-phosphocholine (lyso-C_{12}PC) and 1-oleoyl-2-hydroxy-sn-glycero-3-phosphate (LPA) were obtained from Avanti Polar Lipids (Alabaster, AL).

2.1. Peptide synthesis and peptide preparation

Helix-*Z* (^{465}EHLLV*N*FLQSLS^{476}) and native peptide (^{465}EHLLVDFLQSLS^{476}) derived from the C-terminus of CETP were synthesized by GenScript (Piscataway, NJ) and dissolved in a carbonate buffer pH 9.5 (1 mg/ml). From this solution a further 1:5 dilution was carried out. To evaluate the structure at pH 7.2 in the different lipid environments, a sodium phosphate buffer was also used. Under the same conditions, the control peptide ^{460}DFGFPEHL^{46} was employed. Solutions were filtered through 0.22 μm membrane filters before carrying out the experiments. Purity of peptides was greater than 98% confirmed by mass spectrometry and HPLC analysis. Peptide concentration was determined by measuring the peptide bond absorbance at 205 nm.

Peptide samples at a concentration of 200 μg/ml were incubated with the different lipid preparations for 12 h at 25 °C before their structural characterization, employing circular dichroism, thioflavin T fluorescence, peptide bond spectroscopy and electron microscopy.

2.2. Circular dichroism spectroscopy

Circular dichroism (CD) spectra were recorded with an AVIV 62DS spectropolarimeter (AVIV Instruments) at 25 °C employing far UV wavelength (190–260 nm). Experiments were performed at a peptide concentration of 200 μg/ml in a 1.0 mm quartz path length cuvette, running AVIV software. Spectra were recorded with a 1 mm bandwidth, using 1 nm increments and 2.5 s accumulation time averaged over 3 scans. CD results are reported as mean molar ellipticity (Θ, deg cm^2 dmol^{-1}) considering the baseline correction.

2.3. Thioflavin T fluorescence and peptide bond spectroscopy

Employing 180 μg/ml of peptide, the absorbance was measured every 1 nm using a Perkin Elmer UV/Vis Lambda 2*S* spectrophotometer scanning from 200 to 240 nm. Peptide spectra were corrected by subtracting the corresponding control spectra obtained under identical conditions. Additionally, the β-structure was characterized with ThT fluorescence assay. Fluorescence emission spectra were registered at 25 °C from 470 to 540 nm with an excitation wavelength of 450 nm. A scan velocity of 60 nm/min using an Olis DM45 spectrofluorimeter was used. The concentrations of ThT and peptides were 10 μM and 36 μM, respectively.

2.4. Preparation of micelles formed by phosphatidylcholine/cholesteryl-esters

Lipids were mixed in chloroform and dried for 6 h under a gentle stream of N_2, and an additional period of 24 h in a SpeedVac concentrator (Savant). Lipid mixtures were prepared with a molar ratio of PC 2 mM and cholesteryl-ester 100 μM (20:1). After drying, lipids were resuspended in pH 6.8 buffer and subsequently sonicated 15 s on/30 s off pulses for 4 cycles of 10 min in an ice bath under a flow of N_2 using a Sonifier 250 ultrasonicator (Branson). Samples were left to equilibrate for 2 h and centrifuged at 13,000 rpm for 10 min before being used.

2.5. Preparation of micelles formed by lyso-C_{12}PC, LPA and PA

The required amounts of lyso-C_{12}PC dissolved in chloroform were placed under a gentle stream of N_2 for 4 h, complete solvent free treatment was achieved by an additional 22 h in a vacuum equipment. Samples were resuspended in a phosphate buffer pH 6.8 at 37 °C (50 mM). Samples were kept 2 h at 25 °C and subsequently centrifuged at 13,000 rpm for 10 min at 12 °C.

LPA samples in chloroform were placed under a gentle flow of N_2 for 6 h, and additional 12 h in vacuum equipment. The samples were hydrated in phosphate buffer and afterwards processed through 4 cycles of freezing in liquid N_2, and thawing at 37 °C. Solutions were left to equilibrate for 2 h and centrifuged at 13,000 rpm for 10 min. Under the same experimental conditions, PA vesicles were prepared with an additional step of sonication for 4 cycles of 10 min.

2.6. Preparation of micelles by phospholipids and LPA

PC and LPA were mixed in chloroform and dried for 6 h under a gentle stream of N_2 with an additional treatment using a SpeedVac concentrator 22 h in vacuum. Lipid mixtures were prepared with a molar ratio of PC 3.06 mM and LPA 0.92 mM. After drying, lipid mixture was resuspended in pH 6.8 buffer and subsequently sonicated for 4 cycles. Samples were left to equilibrate for 2 h and centrifuged at 13,000 rpm for 10 min. Employing the same methodology, micelles consisting of DPPC/LPA and PE/LPA were prepared. Under a ratio of POPC 75% and POPG 25%, negatively charged micelles were prepared with the addition of LPA.

2.7. Electron microscopy

Peptide samples incubated under different conditions were processed employing a negative staining technique and visualized using transmission electron microscopy (NS-TEM). Samples (10 μl) were placed on carbon-coated copper grids (400 mesh) for 10 min at 25 °C. Excessive liquid was removed and the grids were negatively stained with uranyl acetate solution (2%, w/v) for 5 min. Samples were dried for 20 min. NS-TEM images were acquired using a JEM-1200EX11 JEOL microscope at 70 kV with a magnification of 60,000×.

3. Results and discussion

Previous studies from our laboratory have shown that peptide helix-*Z* shows the formation of a β-type secondary structure dependent on pH and peptide concentration [5]. Conditions such as ionic strength did not modify the content of β-structure, and only temperatures above 70 °C promote a decrease in the percentage of this type of secondary structure [5]. In this study we evaluated the effect of several lipid arrangements upon helix-*Z* structure at pH 7.2 under physiological conditions. Specifically, we conducted a series of experiments by changing regional characteristics of lipid such as: polar head size, acyl chain length, electrostatic charge and degree of solvation, all of them able to modify the secondary structure of helix-*Z*.

Treatment with increasing incubation concentrations of lyso-C_{12}PC (0.01–40 mM) showed that lipid concentrations below 5 mM allow helix-*Z* to maintain a β-sheet conformation when monitored by CD (Fig. 2A). Incubation with 1 mM lyso-C_{12}PC, a concentration close to the critical micelle concentration (0.9 mM) for this lipid, increased values that correspond to a β-structure (Fig. 2A and B). Under this condition, interactions of helix-*Z* and lyso-C_{12}PC in an aqueous environment must have taken place in a dynamic equilibrium between lipid monomers as well as formed micelles. In this regard, it has been reported that molecules with a similar structure to lyso-C_{12}PC trigger the aggregation phenomenon in amyloidogenic proteins at concentrations equivalent to those used in this study [16]. In our hands, concentrations of lyso-C_{12}PC close to 10 mM induced a transition point between β-sheet structures and the formation of α-helical structures. This change was followed by evaluating the CD characteristics for a β-sheet conformation at 201 nm (Θ_{201nm}) (Fig. 2B). This phenomenon was also studied following changes in peptide bond absorbance at 218 nm (Fig. 2C) and by fluorescence coupled to ThT (Fig. 2D). Under treatment with lyso-C_{12}PC (10 mM), fibrillar structures were still identified in smaller quantities but more extended

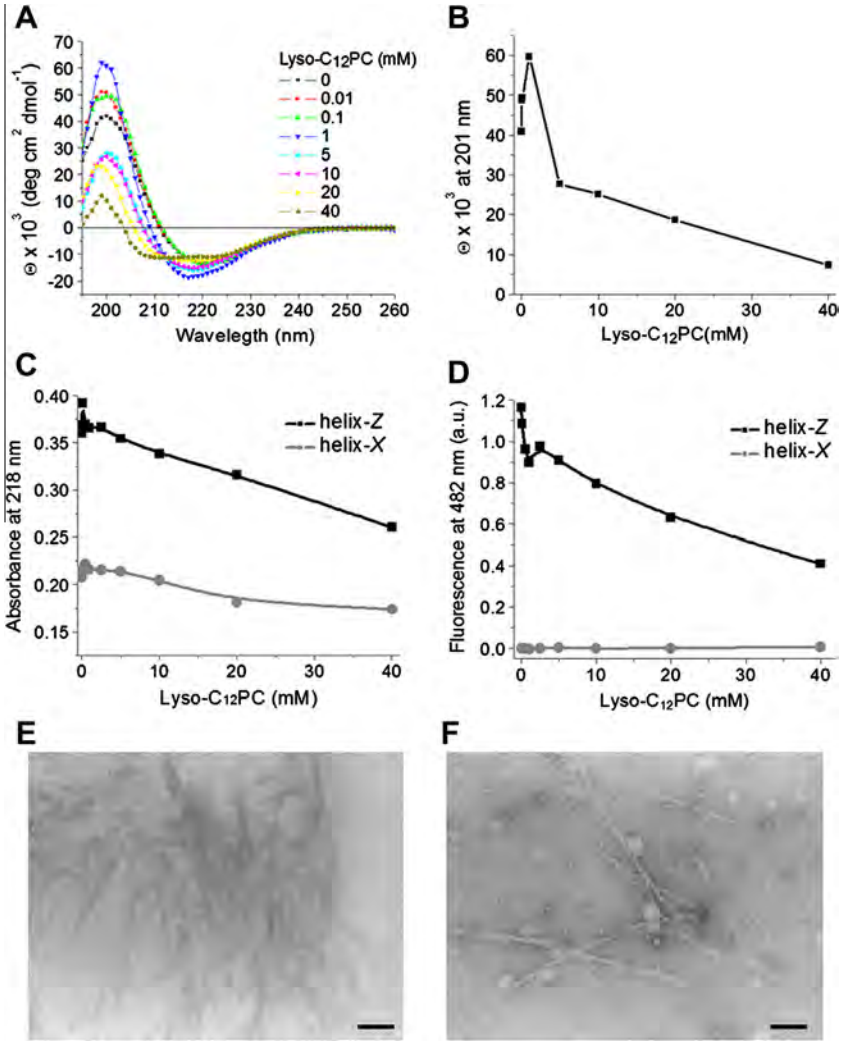

Fig. 2. Effect of lysophosphatidylcholine upon the structure of helix-*Z*. (A) CD spectra obtained under treatment with increasing concentrations of lyso-C_{12}PC. (B) Mean molar ellipticity values at 201 nm. (C) Under the same conditions, absorbance at 218 nm, (D) fluorescence coupled to ThT at 482 nm. Native peptide was used as control. (E) Amyloid fibrils formed by helix-*Z*. (F) Helix-*Z* incubated with lyso-C_{12}PC vesicles (10 mM). Bars correspond to 100 nm.

with respect to helix-*Z* samples not incubated with lipid (Fig. 2E and F). At higher concentrations of lyso-C_{12}PC (20 and 40 mM), although a residual signal for β-structures was detected following peptide bond absorbance and fluorescence coupled to ThT, CD measurements showed the formation of well-defined α-helix structures.

In another series of experiments, considering that the hydrophobic characteristics of the surrounding microenvironment are key conditions that favor structural changes in specific domains of lipid binding proteins, we evaluated several lipid molecules with structures similar to lyso-C_{12}PC. Using a concentration range between 0.1 and 10 mM LPA, a lipid with a small polar head close to the acyl chain, a series of experiments were carried out and the conformational changes from β-structures to α-helices studied. Spectra obtained showed an isodichroic point near to 215 nm associated with the presence of only two conformational states (Fig. 3A).

CD experiments show that this β to α transition was also identified by plotting the signal at Θ_{201nm}, where it was found that incubation with concentrations of LPA above 1 mM induces a drastic decrease in CD values associated with the loss of β-structure (Fig. 3B). In parallel, conformational changes were followed recording absorbance of peptide bonds at 218 nm (Fig. 3C) and by measurements of fluorescence coupled to ThT (Fig. 3D).

The present data indicate that LPA induces a well-defined structural transition in secondary structure from β-sheet towards an α-helix at concentrations above its cmc. In fact, after treatment with 2.5 mM LPA, ThT fluorescence was suppressed (Fig. 3D insert), indicating a complete loss of β-structure content. Fibrillar structures were not found in LPA samples analyzed below 10 mM and processed through NS-TEM (Fig. 3F). Our results suggest that conformational changes in secondary structure dependent of LPA are associated with a cooperative process, where helix-*Z* recovers the levels of an α-helical structure similar to what it is found when the native peptide is studied (Supplementary Fig. 1). However, this might not be considered a general phenomenon for lipids with a free hydroxyl groups at the polar head. At the highest lyso-C_{12}PC concentrations (20 and 40 mM), the fluorescence signal coupled to ThT was not completely abolished; therefore, incubation with lyso-C_{12}PC is associated with a partial transition towards the formation of α-helices.

Polar head size and the presence of a free hydroxyl group in position sn2 of the glycerol backbone, properties that should modify the degree of solvation at the surface of interfaces [7], should play a key role in the mechanisms that modulate lipid-dependent amyloid fibril formation [7,9]. In this case, the hydrophilic components of phospholipids such as a free hydroxyl group in LPA, may affect

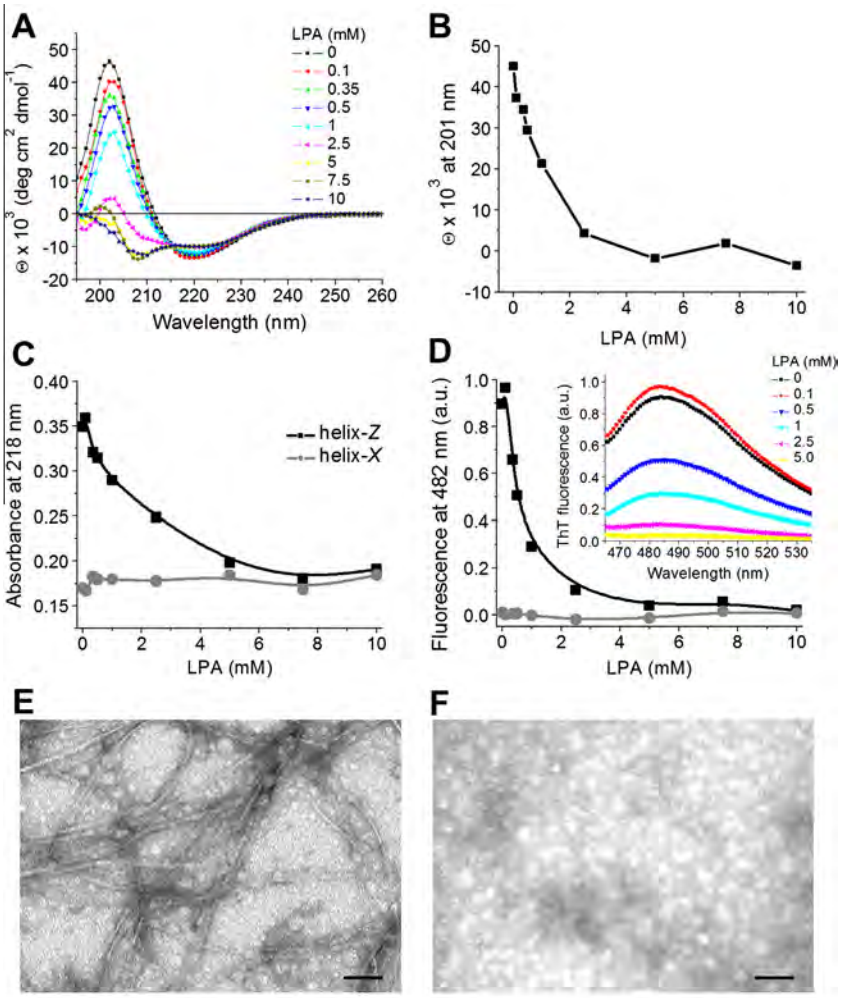

Fig. 3. Lysophosphatidic acid prevents the formation of amyloid fibrils by helix-*Z*. (A) CD spectra of helix-*Z* incubated with increasing concentrations of LPA. (B) Mean molar ellipticity values at 201 nm. (C) Absorbance values at 218 nm. (D) ThT-fluorescence at 482 nm. The native peptide was used as control. The insert shows the emission spectra of helix-*Z* at different concentrations of LPA. (E) Amyloid fibrils formed by helix-*Z*. (F) Effect of LPA treatment in the formation of fibrils. Four samples were processed on different days. Bars correspond to 100 nm.

the position and the array of the hydrophobic assemblies in relation to the interface [17]. We tested this possibility by treatment with increasing concentrations of PA, a lipid molecule with two acyl chains associated to the glycerol backbone, conditions that should not favor the conformational change from β-sheet structures to an α-helix. Employing spectroscopic techniques, this thesis was corroborated using a concentration range of 0.1–5 mM PA, when a β-sheet structure was maintained and the property to form amyloid fibrils was observed when peptide helix-*Z* was studied (Supplementary Fig. 2).

Considering that the electrostatic charge on lipid surfaces is a factor that could modulate the secondary structure of helix-*Z*, we studied the effect of a series of phospholipids mixed with LPA (76%/24%) (Fig. 4). Peptide treatment with micelles formed with POPC/POPG and LPA does not modify the profile of the β-secondary structure evaluated by CD and ThT fluorescence (Fig. 4A and B). This condition is maintained throughout the concentration range of 0.1–2.4 mM of these mixtures, showing micelle formation at the highest concentrations (data not shown).

When helix-*Z* was incubated with neutral vesicles composed of POPC (1.23 mM) and LPA (0.37 mM), CD spectra and fluorescence emission values were similar to the control values without the addition of lipids (Fig. 4A and B). A similar response was obtained when neutral micelles formed by phosphatidylcholine (PC) were studied, a condition in which the formation of well-defined amyloid fibrils is maintained (Fig. 4C and D). Since an extended incubation time (24 h) was used, the presence of oligomeric structures was reduced [5]. However, in these samples it was possible to identify amyloid fibrils located at the surface of lipid micelles (Fig. 4D insert), a condition that suggests there might be interactions at the surface of micelles without the presence of a structural change in helix-*Z*.

Treatment with increasing concentrations of lipids contained in mixtures composed of PC/cholesteryl-esters extensively used in a previous work employing CETP [18], did not modulate the structural changes described above for LPA and lyso-C_{12}PC and only a slight decrease in β-structure content was recorded (data not shown).

Under the same conditions, incubation with neutral micelles formed by DPPC and LPA maintains a β-sheet conformation in helix-*Z*. Nevertheless, in this case an increase in the fluorescence spectrum of ThT was registered, condition that is related to the presence of high concentrations of fibrils shown by samples processed for NS-TEM. Several characteristics related to the morphology of these fibrils showing a highly heterogeneous pattern, were registered (Fig. 4E).

Treatment with micelles composed of phosphatidylethanolamine (PE) and LPA presenting a positive charge at their surface and a small polar head group, induced a moderate decrease in the content of β-structures of helix-*Z* (Fig. 4A and B). Likewise, lower amounts of amyloid fibrils were recorded with respect to previous lipid treatments (Fig. 4F). Under our experimental conditions, at neutral pH helix-*Z* maintains a net negative charge (−1), in such a way that these results could be associated with a low electrostatic binding capacity at the surface of positive charged vesicles. Interestingly, when helix-*X*, the native C-terminus domain of CETP in a disordered state was evaluated in the presence of PE/LPA vesicles, the highest levels of α-helix are promoted (Supplementary Fig. 3).

A hydrophobic cluster at the C-terminus domain of CETP ^{467}LLVNFLQ^{473} originated by mutation $D_{470}N$ shares similar characteristics with the hydrophobic structural motifs for *steric zippers*, which have been described to integrate the molecular structure of amyloid fibrils [19,20]. In this sense, mutation $D_{470}N$ minimizes the electrostatic repulsion between peptide monomers, promoting the formation of hydrogen bonds in the backbone and triggering β-sheet and fibril formation in helix-*Z* [5]. These phenomena are restricted to the C-terminus end (residues 465–476), since peptide sequences that corresponds to ^{460}DFGFPEHL^{467}, do not show β-sheet formation, and even in the presence of lipids the peptide remains in a disordered state (data not shown).

The inhibition of fibril formation and stabilization of an α-helical structure in helix-*Z* seem to be directly associated with the specific physicochemical properties of LPA. The presence of a free hydroxyl group and a small polar head group may facilitate the molecular recognition for helix-*Z*, allowing the interaction of

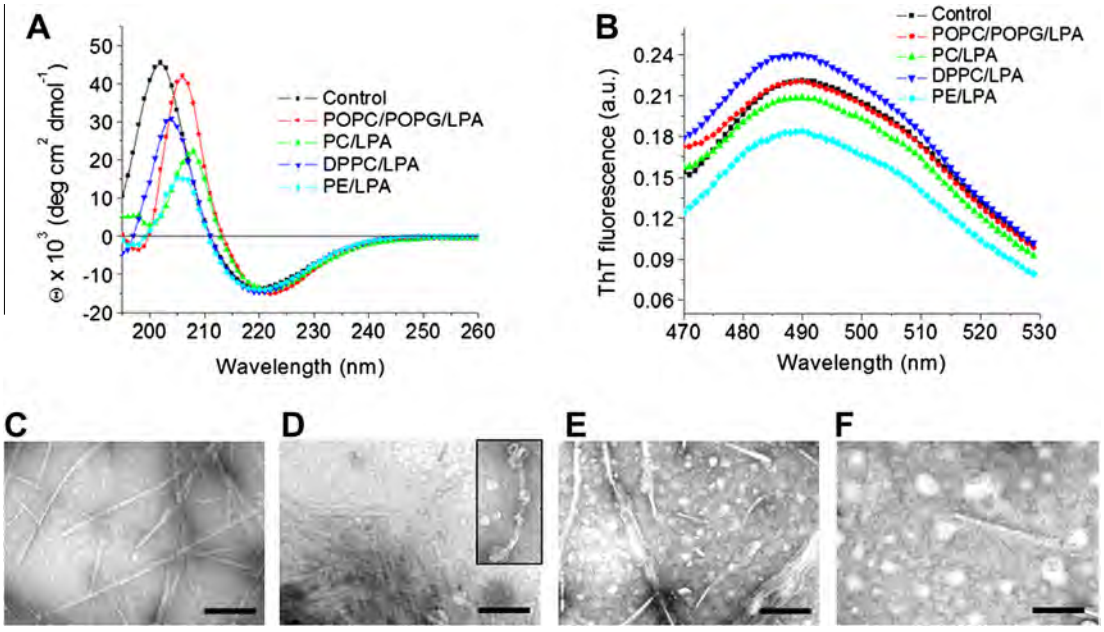

Fig. 4. Effect of lipid electrostatic charge upon the structure of helix-*Z*. (A) CD spectra of helix-*Z* incubated with lipid micelles of different composition. (B) Emission spectra ofThT-fluorescence. NS-TEM of helix-*Z* without lipid treatment (C), and with micelles composed of PC/LPA (D), DPPC/LPA (E) and PE/LPA (F). Bars correspond to 200 nm.

monomeric peptides at the surface of micelles. Therefore, nucleation and stacking of peptides, phenomena that lead to aggregation and ultimately to fibril formation are suppressed. In this sense, it has been reported that the stability of native folding is primarily determined by hydrophobic interactions between side chains, whereas the stability of amyloid fibrils is more dependent on backbone intermolecular hydrogen bonding interactions [21].

On the other hand, a large group of events occurring at the surface of lipids are influenced by hydrogen bonding networks [22], in such a way that binding of lipid/helix-*Z* at the surface of micelles or lipoproteins may involve the release of highly ordered water molecules located at the first layers of hydration, with the consequent reorganization of hydrogen bonds and hydrophobic interactions. Hence, conformational changes and modulation of secondary structure of peptides requires key conditions associated to the microenvironment, being key components the degree of solvation and the size of the polar head of lipids. In conclusion, our results suggest a regulatory role for LPA by modulating the mechanisms that maintain the C-terminus domain of CETP in a functional conformation directly associated to the presence of an α-helical structure for this segment.

Acknowledgments

We would like to thank Blanca Delgado for technical assistance and Rodolfo Paredes for technical support with NS-TEM samples. The authors also thank José Luis Perez-García and Nadia Gutierrez for text editing. This study was partially supported by Consejo Nacional de Ciencia y Tecnología (CONACyT) (Grant 083673) and DGAPA/UNAM (Grant IN205711), both awarded to J.M-O. V.G.-G. receives a scholarship from CONACyT.

Appendix A. Supplementary data

Supplementary data associated with this article can be found, in the online version, at http://dx.doi.org/10.1016/j.bbrc.2013.03.067.

References

[1] A.L. Alonso, A. Zentella-Dehesa, J. Mas-Oliva, Characterization of a naturally occurring new version of the cholesterol ester transfer protein (CETP) from small intestine, Mol. Cell. Biochem. 245 (2003) 173–182.
[2] S. Wang, P. Kussie, L. Deng, A. Tall, Defective binding of neutral lipids by a carboxyl-terminal deletion mutant of cholesteryl ester transfer protein. Evidence for a carboxyl-terminal cholesteryl ester binding site essential for neutral lipid transfer activity, J. Biol. Chem. 270 (1995) 612–618.
[3] S. Wang, X. Wang, L. Deng, E. Rassart, R.W. Milne, A.R. Tall, Point mutagenesis of carboxyl-terminal amino acids of cholesteryl ester transfer protein. Opposite faces of an amphipathic helix important for cholesteryl ester transfer or for binding neutralizing antibody, J. Biol. Chem. 268 (1993) 1955–1959.
[4] V.M. Bolaños-García, M. Soriano-García, J. Mas-Oliva, Stability of the C-terminal peptide of CETP mediated through an (i, i + 4) array, Biochim. Biophys. Acta 1384 (1998) 7–15.
[5] V. García-González, J. Mas-Oliva, Amyloidogenic properties of a D/N mutated 12 amino acid fragment of the C-terminal domain of the cholesteryl-ester transfer protein (CETP), Int. J. Mol. Sci. 12 (2011) 2019–2035.
[6] A. Andreola, V. Bellotti, S. Giorgetti, P. Mangione, L. Obici, M. Stoppini, J. Torres, E. Monzani, G. Merlini, M. Sunde, Conformational switching and fibrillogenesis in the amyloidogenic fragment of apolipoprotein A-I, J. Biol. Chem. 278 (2003) 2444–2451.
[7] P. Mendoza-Espinosa, A. Moreno, R. Castillo, J. Mas-Oliva, Lipid dependant disorder-to-order conformational transitions in apolipoprotein CI derived peptides, Biochem. Biophys. Res. Commun. 365 (2008) 8–15.
[8] A.M. Sheikh, A. Nagai, Lysophosphatidylcholine modulates fibril formation of amyloid beta peptide, FEBS J. 278 (2011) 634–642.
[9] P. Mendoza-Espinosa, V. García-González, A. Moreno, R. Castillo, J. Mas-Oliva, Disorder-to-order conformational transitions in protein structure and its relationship to disease, Mol. Cell. Biochem. 330 (2009) 105–112.
[10] E. Evangelisti, C. Cecchi, R. Cascella, C. Sgromo, M. Becatti, C.M. Dobson, F. Chiti, M. Stefani, Membrane lipid composition and its physicochemical properties define cell vulnerability to aberrant protein oligomers, J. Cell Sci. 125 (2012) 2416–2427.
[11] V.G. García-González, J. Mas-Oliva, El Concepto de Enfermedad Asociado a la Conformación de Proteínas, first ed., Universidad Nacional Autónoma de México and El Manual Moderno, Mexico, 2012.
[12] T. Ookoshi, K. Hasegawa, Y. Ohhashi, H. Kimura, N. Takahashi, H. Yoshida, R. Miyazaki, Y. Goto, H. Naiki, Lysophospholipids induce the nucleation and extension of beta2-microglobulin-related amyloid fibrils at a neutral pH, Nephrol. Dial. Transplant. 23 (2008) 3247–3255.
[13] H. Pál-Gábor, L. Gombos, A. Micsonai, E. Kovács, E. Petrik, J. Kovács, L. Gráf, J. Fidy, H. Naiki, Y. Goto, K. Liliom, J. Kardos, Mechanism of lysophosphatidic acid-induced amyloid fibril formation of beta(2)-microglobulin in vitro under physiological conditions, Biochemistry 48 (2009) 5689–5699.
[14] K. Nakanaga, K. Hama, J. Aoki, Autotaxin an LPA producing enzyme with diverse functions, J. Biochem. 148 (2010) 13–24.
[15] S. Okudaira, H. Yukiura, J. Aoki, Biological roles of lysophosphatidic acid signaling through its production by autotaxin, Biochimie 92 (2010) 698–706.
[16] S. Yamamoto, K. Hasegawa, I. Yamaguchi, S. Tsutsumi, J. Kardos, Y. Goto, F. Gejyo, H. Naiki, Low concentrations of sodium dodecyl sulfate induce the extension of beta 2-microglobulin-related amyloid fibrils at a neutral pH, Biochemistry 43 (2004) 11075–11082.
[17] D. Chandler, Interfaces and the driving force of hydrophobic assembly, Nature 437 (2005) 640–647.
[18] V. García-González, N. Gutiérrez-Quintanar, P. Mendoza-Espinosa, P. Brocos, Á. Piñeiro, R. Castillo, J. Mas-Oliva, Key structural arrangements at the C-terminus domain of CETP promote a mechanism for lipid-transfer activity, unpublished results.
[19] M.R. Sawaya, S. Sambashivan, R. Nelson, M.I. Ivanova, S.A. Sievers, M.I. Apostol, M.J. Thompson, M. Balbirnie, J.J. Wiltzius, H.T. McFarlane, A.Ø. Madsen, C. Riekel, D. Eisenberg, Atomic structures of amyloid cross-beta spines reveal varied steric zippers, Nature 447 (2007) 453–457.
[20] S.A. Sievers, J. Karanicolas, H.W. Chang, A. Zhao, L. Jiang, O. Zirafi, J.T. Stevens, J. Münch, D. Baker, D. Eisenberg, Structure-based design of non-natural amino-acid inhibitors of amyloid fibril formation, Nature 475 (2011) 96–100.
[21] A.W. Fitzpatrick, T.P. Knowles, C.A. Waudby, M. Vendruscolo, C.M. Dobson, Inversion of the balance between hydrophobic and hydrogen bonding interactions in protein folding and aggregation, PLoS Comput. Biol. 7 (2011) e1002169.
[22] M.Ø. Jensen, O.G. Mouritsen, G.H. Peters, The hydrophobic effect: molecular dynamics simulations of water confined between extended hydrophobic and hydrophilic surfaces, J. Chem. Phys. 120 (2004) 9729–9744.

Int. J. Mol. Sci. **2011**, *12*, 2019-2035; doi:10.3390/ijms12032019

OPEN ACCESS

International Journal of
Molecular Sciences
ISSN 1422-0067
www.mdpi.com/journal/ijms

Article

Amyloidogenic Properties of a D/N Mutated 12 Amino Acid Fragment of the *C*-Terminal Domain of the Cholesteryl-Ester Transfer Protein (CETP)

Victor García-González and Jaime Mas-Oliva *

Institute of Cell Physiology, National Autonomus University of Mexico (UNAM), AP 70-243, 04510 Mexico, D.F., Mexico; E-Mail: vgarcia@emailifc.unam.mx

* Author to whom correspondence should be addressed; E-Mail: jmas@ifc.unam.mx; Tel.: +52-55-5622-5584; Fax: +52-55-5622-5611.

Received: 10 January 2011; in revised form: 2 March 2011 / Accepted: 14 March 2011 / Published: 21 March 2011

Abstract: The cholesteryl-ester transfer protein (CETP) facilitates the transfer of cholesterol esters and triglycerides between lipoproteins in plasma where the critical site for its function is situated in the *C*-terminal domain. Our group has previously shown that this domain presents conformational changes in a non-lipid environment when the mutation $D_{470}N$ is introduced. Using a series of peptides derived from this *C*-terminal domain, the present study shows that these changes favor the induction of a secondary β-structure as characterized by spectroscopic analysis and fluorescence techniques. From this type of secondary structure, the formation of peptide aggregates and fibrillar structures with amyloid characteristics induced cytotoxicity in microglial cells in culture. These supramolecular structures promote cell cytotoxicity through the formation of reactive oxygen species (ROS) and change the balance of a series of proteins that control the process of endocytosis, similar to that observed when β-amyloid fibrils are employed.Therefore, a fine balance between the highly dynamic secondary structure of the *C*-terminal domain of CETP, the net charge, and the physicochemical characteristics of the surrounding microenvironment define the type of secondary structure acquired. Changes in this balance might favor misfolding in this region, which would alter the lipid transfer capacity conducted by CETP, favoring its propensity to substitute its physiological function.

Keywords: cholesteryl-ester transfer protein (CETP); CETP *C*-terminal domain; α-helix and β-sheet secondary structures; peptide oligomers; amyloids

1. Introduction

To date, a significant number of diseases caused by the aggregation of misfolded proteins have been described. Of these, approximately 40 diseases present amyloid properties associated with the extracellular and intracellular deposition of peptides and proteins [1]. However, self-assembly into fibrillar structures is not a feature restricted to a small group of peptides and proteins with specific patterns in their amino acid sequence or three-dimensional structure, since in the past ten years several peptide sequences have been found not to be related to disease despite their ability to form amyloid structures. The adaptation of specific cellular processes coupled to the formation of amyloids has also been found; for instance, during the polymerization of melanin precursor molecules in melanocytes [2]. Therefore, nowadays the formation of amyloid structures has been considered a property that may be generic to many polypeptide chains and in many cases directly related to function [3].

For several years, our laboratory has been interested in the study of the relationship between structure and function of proteins involved in lipid binding and transport. Secondary to changes found in the secondary structure of specific regions of several of these proteins such as apolipoprotein C–I, we have proposed the possibility that these regions respond to specific changes in the microenvironment that surrounds them, and through specific disorder-to-order transitions these changes act as molecular switches that trigger function [4–6].

The cholesteryl-ester transfer protein (CETP) promotes the transfer of cholesterol esters and triglycerides between lipoproteins, mainly directing the cholesterol flow from high density lipoprotein (HDL) to low and very low density lipoproteins (LDL and VLDL). In this regard, extensive studies on genetic polymorphisms and CETP deficiencies suggest a direct relationship between its activity and cardiovascular disease [7]. Site specific mutagenesis studies have shown that the domain located in the *C*-terminus (E_{465}-S_{476}), structured as an amphipathic α-helix, corresponds to a key region in lipid transfer (Figure 1) [8–10]. During the structural characterization of this domain, we have found that disruption of the H_{466}-D_{470} salt bridge across the $D_{470}N$ mutation causes the loss of native structure, due in part to the change of the negatively charged carboxylate group of D for the amide group in N (Figure 1) [8].

Three-dimensional structure resolution has provided a solid basis for the proposal that CETP operates through a carrier mechanism of lipid transfer [11]. Nevertheless, studies from our laboratory suggest that the lipid transfer process can be also directly related to the formation of a lipid micellar system where conservation of the α-helical structure of this region is critical for the process [12]. Therefore, this work focused on the 12 residues of the *C*-terminal domain of CETP, and the structure and function of two peptides derived from this site, the native sequence named helix-*X* and a peptide with the mutation $D_{470}N$ appointed helix-*Z* (Figure 1), were characterized. Employing helix-*Z* as an example of hydrogen bonding disturbance has allowed us to demonstrate a conformational change of this region from an α-helix to a β-sheet. Ongoing experiments employing CETPI, an isoform of CETP

that lacks the normal C-terminal domain and instead presents a new carboxy-end mainly structured as a β-sheet [13], supports the fact that small order-to-disorder and/or disorder-to-order transitions supported by changes in hydrogen bonding might give proteins an entirely new physiological function [14]. Secondary to the formation of β-sheet structures, helix-*Z*—the D/N mutated 12 amino acid (aa) fragment of the C-terminal domain of CETP—shows the consequent formation of oligomers and amyloid-like fibril structures that in turn cause cytotoxic effects similar to those exercised by the β-amyloid peptide.

2. Results

2.1. Conformational Changes in the C*-Terminal Domain of CETP*

Although previous studies performed by our group have demonstrated the key role of the *C*-terminal domain of CETP during the process of lipid transfer when holding an α-helix conformation (residues E_{465}-S_{476}) [8,13], it has not been determined yet whether this domain presents the ability to undergo conformational changes. Therefore, in order to investigate if this domain might undergo conformational changes by modifying the physicochemical properties of the surrounding media, two peptides were synthesized: the native *C*-terminal peptide called helix-*X*, and a second one containing the mutation $D_{470}N$ and named helix-*Z* (Figure 1).

Figure 1. Structural representation of the *C*-terminal region of cholesteryl-ester transfer protein (CETP), showing the sequences of helix-*X* and helix-*Z*. The H_{466}-D_{470} salt bridge and the hydrophobic cluster are shown. The structure was obtained from the Protein Data Bank, access code: 2obd.

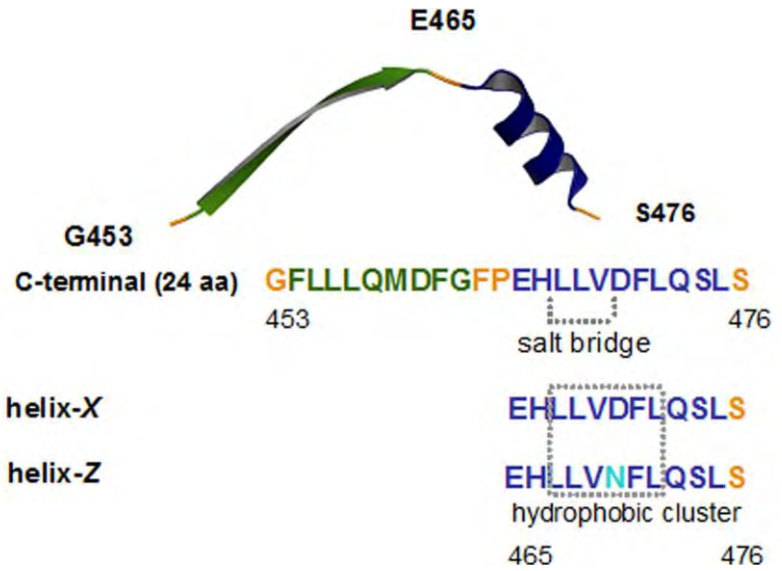

Helix-*X* and helix-*Z* were incubated in water in a pH range of 3.8–9.5 and studied by circular dichroism (CD) spectroscopy, in parallel. The secondary structure of helix-*X* was consistent with the presence of a disordered state over the whole range of pH values tested (Figure 2A). In contrast, CD spectra of helix-*Z* showed a pH specific response with minimum shift signals from 219 nm to 201 nm, which is associated with an increase in ellipticity indicative of the formation of β-type

secondary structures (Figure 2B). This spectrum was only found in a pH range of 7–8, reaching the highest value at pH 7.2 (Figure 2B insert).

Moreover, through the use of thioflavin-T (ThT) fluorescence assays, an increase in the emission spectrum of helix-*Z* with a maximum signal near 482 nm was observed (Figure 2C). Also, by testing with a Congo red-shift assay, the characteristic birefringence change observed in the presence of β-structures with a maximum signal close to 540 nm was determined (Figure 2D). Therefore, these assays confirm the possibility that under specific conditions the *C*-terminal domain of CETP can acquire a secondary structure consistent with the formation of a β-structure.

Figure 2. Circular dichroism (CD) spectra of helix-*X* (**A**) and helix-*Z* (**B**) in a pH range of 3.8–9.5. Inset in (**B**) shows ellipticity values at 219 nm; (**C**) Fluorescence assay coupled to ThT, showing a characteristic peak at 482 nm; (**D**) Birefringence changes of Congo red (Δ absorbance) at different incubation times. The peptide concentration used in all CD assays was 200 μg/mL, for ThT assays was 50 μg/mL, and for Congo red assays 180 μg/mL.

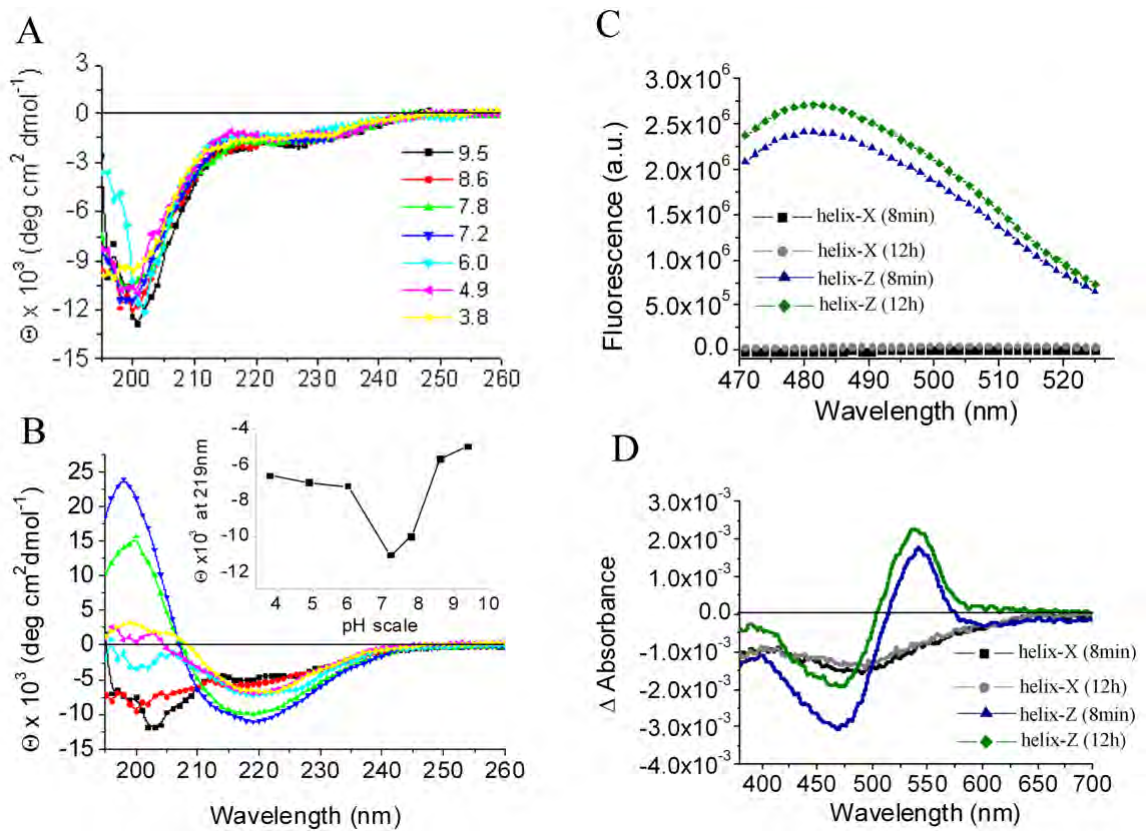

During the evaluation of the stability of helix-*Z* through temperature-induced unfolding CD assays (4–90 °C), only temperatures close to 65 ℃ were found to induce significant loss in its β-type secondary structure, suggesting high stability. The presence of an isodichroic point near 211 nm in the obtained spectra is associated with the presence of only two conformational states (Figure 3). These experiments, together with the fact that helix-*Z* keeps its characteristic CD profile consistent with a β-strand under a range of high ionic strength solutions (up to 2.4 M NaCl, data not shown), show that the acquired β-structure is not determined by long-range electrostatic interactions, but rather by stronger inter- and intra-chain interactions such as hydrogen bonds.

Figure 3. Temperature-induced unfolding of helix-*Z*. CD spectra were obtained from 4 to 90 °C. Inset shows ellipticity values at 219 nm (β-structure signal). The concentration of helix-*Z* employed was 200 μg/mL.

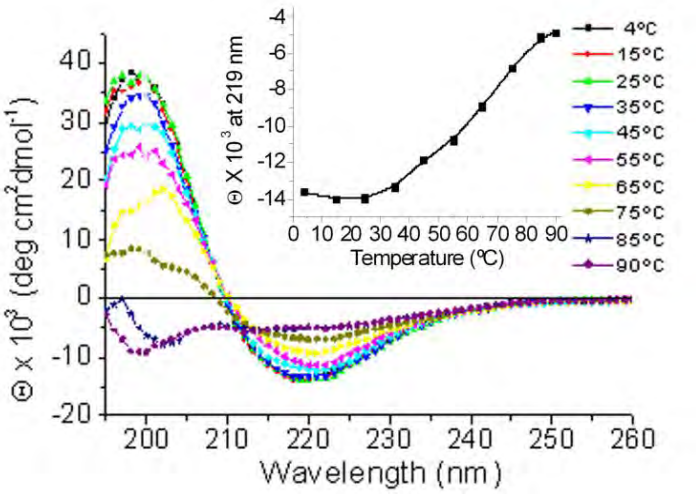

Another set of experiments, where both helix-*X* and helix-*Z* were incubated in a hydrophobic environment composed of sodium dodecyl sulfate (SDS) micelles, shows that both peptides acquire and maintain an α-helical conformation (Figure 4A,B). This transition was monitored in parallel following fluorescence coupled to ThT (Figure 4C) and the change in absorbance of peptide bonds at 205 nm (Figure 4D). Our results suggest that the interaction within a hydrophilic/hydrophobic interface may be the key parameter to maintain both peptides in an α-helix conformation; more importantly, in the case of helix-*Z*, this is a key feature to avoid the formation of a β-structure.

2.2. $D_{470}N$ Mutation in the C*-Terminal Domain of CETP Induces Amyloid Fibril Formation*

In order to extend our structural analysis and considering that an increase in β-signal is not a direct indication of the formation of amyloid fibrils, peptide samples were analyzed by transmission electron microscopy (TEM). Throughout the pH-range evaluated (4–9), helix-*X* samples did not form any kind of structured material, which correlates well with previous results in which helix-*X* remains in a non-ordered state (Figure 5A). In contrast, when helix-*Z* samples were analyzed, even from the first sample without incubation (time 0), small oligomers were clearly identified (Figure 5B,C). It was only after 1 h of incubation that protofilament formation was observed (Figure 5D).

Incubation of helix-*Z* for 6 h with stirring (200 rpm) was the condition that identified a mixture of oligomeric structures, protofilaments, and mature fibrils in some areas (Figure 5E). Samples analyzed after an incubation time of 72 and 120 h at 37 °C clearly showed mature fibrils with high morphological similarities to β-amyloid samples (Figure 5F,G). At this stage, it is interesting to mention that although the formation of fibrils from pH 4–9 was evaluated, aggregates and fibril formation were only observed at pH 7–8, which correlates well with the presence of β-structures at this pH range when monitored by spectrophotometric techniques.

Figure 4. The effect of SDS on the secondary structure of peptides monitored by CD. (**A**) helix-*X*; (**B**) Helix-*Z*; (**C**) ThT fluorescence at 482 nm; (**D**) Absorbance at 205 nm. The peptide concentration used in all CD assays was 200 μg/mL. For ThT assays was 50 μg/mL and for absorbance assays 180 μg/mL.

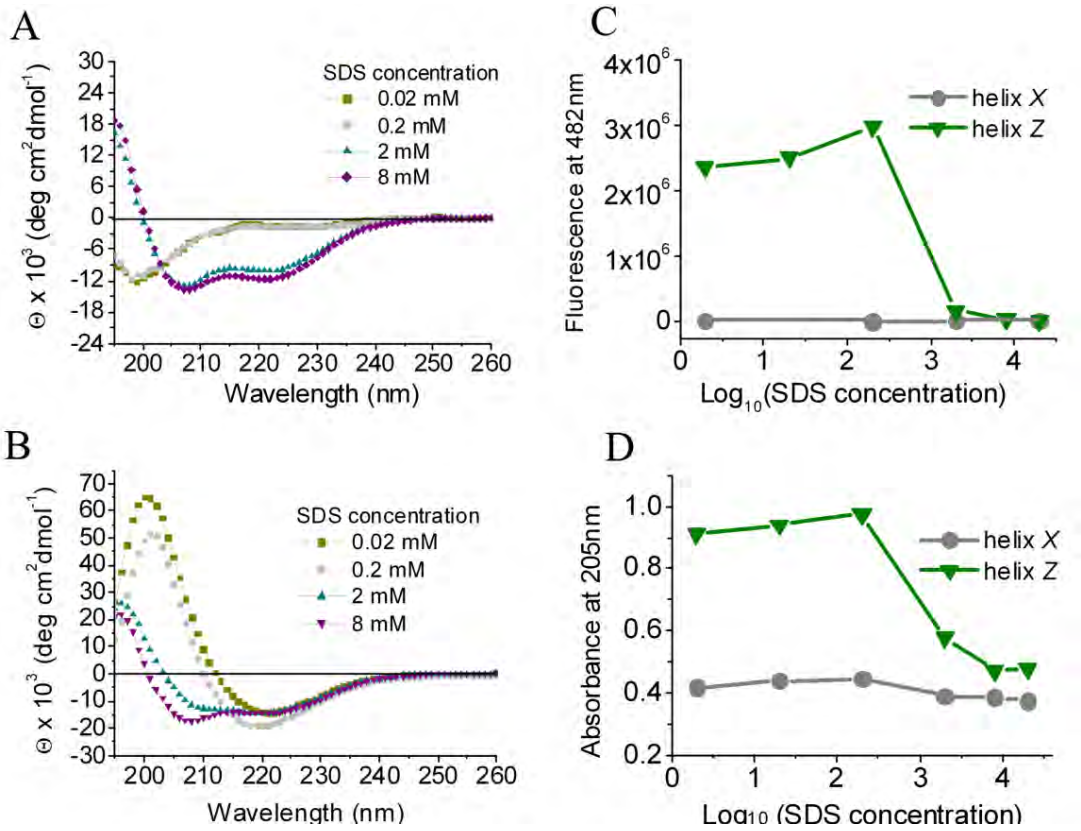

2.3. Cytotoxic Effects Associated with Helix-Z

Taking into account previous studies from several laboratories where microglia and macrophages were employed in the characterization of the cytotoxic effects of the β-amyloid peptide [15–17], when microglial cells were exposed to a gradual increase in concentrations of both peptides, only helix-*Z* was able to significantly reduce cell viability as measured by the 3-(4,5-dimethylthiazol-2-yl)-2,5-diphenyltetrazolium bromide (MTT) reduction assay (Figure 6). It is interesting to observe that independently of the incubation time used for both peptides in solution (0, 6, 120 h) the lowest concentration employed for helix-*Z* (1.7 μM) shows an important reduction in cell viability that is maintained up to 56 μM (Figure 6A–C). At this stage it is important to mention that 0 time actually corresponds to the time employed to place both peptides, first in solution and second into the cell culture plate. This procedure takes approximately 15 min, enough time to apparently produce peptide oligomers as shown in Figure 5B–C. Because cell viability is maintained close to 50% independently of the concentration of helix-*Z* or the time of the incubation needed for the formation of amyloid structures, our experiments indicate that helix-*Z* in the form of oligomers seem to be the highest toxic form for this peptide. Whether or not mature fibrils are also responsible for cell toxicity after the incubation of helix-*Z* for 120 h, will have to be elucidated in experiments where under these conditions

the presence of small amounts of oligomers can be ruled out. At this stage it is interesting to mention that while helix-*Z* oligomers formed at pH 7.2 are cytotoxic, amorphous aggregates of the β-amyloid peptide obtained at the same pH do not present the ability to damage microglial cells in culture (Figure 1 supplementary data). Changes found in cell morphology are possibly related to the presence of a cellular stress condition as described by our group when studying the β-amyloid peptide [17] (Figure 6D). It is noteworthy that the MTT assay is also an indicator of oxidative stress and changes in the vesicular trafficking of cells [18,19].

Figure 5. Ultrastructural analysis of peptides by transmission electron microscopy (TEM); (**A**) Helix-*X* at 48 h of incubation at 37°C; (**B**) Helix-*Z* at 0 h of incubation; (**C**) Helix-*Z* at 0.5 h of incubation; (**D**) Formation of helix-*Z* protofilaments at 1.0 h of incubation; (**E**) Helix-*Z* under constant agitation at 6.0 h of incubation; (**F**) Helix-*Z* under constant agitation and 48 h of incubation; (**G**) Helix-*Z* under constant agitation at 120 h of incubation. Solid arrows indicate oligomeric structures, open arrows show protofibrils and amyloid fibrils. The concentration of peptide used in all conditions was 60 μg/mL. Bar indicates 200 nm.

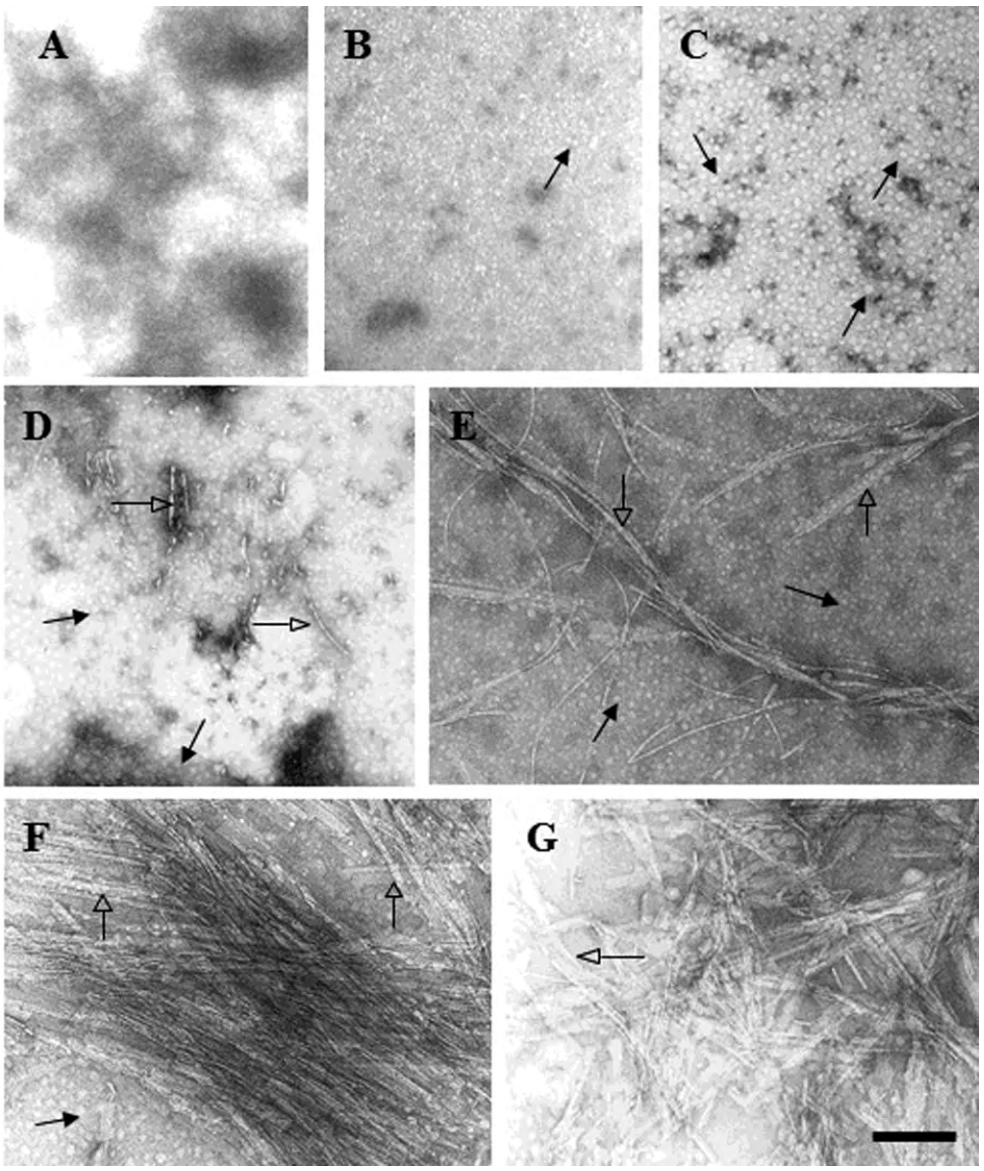

Figure 6. Cytotoxic effects in microglia associated with the exposure of helix-*X* and helix-*Z*. (**A**) Cell viability determined by MTT for cells treated with peptide previously incubated 0.5 h at 37 °C; (**B**) Cells treated with peptide previously incubated 6 h at 37 ℃ ; (**C**) Cells treated with peptide previously incubated 120 h at 37 °C; (**D**) Light microscopy showing microglia treated with both peptides (56 μM) previously incubated 120 h at 37 ℃ .

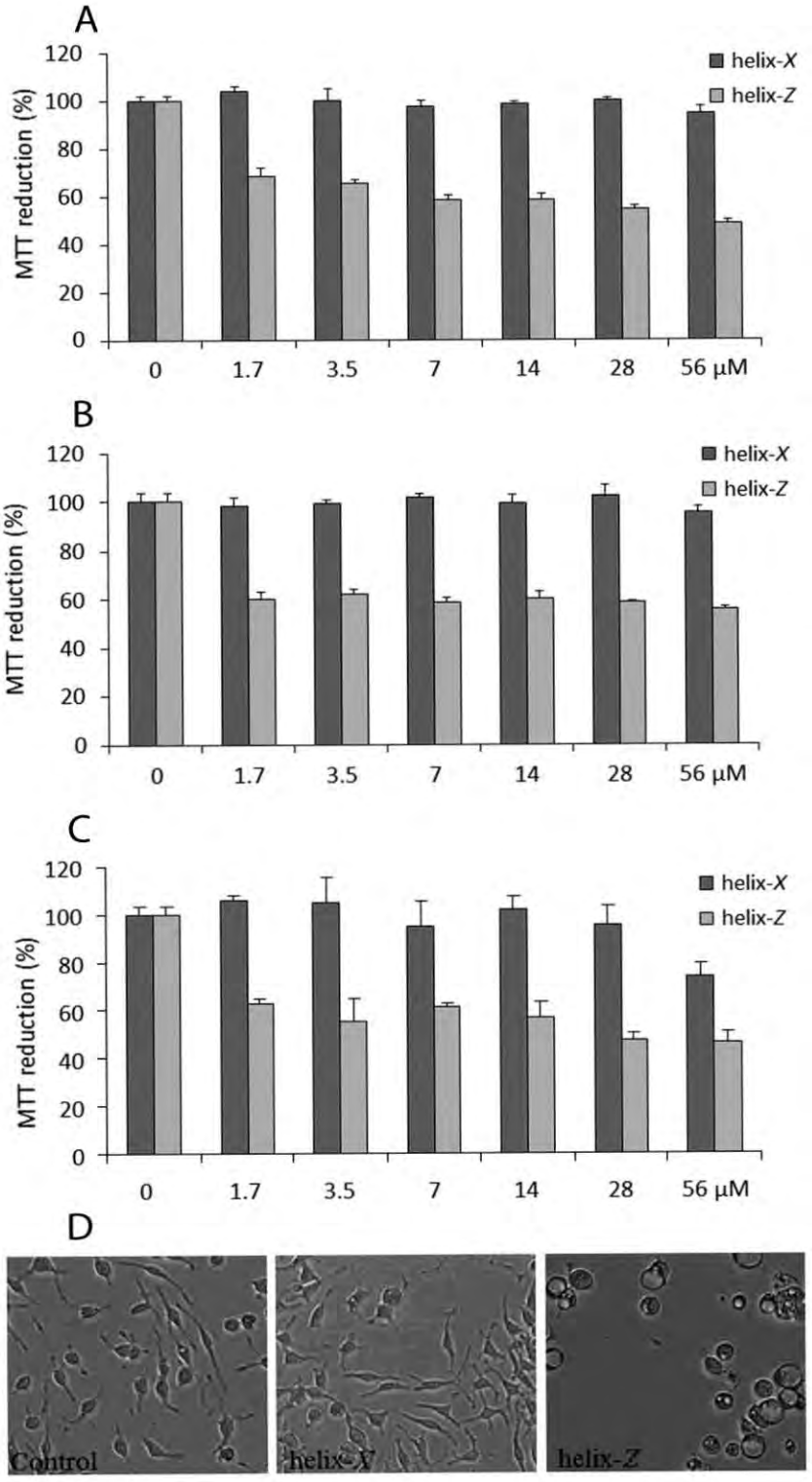

2.4. Endocytic Protein Expression

After an incubation period of 120 h at 37 ℃ (condition at which mature fibrils are obtained with helix-*Z*) microglial cells were treated for 20 h with increasing concentrations of peptides. The experiment was focused on assessing the expression levels of proteins such as β-adaptin, eps 15, and clathrin assembly lymphoid myeloid leukemia (CALM). Cells exposed to helix-*Z* showed differential expression of some of these endocytic proteins, in contrast to experiments performed with helix-*X* in which no changes were found. While the expression of proteins such as eps 15 was held constant, β-adaptin protein expression decreased with respect to exposure to increasing concentrations of helix-*Z* (Figure 7A). In contrast, CALM protein expression increased with respect to the concentration of helix-*Z* (Figure 7B). These results, as shown previously by us, correlate well with the β-amyloid peptide ($A\beta_{25-35}$) experiments that were employed under the same conditions as used here with helix-*Z* (Figure 1 supplementary data).

Figure 7. Endocytic protein expression in microglial cells treated with helix-*X* and helix-*Z*. Both peptides were previously incubated 120 h at 37 °C. (**A**) Western blot analysis of eps 15 and β–adaptin; (**B**) Western blot analysis of clathrin assembly lymphoid myeloid leukemia (CALM) protein. β-actin was used as loading control.

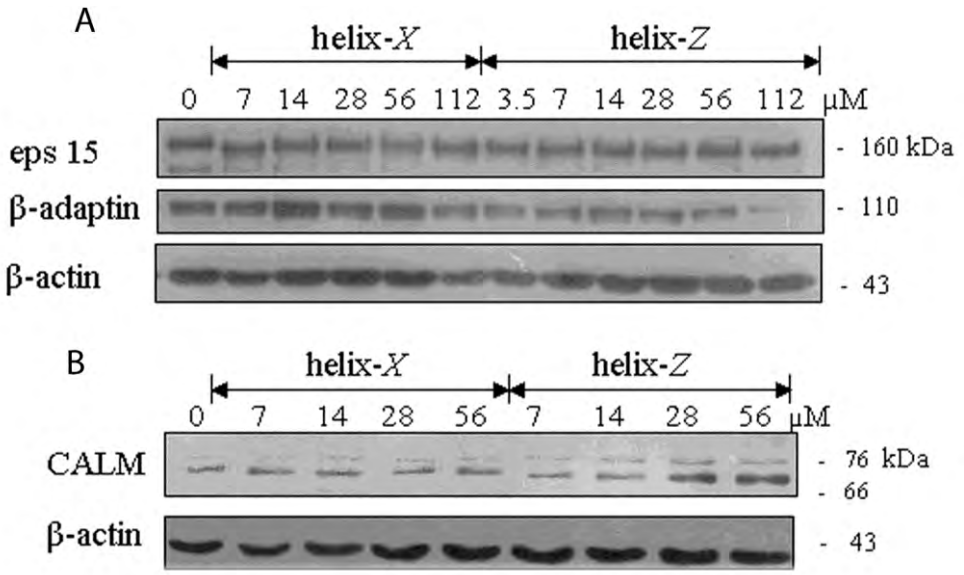

3. Discussion

During the search for factors that might explain the formation of a β-structure in helix-*Z*, we propose that this structural feature is not determined by parameters such as the hydrophobic moment (μH) or the mean hydrophobicity, since differences in values with respect to helix-*X* are minimal (Table 1). However, we found that helix-*Z* presents a β-sheet structure, only when it presents a net charge close to −1 in the pH range of 7–8. In contrast, helix-*X* with a net charge closer to −2 remains in a non-structured state (Table 2).

Table 1. Physicochemical parameters of peptides.

Parameter	helix-*X*	helix-*Z*	$A\beta_{1-42}$	$A\beta_{25-35}$
MW (Da)	1399.8	1399.6	4514	1060.3
Isoelectric point	4.17	5.13	5.21	8.75
Hydrophobicity (kcal/mol)	0.27	0.28	0.21	0.37
μH (kcal/mol)	0.41	0.41	0.08	0.03

Table 2. Net charge distribution of peptides as a function of pH.

pH	helix-*X*	helix-*Z*	$A\beta_{1-42}$	$A\beta_{25-35}$
4	0.07	0.65	3.17	1.02
4.5	−0.47	0.34	1.55	1.01
5	−0.87	0.06	0.38	1.00
5.5	−1.16	−0.18	−0.49	1.00
6	−1.47	−0.48	−1.42	0.99
6.5	−1.75	−0.75	−2.25	0.99
7	−1.91	−0.91	−2.72	0.99
7.5	−1.97	−0.97	−2.92	0.99
8	−2.00	−1.01	−3.01	0.97
8.5	−2.06	−1.06	−3.1	0.93
9	−2.16	−1.17	−3.32	0.79
9.5	−2.39	−1.39	−3.81	0.52

In this sense, there are reports that show a higher propensity to form β-structures when a low net charge and a high hydrophobicity are present in the peptide sequence, conditions that promote amyloid fibril formation [20–22]. Considering these factors, Lopez de la Paz *et al.* [23] have reported that peptide sequences are capable of forming fibrils only when they present a net charge of +1 or −1 and distances between charges are maximized, allowing fibrillogenesis in an orderly form as observed with region 25–35 of the β-amyloid peptide (Table 2). This phenomenon has been proposed as a key feature in molecular evolution preventing the occurrence of misfolding phenomena [24]. Also, there is strong evidence that intrinsically disordered proteins maintain a high net charge as a strategy to prevent aggregation [25]. Therefore, net charge may be the factor that triggers the orderly fibril formation shown by helix-*Z*. It is considered to be a two-stage process with a lag period related to the formation of aggregates and nucleation centers and a second stage related to fast spreading [26].

Taking into account the spectrophotometric results, the evidence of fibrillar structures and the physicochemical properties of helix-*Z* such as μH, hydrophobicity, and a net charge of −0.96 at pH 7.2, we present a model for the amino acid residue disposition within the β-strand (Figure 8A). Since $D_{470}N$ showed the loss of one negative charge, the hydrophobic cluster ($L_{467}LVNFL_{472}$) maintained a β-conformation through hydrophobic interactions. It is also important to consider that along the sequence, there are asparagine and glutamine residues that are considered as inducers of β-structures and therefore allow the stacking of polypeptide chains [27]. Helix-*X* does not show this phenomenon, largely due to an electrostatic repulsion at Asp-470 that prevents the formation of a hydrophobic cluster that maintains the peptide under an extended state (Figure 8B).

Figure 8. Model of an antiparallel β-strand in helix-*Z*. (**A**) The charge of each residue is determined considering a pH of 7.2. *N* and *C* terminal groups are loaded allowing an electrostatic attraction between peptide chains. Shaded regions identify the hydrophobic cluster $L_{467}LVNFL_{472}$, as well as N and Q residues; (**B**) Helix-*X* does not form a β-strand structure due to the electrostatic repulsion between D residues.

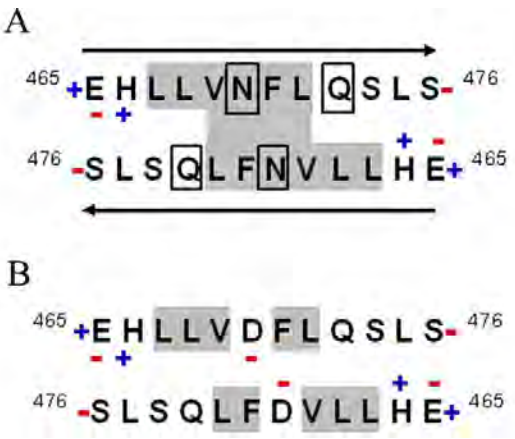

On the other hand, it is surprising that helix-*X* is maintained as an α-helix in the crystallographic data shown for CETP due to its μH value of 0.41 kcal/mol, factor B value, and relative freedom from the main body of the protein. In this regard, peptide sequences showing the potential for intrinsic disorder and domains with high factor-B values are associated with a high thermal vibration of individual atoms and therefore present high intramolecular flexibility [28]. Although helix-*X* presents an α-helix profile in the crystal structure of CETP, when held outside a lipid environment it might adopt a disordered structure with the possibility that this region might undergo disorder-to-order and/or order-to-disorder transitions. This type of transition must probably present a different equilibrium when changes like the one found in helix-*Z* is introduced to this region since the formation of a β-sheet might not be reversible.

Oil-water interfaces also present the ability to promote the stabilization of the secondary structure of peptides believed to the due to hydrogen bonding and a reduction of the energetic cost of partitioning [29]. As previously suggested for the bee venom peptide mellitin, this peptide is largely unstructured when placed in solution, but highly structured as an amphipathic α-helix when partitioned into unilamellar phospholipid vesicles [30]. While the free energy reduction per residue observed for the folding of mellitin in a membrane interface is almost 0.4 kcal mol^{-1} consistent with the formation of hydrogen bonding, values close to 0.6 kcal mol^{-1} have been also shown for β-sheet forming peptides [30].

Studies performed by our group using β-amyloid fibrils as a natural ligand for the scavenger receptor (SR), an association directly related to the development of oxidative stress, have shown changes in the expression of several adaptor proteins involved in the endocytic machinery of macrophages and microglia [17,31]. Proteins α-, β-, μ-, and σ-adaptins integrate into the AP2 adaptor complex, a key component in the initial stages of endocytosis [5]. Within the mechanism of clathrin-mediated endocytosis of the SR, more than 30 proteins have been described, many of which are adaptor molecules involved in the formation of coated pits. In addition to clathrin, proteins such as CALM, epsin, dynamin, amphiphysin, and eps 15 also play an important role in this process [32].

The present results show that when microglial cells are exposed to helix-*Z*, peptide oligomers first and fibrillar species next, are the leading cause for the registered cytotoxic phenomena. Moreover, high concentrations of helix-*Z* fibrils inhibit β-adaptin expression. With the decline of β-adaptin, the increased expression observed for CALM could function as a cellular compensatory mechanism for endocytic function. In this sense, the ANTH domain (AP180 N-Terminal Homology) located in the first 300 residues of CALM allows interaction with PtdIns(4,5)P_2 [33], functioning as a bridge between the plasma membrane clathrin-coated pit and other adaptor proteins [34]. Taking into account that a similar response in β-adaptin and CALM was found in this study when cells were exposed to helix-*Z* fibrils, possibly this condition may be associated with a phenomenon found in cells that come in contact with toxic peptide oligomers and/or amyloid fibrils.

4. Experimental Section

4.1. Materials

All cell culture reagents were purchased from Gibco-Invitrogen (Carlsbard, CA, USA), while tissue culture dishes and other plasticware were obtained from Nulgene Nunc (Rochester, NY, USA). Salts and buffers were purchased from Baker. Tert-butyl hydroperoxide (TBH), ThT, Congo-red, SDS and MTT were obtained from Sigma (St. Louis, MO, USA). Antibodies used in CALM, β-adaptin, and eps 15 protein detection as well as goat secondary antibodies were from Santa Cruz Biotechnoloy Inc.

4.2. Peptide Synthesis and Preparation

Based on the function of the *C*-terminal of CETP, two peptides were synthesized: one named helix-*X* that corresponds to the native peptide, and the second one named helix-*Z* containing the mutation $D_{470}N$. Lyophilized peptides were dissolved in ammonium carbonate buffer (pH 9.5) to a concentration of 1 mg/mL. From this solution a further 1:5 dilution was carried out. To evaluate the structure at pH 3.8 and 4.8, a sodium acetate buffer was used; pH 6.3 and 7.2, a sodium phosphate buffer was used, and at pH 8.6 and 9.5, an ammonium carbonate buffer was employed.

Fragment $A\beta_{25–35}$ (β-amyloid) was employed as a reference molecule for the cytotoxicity assays. Experiments performed with β-amyloid were carried out at two pH conditions using a phosphate buffer (pH 7.2) and ultrapure water (pH 5.5), both with the same peptide concentration (1.5 mg/mL). All buffers were used at 50 mM, and solutions were filtered through 0.22 μm membrane filters before use.

Purity of peptides was greater than 98% (GenScript Corp., Piscataway, NJ, USA). Their identity and purity were confirmed by mass spectrometry and HPLC analysis (data not shown). Protein concentration was determined by peptide bond absorption at 205 nm.

4.3. Circular Dichroism Spectroscopy

Far-UV CD spectra were recorded on an Aviv 62DS spectropolarimeter in a 0.1 cm quartz cell, using an average time of 2.5 s and a step size of 0.5 nm. CD results are reported as mean molar ellipticity (Θ, deg cm^2 $dmol^{-1}$) considering the baseline correction. For the pH studies, CD spectra were obtained from pH 3.8 to −9.5. Peptide unfolding induced by temperature was monitored by CD measurements over a temperature range of 4 to 90 °C.

4.4. Congo Red Spectroscopy and Thioflavin T Fluorescence

Congo red assays were performed based in the protocol designed by Klunk *et al.* [35]. Employing 10.6 μM Congo red and 180 μg/mL of peptide, the absorbance was measured every 2 nm using a Perkin Elmer UV/Vis Lambda 2*S* spectrophotometer scanning from 360 to −700 nm. Peptide spectra were corrected by subtracting the corresponding buffer spectra obtained under identical conditions. Additionally, the presence of β-structures was characterized with the ThT assay. ThT fluorescence emission spectra were registered at 37 °C from 470 to 530 nm with an excitation wavelength of 450 nm. A scan velocity of 73 nm/min using an Olis DM45 spectrofluorimeter was used. The concentrations of ThT and peptides were 10 μM and 36 μM , respectively.

4.5. Cell Culture

EOC cells (mouse microglia, American Type Culture Collection) were grown in Dulbecco's modified Eagle's medium (DMEM) supplemented with 10% fetal bovine serum, and 20% mouse bone marrow, producing colony stimulating factor-1 (LADMAC) conditioned media. Penicillin (50 U/mL) and streptomycin (50 μg/mL) were added to the media. After the initial culture, all experiments were performed using Opti-MEM medium without phenol red and reduced fetal serum.

4.6. Cell Viability Assay

Peptide cytotoxicity was assessed by MTT reduction assays in EOC cells exposed to helix-*X*, helix-*Z*, and the β-amyloid peptide ($A\beta_{25-35}$). Cells were seeded into 96-well plates at a density of 1×10^4 cells/well and allowed to grow to 80% confluence. Next, culture medium was replaced with Opti-MEM medium. After 2 h under this condition, cells were treated with a series of gradually increasing peptide concentrations for 20 h. After this time, 30 μL of an MTT stock solution in Opti-MEM medium was added to the cultures in order to obtain a final concentration of 0.5 mg/mL. Formazan crystals that formed after 4 h of incubation were further dissolved by the addition of cell lysis buffer (20% SDS, 50% *N*,*N*-dimethylformamide, pH 3.7). After 12 h of incubation, absorbance was measured at 570 nm using a microplate reader.

4.7. Western Blot Analysis

With a plate confluence of 80%, cells were treated for 20 h with different doses of peptides. After this procedure, cells were washed with PBS and lysed for 45 min at 4 °C in lysis buffer. Lysed cells were centrifuged at 5000 rpm for 5 min and the supernatant was recovered. Protein concentration was determined with the BCA protein assay (Pierce, Rockford IL, USA) and samples (14 μg/lane) from the total protein fraction were analyzed by SDS-PAGE on 8% gels and further transferred to PVDF membranes (Millipore, Billerica, MA, USA). Membranes were blocked overnight at 4 °C in a solution containing Tris-buffered saline (TBS), 1% tween-20, and 5% non-fat milk. For protein detection, the following primary polyclonal antibodies were used: goat anti-β-adaptin (1:600), CALM (1:600), and rabbit anti-eps 15 (1:2500). In addition, the mouse monoclonal anti β-actin (1:500) was used. The blocked membranes were incubated with the primary antibodies for 1 h a 37 °C. After washing, horseradish peroxidase (HRP) conjugated secondary antibodies (1:5000) were added to the membrane

and were incubated for 1h at 37 ℃ in blocking buffer. The secondary antibodies used were: donkey anti-goat IgG for β-adaptin and CALM, goat anti-rabbit IgG for eps 15, and goat anti-mouse for β-actin. Later, membranes were washed with TBS/1% tween and HRP activity was detected with the Immobilon Western kit (Millipore).

4.8. Optical Microscopy

Under the different exposures using variable concentrations of helix-*X*, helix-*Z*, and the β-amyloid peptide ($A\beta_{25-35}$), EOC cells were visualized and images were taken with an Olympus IX71 microscope (100 and 400×).

4.9. Electron Microscopy

Peptide samples incubated under the different conditions tested were processed using a negative staining technique and visualized using TEM. Samples (10 μL) stained with uranyl acetate solution (2% w/v) were placed on carbon-coated copper grids (400 mesh); and after incubation for 5 min at 25 °C they were dried for 10 min. TEM images were acquired using a JEM-1200EX11 JEOL microscope (70 kV).

5. Conclusions

Since the mutation $D_{470}N$ in the *C*-terminal domain of CETP exemplifies the delicate balance that exists in the conformational changes at the secondary structure level modulated by pH and amino acid-charge modification, disruption of this dynamic equilibrium could lead to the formation of new interactions like hydrogen bonds within the hydrocarbon backbone and between side chains, which promote aggregation and the formation of fibril structures [36]. Although the $D_{470}N$ mutation (helix-*Z*) described in this investigation has not been found in nature, helix-*X*, the natural 12 aa segment of the *C*-terminal domain of CETP, when partitioned into water or into oil-water interfaces might present potential disorder-to-order and/or order-to-disorder transitions that normally are difficult to identify. Therefore, we have used helix-*Z* in order to mimic potential changes in secondary structure of helix-*X* by simply modifying hydrogen bonding that in turn might explain changes in the overall function of native CETP when studied *in vivo*.

Acknowledgements

We thank Blanca Delgado for excellent technical assistance, Rodolfo Paredes for technical support with TEM samples and Kristina Hansen for text editing. This work was supported by grants from the National Council for Science and Technology, Mexico (CONACyT 083673) and DGAPA at the National Autonomous University of Mexico (IN228607).

References

1. Uversky, V.N.; Oldfield, C.J.; Midic, U.; Xie, H.; Xue, B.; Vucetic, S.; Iakoucheva, L.M.; Obradovic, Z.; Dunker, A.K. Unfoldomics of human diseases: linking protein intrinsic disorder with diseases. *BMC Genomics* **2009**, *10*, S7.

2. Berson, J.F.; Theos, A.C.; Harper, D.C.; Tenza, D.; Raposo, G.; Marks, M.S. Proprotein convertase cleavage liberates a fibrillogenic fragment of a resident glycoprotein to initiate melanosome biogenesis. *J. Cell. Biol.* **2003**, *161*, 521–533.
3. Dobson, C.M. Protein folding and misfolding. *Nature* **2003**, *426*, 884–890.
4. Xicohtencatl-Cortes, J.; Castillo, R.; Mas-Oliva, J. In search of new structural states of exchangeable apolipoproteins. *Biochem. Biophys. Res. Commun.* **2004**, *324*, 467–470.
5. Ramos, S.; Campos-Terán, J.; Mas-Oliva, J.; Nylander, T.; Castillo, R. Forces between hydrophilic surfaces adsorbed with apolipoprotein AII alpha helices. *Langmuir* **2008**, *24*, 8568–8575.
6. Mendoza-Espinosa, P.; Moreno, A.; Castillo, R.; Mas-Oliva, J. Lipid dependant disorder-to-order conformational transitions in apolipoprotein CI derived peptides. *Biochem. Biophys. Res. Commun.* **2008**, *365*, 8–15.
7. Klerkx, A.H.; El Harchaoui, K.; van der Steeg, W.A.; Boekholdt, S.M.; Stroes, E.S.; Kastelein, J.J.; Kuivenhoven, J.A. Cholesteryl ester transfer protein (CETP) inhibition beyond raising high-density lipoprotein cholesterol levels: pathways by which modulation of CETP activity may alter atherogenesis. *Arterioscler. Thromb. Vasc. Biol.* **2006**, *26*, 706–715.
8. Bolaños-García, V.M.; Soriano-García, M.; Mas-Oliva, J. Stability of the C-terminal peptide of CETP mediated through an (i, i + 4) array. *Biochim. Biophys. Acta* **1998**, *1384*, 7–15.
9. Wang, S.; Wang, X.; Deng, L.; Rassart, E.; Milne, R.S.; Tall, A.R. Point mutagenesis of carboxyl-terminal amino acids of cholesteryl ester transfer protein. *J. Biol. Chem.* **1993**, *66*, 1955–1959.
10. Wang, S.; Kussie, P.; Deng, L.; Tall, A. Defective binding of neutral lipids by a carboxyl-terminal deletion mutant of cholesteryl ester transfer protein. Evidence for a carboxyl-terminal cholesteryl ester binding site essential for neutral lipid transfer activity. *J. Biol. Chem.* **1995**, *270*, 612–618.
11. Qiu, X.; Mistry, A.; Ammirati, M.J.; Chrunyk, B.A.; Clark, R.W.; Cong, Y.; Culp, J.S.; Danley, D.E.; Freeman, T.B.; Geoghegan, K.F.; Griffor, M.C.; Hawrylik, S.J.; Hayward, C.M.; Hensley, P.; Hoth, L.R.; Karam, G.A.; Lira, M.E.; Lloyd, D.B.; McGrath, K.M.; Stutzman-Engwall, K.J.; Subashi, A.K.; Subashi, T.A.; Thompson, J.F.; Wang, I.K.; Zhao, H.; Seddon, A.P. Crystal structure of cholesteryl ester transfer protein reveals a long tunnel and four bound lipid molecules. *Nat. Struct. Mol. Biol.* **2007**, *14*, 106–113.
12. García-González, V.; Mas-Oliva, J. Structural Arrangement that Supports Lipid Transfer in the cholesteryl-ester transfer protein (CETP). USA-México Workshop in Biological Chemistry: Multidisciplinary Approaches to Protein Folding, Mexico City, Mexico, 25–27 March 2009.
13. Alonso, A.L.; Zentella-Dehesa, A.; Mas-Oliva, J. Characterization of a naturally occurring new version of the cholesterol ester transfer protein (CETP) from small intestine. *Mol. Cell. Biochem.* **2003**, *245*, 173–182.
14. Mendoza-Espinosa, P.; García-González, V.; Moreno, A.; Castillo, R.; Mas-Oliva, J. Disorder-to-order conformational transitions in protein structure and its relationship to disease. *Mol. Cell. Biochem.* **2009**, *330*, 105–120.
15. El Khoury, J.; Luster, A.D. Mechanisms of microglia accumulation in Alzheimer's disease: therapeutic implications. *Trends. Pharmacol. Sci.* **2008**, *29*, 626–632.
16. Hickman, S.E.; Allison, E.K.; El Khoury, J. Microglial dysfunction and defective beta-amyloid clearance pathways in aging Alzheimer's disease mice. *J. Neurosci.* **2008**, *28*, 8354–8360.

17. Manzano-León, N.; Delgado-Coello, N.B.; Guaderrama-Díaz, M.; Mas-Oliva, J. Beta-adaptin: Key molecule for microglial scavenger receptor function under oxidative stress. *Biochem. Biophys. Res. Commun.* **2006**, *351*, 588–594.
18. Abe, K.; Saito, H. Both oxidative stress-dependent and independent effects of amyloid beta protein are detected by 3-(4,5-dimethylthiazol-2-yl)-2,5-diphenyltetrazolium bromide (MTT) reduction assay. *Brain Res.* **1999**, *830*, 146–154.
19. Liu, Y.; Peterson, D.A.; Schubert, D. Amyloid beta peptide alters intracellular vesicle trafficking and cholesterol homeostasis. *Proc. Natl. Acad. Sci. USA* **1998**, *95*, 13266–13271.
20. Broome, B.M.; Hecht, M.H. Nature disfavors sequences of alternating polar and non-polar amino acids: implications for amyloidogenesis. *J. Mol. Biol.* **2000**, *296*, 961–968.
21. Schwartz, R.; Istrail, S.; King, J. Frequencies of amino acid strings in globular protein sequences indicate suppression of blocks of consecutive hydrophobic residues. *Protein Sci.* **2001**, *10*, 1023–1031.
22. Chiti, F.; Calamai, M.; Taddei, N.; Stefani, M.; Ramponi, G.; Dobson, C.M. Studies of the aggregation of mutant proteins *in vitro* provide insights into the genetics of amyloid diseases. *Proc. Natl. Acad. Sci. USA* **2002**, *99*, 16419–16426.
23. López De La Paz, M.; Goldie, K.; Zurdo, J.; Lacroix, E.; Dobson, C.M.; Hoenger, A.; Serrano, L. *De novo* designed peptide-based amyloid fibrils. *Proc. Natl. Acad. Sci. USA* **2002**, 99, 16052–16057.
24. Monsellier, E.; Chiti, F. Prevention of amyloid-like aggregation as a driving force of protein evolution. *EMBO Rep.* **2007**, *8*, 737–742.
25. Uversky, V.N. Natively unfolded proteins: A point where biology waits for physics. *Protein Sci.* **2002**, *11*, 739–756.
26. Wetzel, R. Kinetics and thermodynamics of amyloid fibril assembly. *Acc. Chem. Res.* **2006**, *39*, 671–679.
27. Nelson, R.; Sawaya, M.R.; Balbirnie, M.; Madsen, A.Ø.; Riekel, C.; Grothe, R.; Eisenberg, D. Structure of the cross-beta spine of amyloid-like fibrils. *Nature* **2005**, *435*, 773–778.
28. Radivojac, P.; Obradovic, Z.; Smith, D.K.; Zhu, G.; Vucetic, S.; Brown, C.J.; Lawson, J.D.; Dunker, A.K. Protein flexibility and intrinsic disorder. *Protein Sci.* **2004**, *13*, 71–80.
29. Ladokhin, A.S.; White, S.H. Folding of amphipathic alpha-helices on membranes: energetics of helix formation by melittin. *J. Mol. Biol.* **1999**, *285*, 1363–1369.
30. White, S.H.; Wimley, W.C. Hydrophobic interactions of peptides with membrane interfaces. *Biochim. Biophys. Acta* **1998**, *1376*, 339–352.
31. Aguilar-Gaytan, R.; Mas-Oliva, J. Oxidative stress impairs endocytosis of the scavenger receptor class A. *Biochem. Biophys. Res. Commun.* **2003**, *305*, 510–517.
32. Mousavi, S.A.; Malerød, L.; Berg, T.; Kjeken, R. Clathrin-dependent endocytosis. *Biochem. J.* **2004**, *377*, 1–16.
33. Ford, M.G.; Pearse, B.M.; Higgins, M.K.; Vallis, Y.; Owen, D.J.; Gibson, A.; Hopkins, C.R.; Evans, P.R.; McMahon, H.T. Simultaneous binding of PtdIns(4,5)P2 and clathrin by AP180 in the nucleation of clathrin lattices on membranes. *Science* **2001**, *291*, 1051–1055.
34. Legandre-Guillemin, V.; Wasiak, S.; Hussain, N.K.; Angers, A.; McPherson, P.S. ENTH/ANTH proteins and clatrin-mediated membrane budding. *J. Cell. Sci.* **2004**, *117*, 9–18.
35. Klunk, W.E.; Jacob, R.F.; Mason, R.P. Quantifying amyloid beta-peptide (Abeta) aggregation using the Congo red-Abeta (CR-abeta) spectrophotometric assay. *Anal. Biochem*. **1999**, *266*, 66–76.

36. Knowles, T.P.; Fitzpatrick, A.W.; Meehan, S.; Mott, H.R.; Vendruscolo, M.; Dobson, C.M.; Welland, M.E. Role of intermolecular forces in defining material properties of protein nanofibrils. *Science* **2007**, *318*, 1900–1903.

Supplementary Data

Figure 1S. Effect of pH on $A\beta_{25-35}$ fibril formation. (**A**) $A\beta_{25-35}$ incubated for 72 h at pH 7.2 induces the formation of amorphous aggregates; (**B**) Microglial cells treated with these amorphous aggregates did not produce changes in endocytic protein expression; (**C**) Incubation of $A\beta_{25-35}$ for 72 h at pH 5.5 induces the formation of well-defined fibrils; (**D**) Cells treated with $A\beta_{25-35}$ fibrils show changes in β-adaptin and CALM expression; (**E**) Well-defined fibrils of $A\beta_{25-35}$ induce a gradual decrease in microglial cell viability. TEM images were obtained with a peptide concentration of 60 μg/mL. Bars correspond to 200 nm.

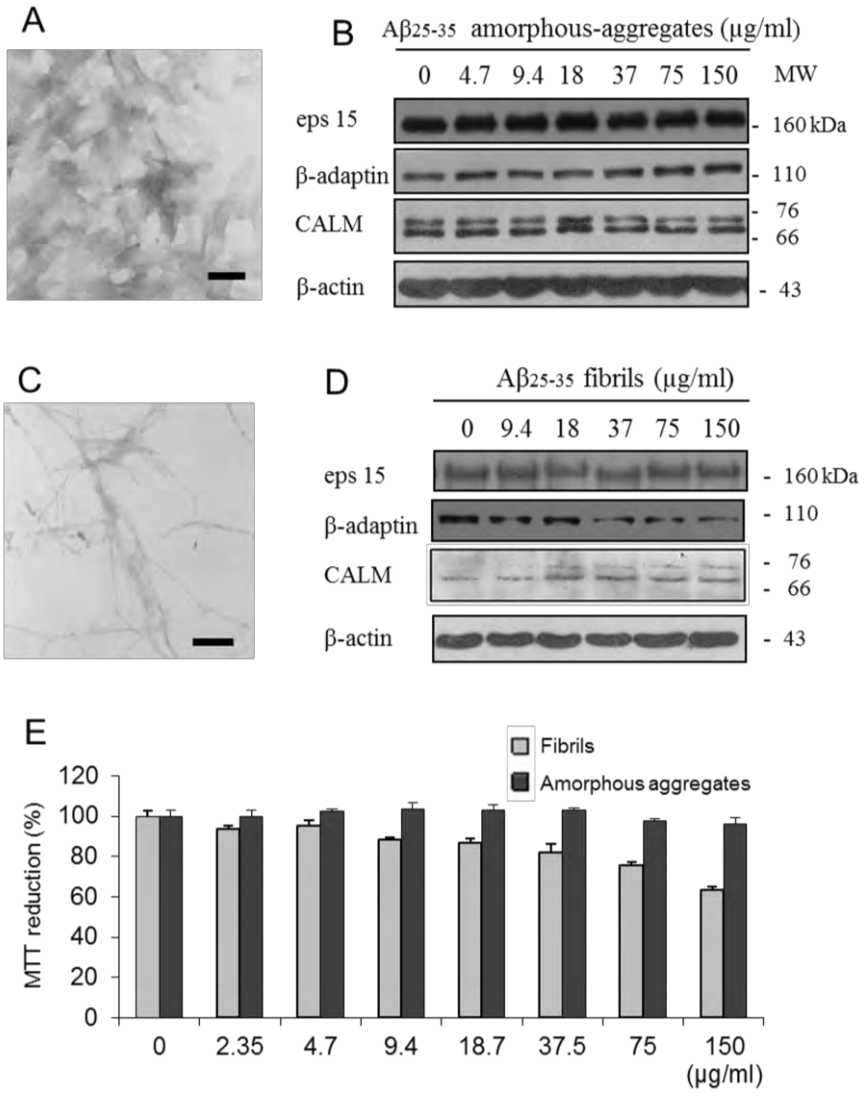

Mol Cell Biochem (2009) 330:105–120
DOI 10.1007/s11010-009-0105-6

Disorder-to-order conformational transitions in protein structure and its relationship to disease

Paola Mendoza-Espinosa · Victor García-González · Abel Moreno · Rolando Castillo · Jaime Mas-Oliva

Received: 4 December 2008 / Accepted: 30 March 2009 / Published online: 9 April 2009

Abstract Function in proteins largely depends on the acquisition of specific structures through folding at physiological time scales. Under both equilibrium and non-equilibrium states, proteins develop partially structured molecules that being intermediates in the process, usually resemble the structure of the fully folded protein. These intermediates, known as molten globules, present the faculty of adopting a large variety of conformations mainly supported by changes in their side chains. Taking into account that the mechanism to obtain a fully packed structure is considered more difficult energetically than forming partially "disordered" folding intermediates, evolution might have conferred upon an important number of proteins the capability to first partially fold and—depending on the presence of specific partner ligands—switch on disorder-to-order transitions to adopt a highly ordered well-folded state and reach the lowest energy conformation possible. Disorder in this context can represent segments of proteins or complete proteins that might exist in the native state. Moreover, because this type of disorder-to-order transition in proteins has been found to be reversible, it has been frequently associated with important signaling events in the cell. Due to the central role of this phenomenon in cell biology, protein misfolding and aberrant disorder-to-order transitions have been at present associated with an important number of diseases.

Keywords Protein structure · Protein misfolding · Disorder-to-order transitions · Disease

P. Mendoza-Espinosa · V. García-González · J. Mas-Oliva (✉)
Instituto de Fisiología Celular, Universidad Nacional Autónoma de México, Apdo. Postal 70-243, 04510 Mexico, D.F., Mexico
e-mail: jmas@ifc.unam.mx

A. Moreno
Instituto de Química, Universidad Nacional Autónoma de México, Mexico, D.F., Mexico

R. Castillo
Instituto de Física, Universidad Nacional Autónoma de México, Mexico, D.F., Mexico

Introduction

Although for many years now human disease has been directly related with specific anomalies in protein–protein, protein–DNA and protein–RNA interactions, in the near future such accumulated knowledge will require expansion in order to take the next technological step with the application of many proteomic concepts to patient-oriented therapies [1]. Recently in this regard, an important number of diseases have been associated with problems specifically related with protein folding. The concept of protein folding is directly related with the process of reversible disorder-to-order transitions, by which an unfolded polypeptide chain folds into a specific functional native structure [2, 3]. Although for a long time it was thought to be only a theoretical concept, it was only recently that it became clear that incorrectly folded proteins might be related with the development of disease. From that time, conformational or protein-folding diseases have been divided basically into two groups. The first, includes errors in the genetic blueprint that leads to incomplete or incorrectly folded proteins directly affecting function; classical examples of this group comprise malfunction of p53 as a critical tumor suppressor protein directly related with cancer [4, 5] and specific alterations in diseases such as cystic fibrosis [6] and sickle cell anemia [7]. The second group, which is made up to excessive quantities of incorrectly conformed proteins

causes the formation of multimolecular structures or plaques with the property of altering normal cell function. Such alterations, known as amyloidosis, are found in diseases like Alzheimer disease [8], Creutzfeldt–Jakob disease [9], Parkinson disease [10], and type II non-insulin-dependent diabetes mellitus [11]. Although in all of the previously mentioned diseases, protein aggregates or plaques are known to be constituted of amyloid fibrils polymerized as beta-sheet structures, important factors involved in the process dealing first with formation and propagation, and second with their stability are far from being understood in vivo.

Physicochemical approach

For folding into a native state, unfolded polypeptide chains require the intervention of weak interactions. Driven by hydrophobic interactions, a polypeptide chain begins to fold when placed in an aqueous medium, and rapidly becomes a molten globule followed by an important release of latent heat. Stabilization of the molten globule is achieved mainly through the distribution of hydrophobic residues away from the water matrix. On the other hand, because the polar residues contained in a protein develop hydrogen bonds with the water network as well as with each other, α-helices and β-sheets can be formed when bonds switch between molecules. It has been calculated that such bonds might be in the order of 10^{-12} s, very similar to those we find in water itself. The random equilibrium can be shifted toward one of these conformations by means of two stages: a fast stage, during which the unfolded polypeptide becomes a molten globule; and a slow stage, in which the molten globule slowly transforms into a fully folded form or native state [12]. These two stages in protein folding can be illustrated by a "folding funnel", during which due to a small change in entropy with a large loss of energy, a molten globule evolves into the native state (Fig. 1) [13, 14]. Although the process is extremely efficient, there is always the possibility that this accurate mechanism might fail, and the possibility of finding a protein folded into a non-native state becomes a reality [15]. Proteins that follow this pathway might present transiently stable conformations, promoting their interaction with other molecules and facilitating the fact that they might form amorphous oligomers and end in a state of aggregation. Aggregation does not arise from a random coil state, but rather from a series of intermediates that—based on the type of secondary structure acquired during folding—might or might not resemble the native state (Fig. 2) [14, 16]. It is well known now that primary polypeptide sequences become the key factor during this process, while the environment surrounding the protein is an important

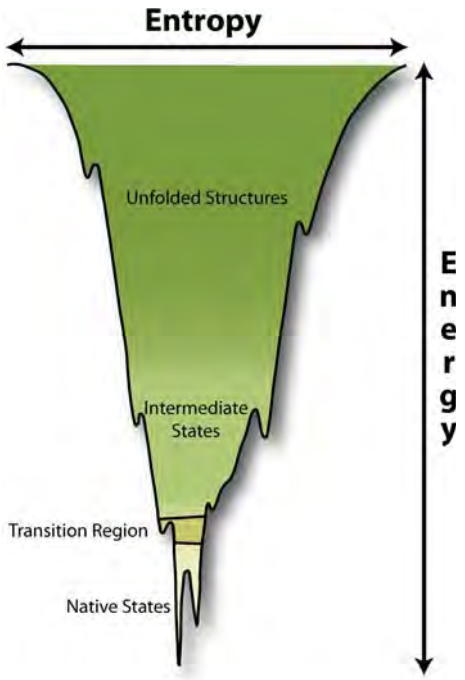

Fig. 1 Folding funnel energy landscape. Globular proteins organize themselves from a random coil to a molten globule during a large loss of entropy and small changes in energy. However, the molten globule becomes transformed to a native state during a low change in entropy at the expense of a large loss of energy. Adapted from references [12–14]

factor for explaining the folding process [17]. On the other hand, natively unfolded proteins, known to lack the presence of permanent secondary and tertiary structures, have been recognized at least in the absence of other proteins, to present the tendency to organize themselves into amyloidogenic structures. This is the case for α-synuclein, an important protein found in Lewy bodies in the brain of patients affected with Parkinson disease [18]. In the case of prion diseases, the P_rP protein has been isolated from amyloid plaques, in which a clear conformational change in secondary structure from α-helix into β-sheet following a templating mechanism has been recognized as the process that causes aggregation [17].

Considering that the native state is located at the lowest minimum of the "folding funnel", it indicates that this region is the most thermodynamically stable configuration of the polypeptide chain under physiological conditions. For proteins, whose functional state is a tightly packed globular fold, a key step in fibril formation related to partial or complete unfolding is less likely to occur and therefore remains protected against aggregation [19]. In this respect, it has been proposed that the more transient structures thus formed in proteins, the better probability for key determinants in amyloid fibril formation to be found [20]. Thus, many of the known forms of amyloid diseases are

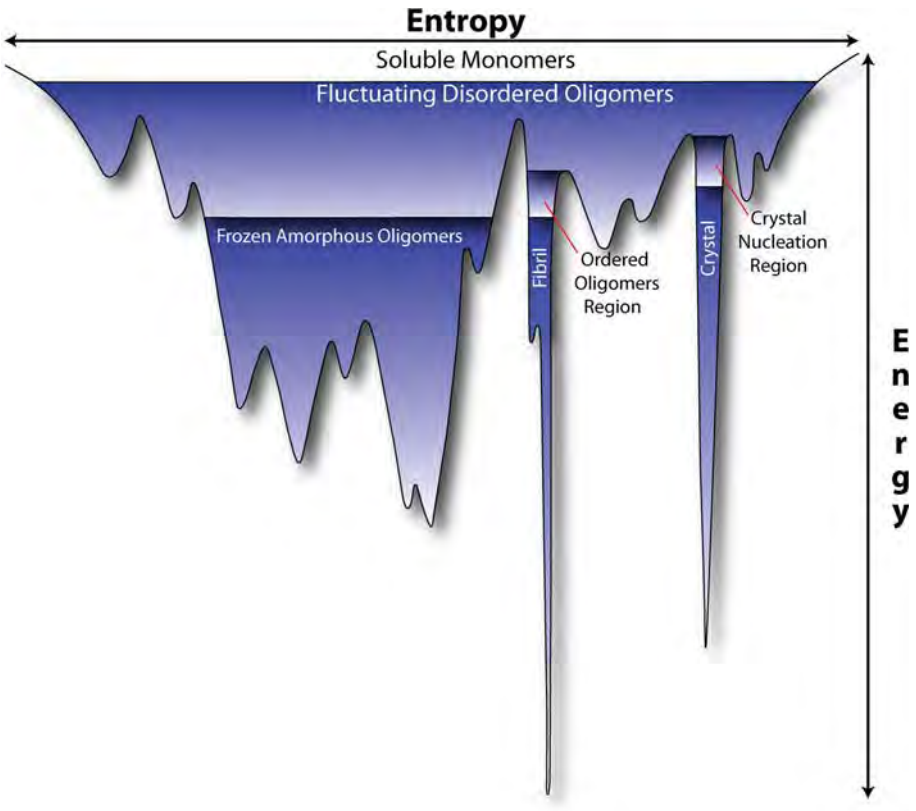

Fig. 2 Protein aggregation energy landscape. Although the funnel shape for protein folding is organized from an active process that results in the selection of forms with favorable native contacts, when a high concentration of polypeptide is present, a large number of interactions appear followed by protein aggregation. Landscape regions characterized by low energy and low entropy are recognized for the appearance of well-ordered species such as fibrils and crystals. Adapted from reference [14]

associated with genetic mutations that decrease protein stability and promote unfolding [20], both related to disorder-to-order conformational transitions.

Chen et al. showed that monomeric polyglutamine in solution represents the nucleus for aggregation and nucleation of a β-sheet aggregate through an initial disorder-to-order transition [21]. Multiple molecular dynamic simulations have provided quantitative characterization of these polyglutamine peptides showing disorder-to-order fluctuations directly related to chain length and average compactness [22]. Here, it was shown that the concentration of side chain primary amides around backbone units and solvation, either by hydrogen bonds or surrounding water molecules, importantly contribute to these average compactness values [22]. In this context, the first experimental evidence about a specific disorder-to-order transition was presented over 30 years ago with the mechanism description for the conversion of trypsinogen to trypsin [23]. This mechanism is characterized by the enzymatic removal of an hexapeptide from the N-terminal region of trypsinogen in order to form trypsin. This basic change promotes the transition from a disordered state of the "specificity pocket" in trypsinogen to an ordered state in trypsin [24].

Since it is known that several amino acids that make up a protein strongly favor a disordered state, at present this "new view" of folding is beginning to be further studied, in which the influence of external or environmental conditions sustains well-tested transitions between disordered and ordered states [25–27]. Specific polypeptide chains contained in proteins or complete proteins lacking defined tertiary structures are known to have the capacity to undergo disorder-to-order transitions upon binding to specific [28] or multiple partners [29]. It is precisely this ability that allows the concept of "protein disorder" to be proposed as an important feature in the capability of proteins to present regions with switching properties [30–32]. Dunker and Obradovic [26] and later Uversky [27] designed a protein/function paradigm extended from the classic form of thought in which ordered 3D structures are indispensable for function due to the fact that the function might arise from ordered structures as efficiently as from disordered functions, namely pre-molten globules and random coils (Fig. 3). An example of the latter would be α-synuclein, shown to be partially folded in the presence of di- and trivalent metal ions, in which in response to cation-binding intrinsic coils change into a pre-molten globular conformation [33]. On the other hand, structural arrangements that take place from a random coil to a molten globule-like conformation have been observed with the myelin basic protein upon binding to lipids [34]. From an evolutionary point of view, it appears that intrinsic disorder in proteins might have been the driving force behind many of the adaptability processes found in proteins [15, 35].

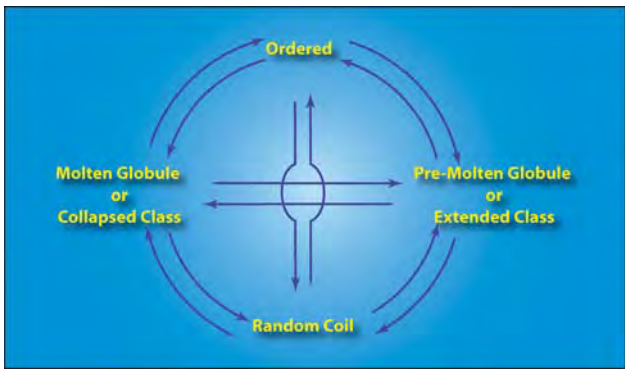

Fig. 3 Protein quartet model for protein structure transitions. Adapted from references [26, 27]

Taking into account that the number of proteins presenting disordered regions directly related with function and therefore with disease is increasingly growing, an interest to also generate accessible data banks for improving information management has increased. Therefore, the database of disordered proteins (DisProt) was created and released in August 2006 by the group of Dunker [36] with extremely good results at present [37]. Since then, other systems for studying disorder in proteins have been released, such as the Integrated Protein Disorder Analyzer, which aims at identifying and predicting disordered region in proteins [38], or algorithms for predicting and evaluating aggregation "hot spots" (AGGRESCAN) [39]. According to Dunker's group and as predicted by PONDR^{r} [40], a large percentage of all proteins involved with some sort of a disease have been identified as directly related with disordered regions in proteins closely associated with signaling.

Protein conformational diseases

From a general point of view, disordered regions in proteins have been divided into the following two classes: the class in which proteins retain a low percentage of secondary structure together with unstable tertiary structures during a molten globule state, recognized as the collapsed class; and second, the class in which proteins with a highly extended backbone resemble a β-sheet conformation related with the extended class [25, 41]. In general, proteins containing disordered regions have been recognized as associated with several human diseases, including cardiovascular disease, cancer, degenerative diseases, and diabetes. Interestingly, because in many of these cases cell signaling function has been involved, there is a strong possibility that disorder-to-order transitions in proteins playing normal switching roles in the cell might become distorted and therefore abolish or transform the normal protein–protein language into an aberrant one. Therefore, the basic properties of a switching mechanism must be based on the equilibrium between high specificity and weak affinities accompanied by a large conformational entropy decrease. This phenomenon is based principally on the fact that upon binding, disorder-to-order transitions can overcome steric restrictions and thereby enable larger interaction surfaces in protein–protein complexes than those that could be obtained for rigid partners [42]. Despite the extraordinary importance of this type of transition, we continue to lack detailed biophysical studies that might demonstrate a close relationship between this type of disorder-to-order organization and protein function.

During the last few years and mainly employing powerful bioinformatics and data mining, many proteins showing intrinsic disorder have been studied in relationship with the disease [43, 44]. A good number of these proteins can be considered as potential candidates in the understanding and treatment of the disease when specific group domains undergoing abnormal disorder-to-order transitions are recognized [42, 45]. An example of this possibility is the lymphoid enhancer-binding factor 1 (LEF-1), which corresponds to a sequence-specific and cell type-specific transcription factor playing a key role in T-cell receptor (TCR)-α gene-enhancer modulation [46]. Based on circular dichroism studies, helix I adopts a helical structure and becomes fully stabilized, reaching a well-folded state in the presence of DNA [47].

Another example corresponds to the p53 tumor-suppressor protein as one of the most studied proteins in history. It is known that p53 activates a large number of genes, with its main function being the arrest of the cell cycle in G1 and G2, allowing the activation of DNA repair mechanisms and therefore the development of its cancer-inhibiting properties. Persons inheriting only one functional copy of the p53 gene are predisposed to develop several tumor types. This condition has been found in the Li-Fraumeni syndrome (LFS), in which individuals are predisposed to develop sarcomas, leukemias, adrenocortical carcinomas, and breast cancer at early ages [48, 49]. More than 50% of human cancers have been associated with mutations in p53, and according to systematic analysis of a large number of mutations, it has been revealed that 304 of the 882 mutations studied affecting the structure of the p53 core domain can be explained by their effects on protein folding [50]. Although reversible aggregation appears to play an important role in p53 core-domain folding [51], it remains to be studied whether a percentage of the structural changes found with this important protein might be associated with localized disorder-to-order transitions, which in turn could modulate—and therefore affect, for example—protein–DNA interactions.

Moreover, with regard to RNA function, several RNA chaperones with key participation in cellular RNA metabolism have been described as organizing several networks of RNA–RNA, RNA–protein, and protein–protein interactions

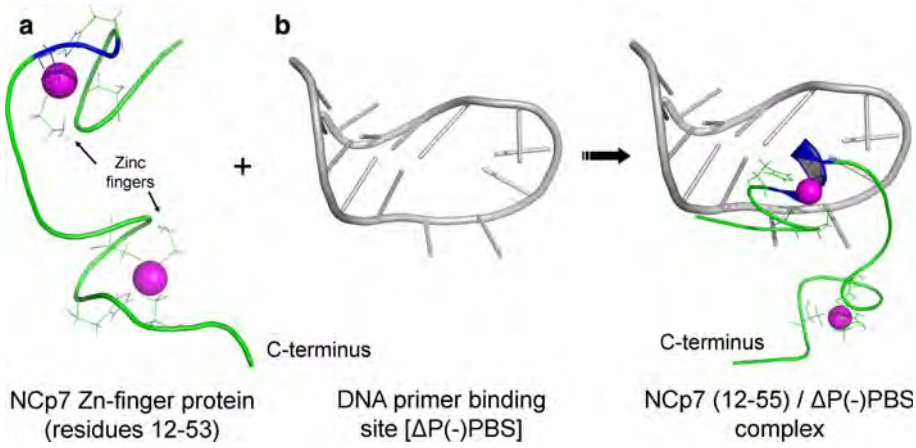

Fig. 4 Structural conformations for the NCp7 (Zn-finger) protein. **a** Relatively unstructured NCp7 (residues 12–53) showing coordination with zinc atoms in purple around a poorly structured section. **b** In the presence of DNA (HIV-1 primer binding site) a change in secondary structure (α-helix, *blue*) is observed, when a complex is formed around the HIV-primer binding site of DNA and the N-terminal region of NCp7 (Zn-finger). Structures were obtained from PDB access code: 1esk and 2jzw. Images visualized employing the Pymol program [212]

[52]. Here, these chaperone proteins presenting an important intrinsic disorder assist RNA function by successive disorder-to-order and order-to-disorder transition cycles to aid RNA in acquiring the most stable conformation required for optimal function [53]. One classical example is NCp7, a nucleocapsid protein from the HIV type 1 virus. NCp7 is a 55 amino-acid nucleic-acid-binding protein that represents an important structural segment of the HIV type 1 virus nucleocapsid. It is characterized by two zinc fingers [54, 55] and participates in several key functions during the HIV-1 viral life cycle [56–58]. The two main activities of NCp7 are destabilization of nucleic acid loop structures [59–61] and nucleic acid aggregation–condensation [62–64]. NCp7 has been mainly studied through its interaction with four contiguous stem-loop structures, where SL1–SL4 of the HIV-1 ψ recognition site [65–67] shows a high degree of disorder [53] and therefore excellent adaptation properties for a wide range of RNA and DNA molecules (Fig. 4) [66–70].

Lipid transfer protein structure and disease

In an attempt to define the possibility that folding key features in proteins could provide us with the manner in which to explain basic issues such as receptor recognition, lipid transfer activity, and self-exchangeability carried out by several lipid transfer proteins including apolipoproteins, our group has attempted to address these points by directly measuring molecular conformational changes of apolipoproteins at air/water and lipid/water interfaces, in order to approach the possible mechanisms that might explain these phenomena [71]. This has been achieved employing Langmuir monolayers in conjunction with Brewster angle microscopy (BAM), atomic force microscopy (AFM) of LB films of protein [72–75], grazing incidence X-ray diffraction on protein monolayers [76], and surface force measurements (SFA) [77]. Because at that time, we were unable to define whether the secondary structure of specific segments of apoCI and -AII remained stable independently of their position at air/water and lipid/water interfaces, more recently we have addressed the possibility that these segments responding to specific environmental changes and following disorder-to-order transitions might function as molecular switches that trigger function [78, 79].

ApoCI is synthesized with a 26-residue signal peptide that is cleaved co-translationally in the rough endoplasmic reticulum which inhibits both phospholipase A2 [80, 81] and hepatic lipase [82] and activates the lecithin-cholesterol acyltransferase (LCAT) [83]. Also, it has been reported that the C-terminal fragment of human apoCI acts as an inhibitor in vitro of the cholesterol ester transfer protein (CETP) [84, 85]. On the other hand, the discovery that apoE-enriched β-migrating very-low-density lipoprotein (β-VLDL) binds to the lipoprotein receptor-related protein (LRP) [86], the effect of apoCI content upon this binding has been studied [87]. When individual members of the C apolipoprotein family were examined, it was found that apoCI is the most potent inhibitor of apoE-mediated β-VLDL binding to the lipoprotein-related protein (LRP) [88]. It has been suggested that in addition to displacement of apoE from the particle, apoCI binding might exert its effect by inducing a change in resident apoE conformation, which in turn abolishes its ability to interact with LRP. Apolipoprotein E is a 299-residue protein that exists as three allelic variants, denominated apo E2, -3, and -4. In Alzheimer disease, the apo E4 allele is a risk factor associated with an earlier age of onset for sporadic cases [89, 90].

Although function that depends specifically on 100% disordered proteins represents the extreme case, the concept of having disordered segments in proteins that only respond and acquire a well-defined secondary structure associated with the binding of specific ligands, might be more common than we thought. We have postulated that changes in lipid composition of HDL particles might promote an alteration in normal disorder-to-order transitions found in apoCI, changing its switching properties, and therefore predisposing the onset of diseases related with LCAT activation and CETP function [79]. Acquisition of a very rapid lipid-specific α-helical conformation following a disorder-to-order transition in the C-terminal peptide of apoCI has provided new insights into how this protein might modulate function [77, 79]. Moreover, following the same approach with specific peptides synthesized from the reported structure of apolipoprotein A1, when left in water at 4°C, a very slow disorder-to-order transition develops over the course of weeks, from a fully disordered state to a well-developed β-sheet secondary structure (Mas-Oliva J, personal communication). This behavior further supports the fact that the physicochemical characteristics of the environment must be considered as a key factor in the equilibrium displacement within the secondary structure of a protein or specific segments toward α-helices or β-sheets [91]. Here, the result that specific segments of apolipoprotein AI slowly develop fibril-like structures indicates the possibility that pathological processes such as atherogenesis might be also considered as an amyloidotic-related process (Fig. 5) [92].

Amyloid-related diseases

At present, an important number of human diseases affecting several tissues and producing a series of common symptoms find their origin in the assembly of proteins into insoluble deposits [93, 94]. Although absolute establishment of this connection is lacking to date, there is solid evidence indicating a strong correlation between the formation of amyloid fibrils and their toxicity upon cells in vitro [95–97]. The missing point continues to reside in basic understanding of the characteristics of the so-called amyloidogenic proteins that define their capacity to organize themselves into a β-structure conformation. This capacity has been, on the one hand, related to a hereditary component with several dominant autosomic diseases [98], and on the other, with a "sporadic" form of the disease [98, 99]. Here, independently of whether the precursor protein is being synthesized as a normal protein, secondary external factors mainly related with the protein environment during synthesis or during transit to its target pathway, define their potential amyloidotic pathway. Because not every protein that aggregates forms amyloid deposits, the study—and eventually the understanding—of the mechanisms that govern, first, protein folding and second, aggregation-related phenomena, include possible implications for disorder-to-order transitions. Again, the potential implications of having disordered segments in these proteins that might present conformational transitions to ordered states still remains to be fully evaluated.

Amyloid-related diseases are in direct association to a failure of the regulatory mechanisms that normally ensure that proteins remain in their correctly folded functional states [13]. Such mechanisms and quality control systems include the action of folding catalysts, molecular chaperones, degrading enzymes, and endoplasmic reticulum-associated degradation, that normally detect misfolded or damaged proteins and either rescue or destroy them [19, 100]. If the function of these protective mechanisms is diminished, the probability of pathogenesis increases [101, 102].

On the other hand, several studies have shown that a certain number of polypeptides not directly related to amyloid disease might be also capable of forming amyloid fibrils under destabilized conditions [103–108]. This shows that amyloid deposition may be a common property of proteins, and not only to the ones associated with disease [109]. In fact, the difference between "functional" amyloids and the ones associated to disease might be explained in terms of evolutionary regulating mechanisms. These mechanisms might have evolved functional amyloids where cellular toxicity associated to their formation might have been quenched by other proteins [110] as in the case of protein Pmel17 [111, 112]. Pmel17 corresponds to a transmembrane protein located in the plasma membrane of melanocytes [113]. This protein is of central importance in the way melanin is polymerized in melanocytes since Mα, a proteolytic fragment of Pmel17 structured as amyloid fibrils

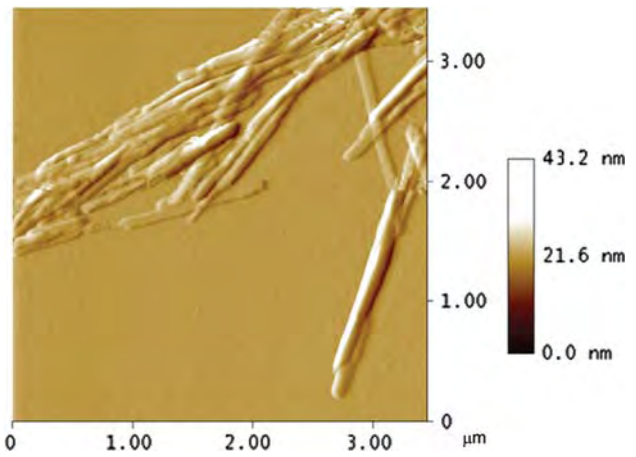

Fig. 5 Atomic force microscopy image of apolipoprotein AI-peptide DRV (amino acids 9–24) (Mas-Oliva J, personal communication). Fibrils show an average length of 300 nm and 25 nm in height

functions as a key support in the polymerization of melanin [111]. Since it has been shown that amyloidogenesis of Mα is four orders of magnitude faster that Aβ and α-synuclein, we can consider this optimized process of fibrillogenesis as an evolutionary way to avoid intrinsic toxicity mostly associated to fibril polymerization [112].

Amyloids are basically classified according to the process-specific protein rather than their clinical manifestations. One of the most important models for studying amyloidogenesis has been the one that occurs during inflammation [114, 115]. This model has been useful in the study of the common characteristics among amyloids, in which an acute phase related with protein synthesis in liver has been described. Because many amyloid peptides/proteins correspond to a fragment of larger precursor molecules, it has been observed that usually a 1,000-fold increase in the plasma concentration of these precursors is needed in order to start the deposition of amyloid. Proteolytic processing of these precursors associated with an altered expression of a series of sorting and trafficking factors appears to be a pathogenic factor in the formation of amyloid deposits [116].

To date, many proteins have been proposed as presenting amyloidogenic properties. Interestingly, on examining their shared characteristics from the perspective of primary structure, no common features are found among them. Therefore, their amyloidogenic properties must rely on the secondary and tertiary levels. Kinetic data are consistent with the possibility that "intermediate" or "molten globule-like" conformational states are in equilibrium, and that the process of fibril formation takes place only by shifting this equilibrium [117]. Since amyloidogenesis corresponds to a two-step reaction with a slow lag period related with the formation of a nucleation center and as a secondary stage its propagation, this process has been compared with protein crystallization [118]. The presence of metal ions and the association with accessory proteins such as apolipoproteins and sulfated proteoglycans has shown the property to modulate amyloidogenesis [119–121]. Therefore, the sometimes denominated *pathological chaperones* have also been shown to contribute to amyloid toxicity [122].

Amyloid-associated proteoglycans

Perhaps the most common amyloid-associated molecules are proteoglycans, which contain a large number of sulfate glycosaminoglycan (GAG) chains linked to large molecular-weight protein cores [123, 124]. The possibility that GAG interaction contributes as a driving force in fibril assembly and amyloid plaque formation has been suggested [125]. In this context, sulfated proteoglycans are ubiquitously expressed on various cell membranes and they are common to all type of amyloids studied to date. They have been also suggested as key factors in the formation of mature plaques serving as scaffolds and protecting against proteolysis [126–128]. Several subtypes have been associated with Aβ plaques, including heparin, dermatan, keratin, and chondroitin sulfate proteoglycans [129, 130].

It seems that the most common amyloid-associated proteoglycan is perlecan [130, 131] that constitutes the major component of the basement membrane/extracellular matrix proteoglycan of the cell [127, 132, 133]. Perlecan has been associated to virtually all human amyloid diseases including Alzheimer's disease, familial amyloidosis, and type 2 diabetes [128, 134–137]. Although several in vitro studies have shown that sulfated GAG chains can induce extensive Aβ aggregation via electrostatic interactions [138] and have been found to increase the β-sheet content of several amyloidogenic proteins such as serum amyloid A protein (SAA) [139], sulfated GAG chains also seem to reduce amyloid fibril degradation [140]. The SAA [139] has been reported to contain specific binding sites for heparin and heparan sulfate, associated to phylogenetically conserved basic residues. The occupation of these sites is likely to increase the amyloid conformation of SAA [141].

β amyloid precursor protein (AβPP) and β amyloid (Aβ)

Together with its precursor protein, the amyloid peptide is considered a normal molecule found in plasma, cerebrospinal fluid, and the extracellular space. AβPP corresponds to a transmembrane protein with a low amyloidogenesis potential in vitro. This is in contrast with the high tendency of Aβ to form fibril aggregates [142]. Three AβPP isoforms are shown to date (751, 770, and 695 amino-acids) [143] and all of them, followed by the action of an α-secretase, form a soluble ectodomain with the retention in the membrane of the carboxy end fragment [144]. Secondary to the action of β and γ secretases, Aβ is liberated generating diverse forms of the β amyloid peptides ranging in size from 39 to 43 residues, being $A\beta_{42}$, the one with the highest fibrillogenic potential (Fig. 6) [145]. Several years ago, we found that upon activation platelets secrete a 120 kDa proteoglycan that presents the ability to inhibit acetylated-low-density-lipoprotein internalization through binding to the scavenger receptor class A (SR-A) in macrophages [124]. This proteoglycan was identified as an α-secretase product of AβPP [146]. This finding supports the possibility that SR-A might participate in the clearance of several forms of AβPP from atherosclerotic lesions, thus contributing to the reduction of foam cell formation. Moreover, competition of AβPP for β-amyloid uptake by microglial cells through the SR-A, might contribute to β-amyloid accumulation in the brain's extracellular space. Although changes in secondary structure of AβPP related to a disorder-to-order transition has not been addressed, at

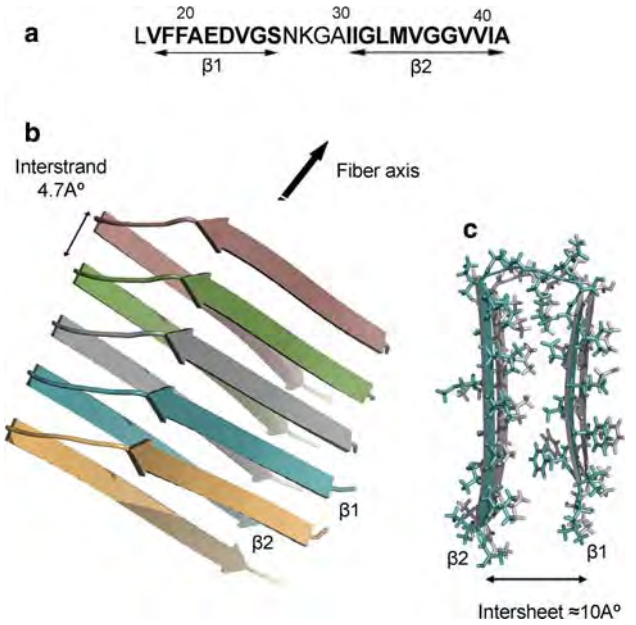

Fig. 6 Structural representation of Aβ peptides. **a** Primary sequence of Aβ fragment 17–42 showing segments that correspond to β1 (18–26) and β2 (31–42) connected through a poorly structured region (residues 27–30). **b** Fibrilar structure of Aβ (17–42) obtained with NMR and mutagenesis complementation methodologies. The structure shows a pentamer with interchain distances of approximately 4.7 Å. **c** Lateral view through the axis of a Aβ fiber showing the lateral amino-acid residues of both β-sheets separated by a 10 Å gap. PDB access code: 2beg. Images visualized employing the Pymol program [212]

this stage this possibility can not be discarded. β-amyloid has been also shown to promote an important cellular oxidative state [147] and further promote, for example, the development of Alzheimer disease, the most common amyloidosis and leading cause of dementia among the elderly.

The amyloid-enhancing factor (AEF) is defined as a factor that dramatically shortens the induction time for amyloid development during inflammatory processes (from 36 h to 2–3 weeks). This characteristic is consistent with amyloidogenesis requiring a nucleating event that shortens initiation of the process. Likewise, many AEF characteristics are related with experiments in which exogenously delivered prions have been injected, and apparently served as templates for endogenously synthesized prions transformed into pathologically active agents [148, 149]. However, different from prions, AEF generates amyloidosis only in the presence of an inflammatory event, reason why instead of being an infective agent it is considered a potentiator of the disease [150].

Prion disease

Prion diseases are chronic neurodegenerative disorders associated with the accumulation of abnormal isoforms of PrP protein in the brain. Among these diseases, we recognize at present scrapie (in sheep and goat), spongiform encephalopathy (in cattle) [151, 152], and in the human, Kuru [153], Creutzfeldt–Jakob disease (CJD) [154], fatal familial insomnia (FFI), Gerstmann–Sträusler–Scheiker disease (GSS), and PrP-cerebral amyloid angiopathy (PrP-CAA) [155–157]. The cellular prion protein (PrP^c) corresponds to a single gene-encoded 35 kDa sialoglycoprotein [158]. The translated protein contains 253 amino acids with glycine/proline-rich octopeptide repeats spanning residues 51–91. It is polymorphic at residue 129 with methionine/valine and at residue 219 with glutamic acid/lysine, and is glycosylated at residues 181 and 197 [159]. Circular dichroism has shown that PrP^c presents a high content of α-helical secondary structure and shows no β-sheet conformation [160]. It is transported in secretory vesicles while anchored to these structures through a GPI moiety [161]. Although the normal function for PrP^c remains unknown, it has been suggested that it might play a role in synaptic function [162]. Because PrP knockout mice have shown to be resistant to development of scrapie, it has been postulated that synthesis of the normal form of PrP^c is an absolute pre-requisite in this protein's abnormal form (PrP^{sc}), which involves a conformational change from an

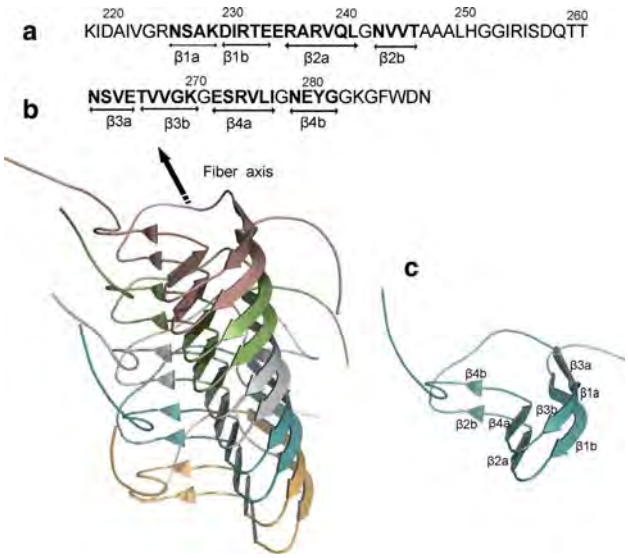

Fig. 7 Structure of the prion like domain of HET-s (218–289). **a** Primary sequence of HET-s fragment 218–289 showing segments that correspond to β-strands β1a (226–229), β1b (230–234), β2a (236–241), β2b (243–246) and β3a (262–265), β3b (266–270), β4a (272–277) and β4b (279–282) separated by a poorly structured region (residues 247–261). **b** Side view of five domains of HET-s (218–289) calculated from solid state NMR with a tridimensional structure in the form of a left-handed-β-solenoid. Each color represents a single domain. **c** Side view of a single domain showing β-structured regions as marked in (**a**). PDB access code: 2rnm. Images visualized employing the Pymol program [212]

α-helix-based structure into β-sheets [163]. Prion rods possess the same tinctorial properties of amyloid fibers (binding the amyloidophilic fluorophores thioflavin and Congo red) [164] and resemble amyloid fibrils found in vivo (Fig. 7) [165, 166].

Peripheral nerve amyloidosis and transthyretin (TTR)

Peripheral nerve amyloidosis is common in familial amyloid polyneuropathy (FAP) [167] and can be a key feature in primary light chain amyloidosis and β2-microglobulin-related amyloidosis. FAPs are a heterogenous group of autosomal dominant disorders characterized by deposition of a fibrillar protein associated to transthyretin (TTR) in the form of amyloid [168, 169]. TTR composed of four identical 127 residue subunits is the plasma protein responsible for transport of thyroxin and vitamin A [170, 171]. Although several mutations in TTR causing extracellular tissue-selective deposition have been described [172], the clinical basis for the predominant manifestation of each mutation has not been established yet [173]. Nevertheless, pathogenesis has been associated with dissociation of the native tetramer molecule into partially unfolded species, which can subsequently self-assemble in the form of amyloid fibrils (Fig. 8) [174–177].

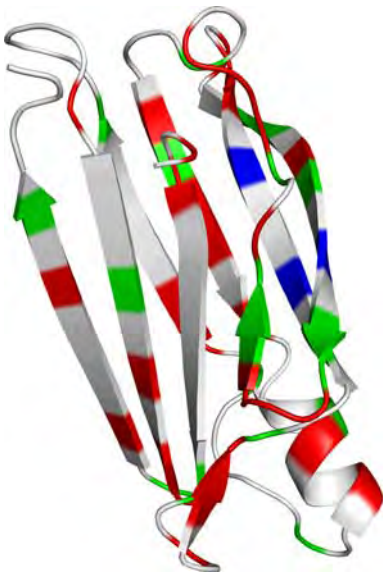

Fig. 8 Three-dimensional structure of the transthyretin monomer obtained from X-ray diffraction. *Arrows* represent β-sheet secondary structure showing in color the position of regions with the most common amyloidogenic mutations. *White color* represents regions with no incidence of mutation, *red* one mutation, *green* two-three mutations, and *blue* four or more mutations. Citation for each mutation can be found at the TTR database of mutations maintained by C. E. Costello at Boston University School of Medicine (http://www.bumc.bu.edu/msr/ttr-database/). PDB access code: 1rlb. Image visualized employing the Pymol program [212]

FAP can also occur secondary to apolipoprotein A-I [178] and gelsolin deposition [179], where two mutations described in the gelsolin gene have been directly associated to this type of disease [180, 181]. In this respect, it has been also shown that serum apo A-II concentrations are much higher in patients with FAP than in normal controls or asymptomatic carriers, suggesting that apo A-II may play a role in amyloid formation in these patients [182]. Moreover, the disease known as familial amyloidosis of Finnish type (FAF) related to gelsolin deposition is characterized by progressive cranial neuropathy, corneal dystrophy, and skin elasticity complications [183, 184]. The first step in FAF is determined by an aberrant proteolysis carried out by furin [185] followed by the proteolytic cut of a MT1-matrix metalloprotease generating amyloidogenic peptides of 5 or 8 kDa [186].

Islet amyloid polypeptide (IAPP) and Beta 2 microglobulin (β2m)

IAAP or amylin synthesized in pancreatic islet β-cells suffers a series of post-translational modifications to yield a mature 37-amino acid peptide (Fig. 9) [187, 188]. IAPP is a molecule involved in the modulation of glucose metabolism [189, 190] as well as in calcium metabolism [191]. IAPP aggregates are the primary component of amyloid deposits found in the pancreatic β-cells of patients with type 2 diabetes mellitus [192]. Prefibrillar oligomeric IAAP has been shown the property to permeabilize membranes through a pore-like mechanism, suggesting that this process might be related to the pathogenic mechanism involved in the genesis of non-insulin-dependent (type II) diabetes mellitus (NIDDM) and other amyloid-related diseases [193]. In adult diabetes (type II), it has been

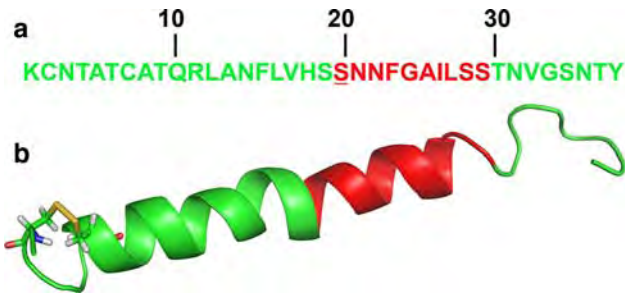

Fig. 9 Three-dimensional structure of human amylin. **a** Primary amino-acid sequence of the entire amylin molecule (1–37) showing in red the amyloidogenic region in between S20 and S29. A mutation that changes S20 for G20 has been directly related to the most severe cases of non insulin dependent diabetes mellitus (NIDDM). **b** Secondary structure of amylin determined by NMR using SDS micelles. The amyloidogenic region of amylin is shown in *red* as in (**a**). PDB access code: 2kb8. Image visualized employing the Pymol program [212]

observed that 90% or more of patients with this disorder present amyloid deposits in the islets of Langerhans [194].

β2m is a protein found in a noncovalently association with the heavy chain of major histocompatibility class I complex (MHCI). Due to the natural turnover of β2m, it is normally found in plasma and therefore carried to the kidneys where it is degraded and excreted [195]. Due to renal disfunction, the concentration of β2m in plasma can increase up to 60-fold, where it accumulates as a filamentous structure in connective tissues and leads to dialysis-related amyloidosis [196–198]. Although it is known that dissociation from MHCI predisposes the amyloid-transition of β2m [199], the mechanism underlying β2m fibrillogenesis in vivo is still largely unknown [200, 201].

Concluding remarks

According to scientists working in different fields of knowledge, nature appears to have employed disorder to create high levels of organization. Moreover, in some cases nature seems to have created disorder, when there is, in the first place a lack of it [202]. This latter situation extrapolated to medicine has shown that many diseases find their origin in the way proteins carry out many structural changes employing finely tuned disorder-to-order and order-to-disorder transitions.

Taking into account that several amyloid-functional-structures have been characterized in bacteria [203, 204], fungi [205–207], insects [208, 209], and mammals [111, 210], there is consensus that the formation of amyloid fibrils represents a well conserved evolutive pathway in protein structure [110, 211]. Therefore, differences between "functional" and "pathological" amyloids might simply reside in the modulatory pathways involved along their synthesis. As professor Christopher M. Dobson has stated, "One can therefore think of the amyloid diseases as resulting from the reversion of the highly evolved biologically functional forms of peptides and proteins into an alternative and unwelcome structural state that exists as a result of the inherent physicochemical nature of polypeptide chains" [19]. Without a doubt we can state that in the near future, many diseases with still unknown origins will find their explanation in the way this class of phenomenon is regulated.

Acknowledgments Research described in this article carried out during the last few years in the laboratory of JM-O has been supported by Consejo Nacional de Ciencia y Tecnología, México (CONACyT-México) grant 47333/A-1 and by Universidad Nacional Autónoma de México (DGAPA-UNAM) grant IN228607. We want to thank Blanca Delgado-Coello for her technical help and Jorge Bravo-Martínez for his work in visualization and structure analysis, Mrs. Margaret Brunner for editorial services and Ma. Elena Gutierrez for manuscript preparation.

References

1. Beretta L (2007) Proteomics from the clinical perspective: many hopes and much debate. Nat Methods 4:785–786. doi:10.1038/nmeth1007-785
2. Rose GD, Fleming PJ, Banavar JR, Maritan A (2006) A backbone-based theory of protein folding. Proc Natl Acad Sci USA 103:16623–16633. doi:10.1073/pnas.0606843103
3. Eaton WA, Muñoz V, Hagen SJ, Jas GS, Lapidus LJ, Henry ER (2000) Fast kinetics and mechanisms in protein folding. Annu Rev Biophys Biomol Struct 29:327–359. doi:10.1146/annurev.biophys.29.1.327
4. Levine AJ (1997) p53, the cellular gatekeeper for growth and division. Cell 88:323–331. doi:10.1016/S0092-8674(00)81871-1
5. Vogelstein B, Lane D, Levine AJ (2000) Surfing the p53 network. Nature 408:307–310. doi:10.1038/35042675
6. Quist A, Doudevski I, Lin H, Azimova R, Ng D, Frangione B, Kagan B, Ghiso J, Lal R (2005) Amyloid ion channels: a common structural link for protein-misfolding disease. Proc Natl Acad Sci USA 102:10427–10432. doi:10.1073/pnas.0502066102
7. Frenette PS, Atweh GF (2007) Sickle cell disease: old discoveries, new concepts, and future promise. J Clin Invest 117:850–858. doi:10.1172/JCI30920
8. Petkova AT, Leapman RD, Guo Z, Yau WM, Mattson MP, Tycko R (2005) Self-propagating, molecular-level polymorphism in Alzheimer's beta-amyloid fibrils. Science 307:262–265. doi:10.1126/science.1105850
9. Yull HM, Ritchie DL, Langeveld JP, van Zijderveld FG, Bruce ME, Ironside JW, Head MW (2006) Detection of type 1 prion protein in variant Creutzfeldt–Jakob disease. Am J Pathol 168:151–157. doi:10.2353/ajpath.2006.050766
10. Selkoe DJ (2003) Folding proteins in fatal ways. Nature 426:900–904. doi:10.1038/nature02264
11. Hoenig M, Hall G, Ferguson D, Jordan K, Henson M, Johnson K, O'Brien T (2000) A feline model of experimentally induced islet amyloidosis. Am J Pathol 157:2143–2150
12. Huang K (2005) Lectures on statistical physics and protein folding. World Scientific, New Jersey
13. Dobson CM (2003) Protein folding and misfolding. Nature 426:884–890. doi:10.1038/nature02261
14. Gsponer J, Vendruscolo M (2006) Theoretical approaches to protein aggregation. Protein Pept Lett 13:287–293. doi:10.2174/092986606775338407
15. Dobson CM (1999) Protein misfolding, evolution and disease. Trends Biochem Sci 24:329–332. doi:10.1016/S0968-0004(99)01445-0
16. Eisenberg D, Nelson R, Sawaya MR, Balbirnie M, Sambashivan S, Ivanova MI, Madsen AO, Riekel C (2006) The structural biology of protein aggregation diseases: fundamental questions and some answers. Acc Chem Res 39:568–575. doi:10.1021/ar0500618
17. Fink AL (1998) Protein aggregation: folding aggregates, inclusion bodies and amyloid. Fold Des 3:R9–R23. doi:10.1016/S1359-0278(98)00002-9
18. Chandra S, Chen X, Rizo J, Jahn R, Südhof TC (2003) A broken alpha-helix in folded alpha-synuclein. J Biol Chem 278:15313–15318. doi:10.1074/jbc.M213128200
19. Dobson MC (2004) Protein chemistry: in the footsteps of alchemists. Science 304:1259–1262. doi:10.1126/science.1093078
20. Ohnishi S, Takano K (2004) Amyloid fibrils from the viewpoint of protein folding. Cell Mol Life Sci 61:511–524. doi:10.1007/s00018-003-3264-8

21. Chen S, Ferrone FA, Wetzel R (2002) Huntington's disease age-of-onset linked to polyglutamine aggregation nucleation. Proc Natl Acad Sci USA 99:11884–11889. doi:10.1073/pnas.182276099
22. Wang X, Vitalis A, Wyczalkowski MA, Pappu RV (2006) Characterizing the conformational ensemble of monomeric polyglutamine. Proteins 63:297–311. doi:10.1002/prot.20761
23. Bode W, Huber R (1976) Induction of the bovine trypsinogen-trypsin transition by peptides sequentially similar to the N-terminus of trypsin. FEBS Lett 68:231–236. doi:10.1016/0014-5793(76)80443-7
24. Huber R, Bode W (1978) Structural basis of the activation and action of trypsin. Acc Chem Res 11:114–122. doi:10.1021/ar50123a006
25. Dunker AK, Lawson JD, Brown CJ, Williams RM, Romero P, Oh JS, Oldfield CJ, Campen AM, Ratliff CM, Hipps KW, Ausio J, Nissen MS, Reeves R, Kang C, Kissinger CR, Bailey RW, Griswold MD, Chiu W, Garner EC, Obradovic ZJ (2001) Intrinsically disordered protein. J Mol Graph Model 19:26–59. doi:10.1016/S1093-3263(00)00138-8
26. Dunker AK, Obradovic Z (2001) The protein trinity-linking function and disorder. Nat Biotechnol 19:805–806. doi:10.1038/nbt0901-805
27. Uversky VN (2002) Natively unfolded proteins: a point where biology waits for physics. Protein Sci 11:739–756. doi:10.1110/ps.4210102
28. Tompa P (2002) Intrinsically unstructured proteins. Trends Biochem Sci 27:527–533. doi:10.1016/S0968-0004(02)02169-2
29. James C, Tawfik DS (2003) Conformational diversity and protein evolution—a 60-year-old hypothesis revisited. Trends Biochem Sci 28:361–368. doi:10.1016/S0968-0004(03)00135-X
30. Bustos DM, Iglesias AA (2006) Intrinsic disorder is a key characteristic in partners that bind 14-3-3 proteins. Proteins 63:35–42. doi:10.1002/prot.20888
31. Kriwacki RW, Hengst L, Tennant L, Reed SI, Wright PE (1996) Structural studies of p21Waf1/Cip1/Sdi1 in the free and Cdk2-bound state: conformational disorder mediates binding diversity. Proc Natl Acad Sci USA 93:11504–11509. doi:10.1073/pnas.93.21.11504
32. Dalal S, Regan L (2000) Understanding the sequence determinants of conformational switching using protein design. Protein Sci 9:1651–1659. doi:10.1110/ps.9.9.1651
33. Pagel K, Vagt T, Koksch B (2005) Directing the secondary structure of polypeptides at will: from helices to amyloids and back again? Org Biomol Chem 3:3843–3850. doi:10.1039/b510098d
34. Polverini E, Fasano A, Zito F, Riccio P, Cavatorta P (1999) Conformation of bovine myelin basic protein purified with bound lipids. Eur Biophys J 28:351–355. doi:10.1007/s002490050218
35. Dunker AK, Garner E, Guilliot S, Romero P, Albrecht K, Hart J, Obradovic Z, Kissinger C, Villafranca JE (1998) Protein disorder and the evolution of molecular recognition: theory, predictions and observations. Pac Symp Biocomput 473–484
36. Sickmeier M, Hamilton JA, LeGall T, Vacic V, Cortese MS, Tatos A, Szabo B, Tompa P, Chen J, Uversky VN, Obradovic Z, Dunker AK (2007) DisProt: the database of disordered proteins. Nucleic Acids Res 35:D786–D793. doi:10.1093/nar/gkl893
37. Cortese MS, Uversky VN, Dunker AK (2008) Intrinsic disorder in scaffold proteins: getting more from less. Prog Biophys Mol Biol 98:85–106. doi:10.1016/j.pbiomolbio.2008.05.007
38. Su C-T, Chen C-Y, Hsu C-M (2007) iPDA: integrated protein disorder analyzer. Nucleic Acids Res 35:W465–W472. doi:10.1093/nar/gkm080
39. Conchillo-Solé O, de Groot NS, Avilés FX, Vendrell J, Daura X, Ventura S (2007) AGGRESCAN: a server for the prediction and evaluation of "hot spots" of aggregation in polypeptides. BMC Bioinformatics 8:65. doi:10.1186/1471-2105-8-65
40. Romero PZ, Obradovic C, Dunker AK (2001) Intelligent data analysis for protein disorder prediction. Artif Intell Rev 14:447–484. doi:10.1023/A:1006678623815
41. Uversky VN (2002) What does it mean to be natively unfolded? Eur J Biochem 269:2–12. doi:10.1046/j.0014-2956.2001.02649.x
42. Cheng Y, LeGall T, Oldfield CJ, Mueller JP, Van YY, Romero P, Cortese MS, Uversky VN, Dunker AK (2006) Rational drug design via intrinsically disordered protein. Trends Biotechnol 24:435–442. doi:10.1016/j.tibtech.2006.07.005
43. Xie Q, Arnold GE, Romero P, Obradovic Z, Garner E, Dunker AK (1998) The sequence attribute method for determining relationships between sequence and protein disorder. Genome Inform Ser Workshop Genome Inform 9:193–200
44. Romero P, Obradovic Z, Li X, Garner EC, Brown CJ, Dunker AK (2001) Sequence complexity of disordered protein. Proteins 42:38–48. doi:10.1002/1097-0134(20010101)42:1<38::AID-PROT50>3.0.CO;2-3
45. Dunker AK, Brown CJ, Lawson JD, Iakoucheva LM, Obradovic Z (2002) Intrinsic disorder and protein function. Biochemistry 41:6573–6582. doi:10.1021/bi012159+
46. Held W, Clevers H, Grosschedl R (2003) Redundant functions of TCF-1 and LEF-1 during T and NK cell development, but unique role of TCF-1 for Ly49 NK cell receptor acquisition. Eur J Immunol 33:1393–1398. doi:10.1002/eji.200323840
47. Love JJ, Li X, Chung J, Dyson HJ, Wright PE (2004) The LEF-1 high-mobility group domain undergoes a disorder-to-order transition upon formation of a complex with cognate DNA. Biochemistry 43:8725–8734. doi:10.1021/bi049591m
48. Birch JM, Hartley AL, Tricker KJ, Prosser J, Condie A, Kelsey AM, Harris M, Jones PH, Binchy A, Crowther D, Craft AW, Edem PB, Evans DGR, Thompson E, Mann JR, Martin J, Mithel ELD, Santibáñez-Koref F (1994) Prevalence and diversity of constitutional mutations in the p53 gene among 21 Li-Fraumeni families. Cancer Res 54:1298–1304
49. Olivier M, Goldgar DE, Sodha N, Ohgaki H, Kleihues P, Hainaut P, Eeles RA (2003) Li-Fraumeni and related syndromes: correlation between tumor type, family structure, and TP53 genotype. Cancer Res 63:6643–6650
50. Martin AC, Facchiano AM, Cuff AL, Hernandez-Boussard T, Olivier M, Hainaut P, Thornton JM (2002) Integrating mutation data and structural analysis of the TP53 tumor-suppressor protein. Hum Mutat 19:149–164. doi:10.1002/humu.10032
51. Ishimaru D, Lima LMTR, Naia LF, Lopez PM, Bom APA, Valente AP, Silva JL (2004) Reversible aggregation plays a crucial role on the folding landscape of p53 core domain. Biophys J 87:2691–2700. doi:10.1529/biophysj.104.044685
52. Ivanyi-Nagy R, Davidovic L, Khandjian EW, Darlix JL (2005) Disordered RNA chaperone proteins: from functions to disease. Cell Mol Life Sci 62:1409–1417. doi:10.1007/s00018-005-5100-9
53. Tompa P, Csermely P (2004) The role of structural disorder in the function of RNA and protein chaperones. FASEB J 18:1169–1175. doi:10.1096/fj.04-1584rev
54. Mély Y, De Rocquigny H, Morellet N, Roques BP, Gerad D (1996) Zinc binding to the HIV-1 nucleocapsid protein: a thermodynamic investigation by fluorescence spectroscopy. Biochemistry 35:5175–5182. doi:10.1021/bi952587d
55. South TL, Blake PR, Sowder RC 3rd, Arthur LO, Henderson LE, Summers MF (1990) The nucleocapsid protein isolated from HIV-1 particles binds zinc and forms retroviral-type zinc fingers. Biochemistry 29:7786–7789. doi:10.1021/bi00486a002
56. Carteau S, Gorelick RJ, Bushman FD (1999) Coupled integration of human immunodeficiency virus type 1 cDNA ends by purified integrase in vitro: stimulation by the viral nucleocapsid protein. J Virol 73:6670–6679

57. Cristofari G, Darlix JL (2002) The ubiquitous nature of RNA chaperone proteins. Prog Nucleic Acid Res Mol Biol 72:223–268. doi:10.1016/S0079-6603(02)72071-0
58. Tsuchihashi Z, Brown PO (1994) DNA strand exchange and selective DNA annealing promoted by the human immunodeficiency virus type 1 nucleocapsid protein. J Virol 68:5863–5870
59. Hargittai MR, Gorelick RJ, Rouzina I, Musier-Forsyth K (2004) Mechanistic insights into the kinetics of HIV-1 nucleocapsid protein-facilitated tRNA annealing to the primer binding site. J Mol Biol 337:951–968. doi:10.1016/j.jmb.2004.01.054
60. Urbaneja MA, Wu M, Casas-Finet JR, Karpel RL (2002) HIV-1 nucleocapsid protein as a nucleic acid chaperone: spectroscopic study of its helix-destabilizing properties, structural binding specificity, and annealing activity. J Mol Biol 318:749–764. doi:10.1016/S0022-2836(02)00043-8
61. Williams MC, Rouzina I, Wenner JR, Gorelick RJ, Musier-Forsyth K, Bloomfield VA (2001) Mechanism for nucleic acid chaperone activity of HIV-1 nucleocapsid protein revealed by single molecule stretching. Proc Natl Acad Sci USA 98:6121–6126. doi:10.1073/pnas.101033198
62. Dib-Hajj F, Khan R, Giedroc DP (1993) Retroviral nucleocapsid proteins possess potent nucleic acid strand renaturation activity. Protein Sci 2:231–243
63. Kankia BI, Barany G, Musier-Forsyth K (2005) Unfolding of DNA quadruplexes induced by HIV-1 nucleocapsid protein. Nucleic Acids Res 33:4395–4403. doi:10.1093/nar/gki741
64. Stoylov SP, Vuilleumier C, Stoylova E, De Rocquigny H, Roques BP, Gérard D, Mély Y (1997) Ordered aggregation of ribonucleic acids by the human immunodeficiency virus type 1 nucleocapsid protein. Biopolymers 41:301–312. doi:10.1002/(SICI)1097-0282(199703)41:3<301::AID-BIP5>3.0.CO;2-W
65. De Guzman RN, Wu ZR, Stalling CC, Pappalardo L, Borer PN, Summers MF (1998) Structure of the HIV-1 nucleocapsid protein bound to the SL3 psi-RNA recognition element. Science 279:384–388. doi:10.1126/science.279.5349.384
66. Amarasinghe GK, De Guzman RN, Turner RB, Chancellor KJ, Wu ZR, Summers MF (2000) NMR structure of the HIV-1 nucleocapsid protein bound to stem-loop SL2 of the psi-RNA packaging signal. Implications for genome recognition. J Mol Biol 301:491–511. doi:10.1006/jmbi.2000.3979
67. Amarasinghe GK, Zhou J, Miskimon M, Chancellor KJ, McDonald JA, Matthews AG, Miller RR, Rouse MD, Summers MF (2001) Stem-loop SL4 of the HIV-1 psi RNA packaging signal exhibits weak affinity for the nucleocapsid protein. Structural studies and implications for genome recognition. J Mol Biol 314:961–970. doi:10.1006/jmbi.2000.5182
68. Tisné C, Roques BP, Dardel F (2001) Heteronuclear NMR studies of the interaction of tRNA(Lys)3 with HIV-1 nucleocapsid protein. J Mol Biol 306:443–454. doi:10.1006/jmbi.2000.4391
69. Johnson PE, Turner RB, Wu ZR, Hairston L, Guo J, Levin JG, Summers MF (2000) A mechanism for plus-strand transfer enhancement by the HIV-1 nucleocapsid protein during reverse transcription. Biochemistry 39:9084–9091. doi:10.1021/bi000841i
70. Bourbigot S, Ramalanjaona N, Boudier C, Salgado GF, Roques BP, Mély Y, Bouaziz S, Morellet N (2008) How the HIV-1 nucleocapsid protein binds and destabilises the (−)primer binding site during reverse transcription. J Mol Biol 383:1112–1128. doi:10.1016/j.jmb.2008.08.046
71. Xicohtencatl-Cortes J, Castillo R, Mas-Oliva J (2004) In search of new structural states of exchangeable apolipoproteins. Biochem Biophys Res Commun 324:467–470. doi:10.1016/j.bbrc.2004.09.045
72. Bolaños-García VM, Mas-Oliva J, Ramos S, Castillo R (1999) Phase transitions in monolayers of human apolipoprotein C-I. J Phys Chem B 103:6236–6242. doi:10.1021/jp984342r
73. Bolaños-García VM, Ramos S, Xicohtencatl-Cortés J, Castillo R, Mas-Oliva J (2001) Monolayers of apolipoproteins at the air/water interface. J Phys Chem B 105:5757–5765. doi:10.1021/jp010714b
74. Mas-Oliva J, Moreno A, Ramos S, Xicohtencatl-Cortés J, Campos J, Castillo R (2003) Frontiers in cardiovascular health. In: Dhalla NS et al (eds) Monolayers of apolipoprotein AII at the air/water interface. Kluwer, Dordrecht, pp 341–352
75. Xicohtencatl-Cortes J, Mas-Oliva J, Castillo R (2004) Phase transitions of phospholipid monolayers penetrated by apolipoproteins. J Phys Chem B 108:7307–7315. doi:10.1021/jp036943
76. Ruíz-García J, Moreno A, Brezesinski G, Möhwald H, Mas-Oliva J, Castillo R (2003) Phase transitions, conformational changes in monolayers of human apolipoprotein CI and AII. J Phys Chem B 107:11117–11124. doi:10.1021/jp034801a
77. Campos-Terán J, Mas-Oliva J, Castillo R (2004) Interactions and conformations of α-helical human apolipoprotein CI on hydrophilic and on hydrophobic substrates. J Phys Chem B 108:20442–20450. doi:10.1021/jp048305d
78. Ramos S, Campos-Terán J, Mas-Oliva J, Nylander T, Castillo R (2008) Forces between hydrophilic surfaces adsorbed with apolipoprotein AII alpha helices. Langmuir 24:8568–8575. doi:10.1021/la800348y
79. Mendoza-Espinosa P, Moreno A, Castillo R, Mas-Oliva J (2008) Lipid dependant disorder-to-order conformational transitions in apolipoprotein CI derived peptides. Biochem Biophys Res Commun 365:8–15. doi:10.1016/j.bbrc.2007.10.112
80. Conde-Knape K, Bensadoun A, Sobel JH, Cohn JS, Shachter NS (2002) Overexpression of apoC-I in apoE-null mice: severe hypertriglyceridemia due to inhibition of hepatic lipase. J Lipid Res 43:2136–2145. doi:10.1194/jlr.M200210-JLR200
81. Poensgen J (1990) Apolipoprotein C-1 inhibits the hydrolysis by phospholipase A2 of phospholipids in liposomes and cell membranes. Biochim Biophys Acta 1042:188–192
82. Kinnunen PK, Ehnolm C (1976) Effect of serum and C-apoproteins from very low density lipoproteins on human postheparin plasma hepatic lipase. FEBS Lett 65:354–357. doi:10.1016/0014-5793(76)80145-7
83. Soutar AK, Garner CW, Baker HN, Sparrow JT, Jackson RL, Gotto AM, Smith LC (1975) Effect of the human plasma apolipoproteins and phosphatidylcholine acyl donor on the activity of lecithin: cholesterol acyltransferase. Biochemistry 14:3057–3064. doi:10.1021/bi00685a003
84. Gautier T, Masson D, de Barros JP, Athias A, Gambert P, Aunis D, Metz-Boutique MH, Lagrost L (2000) Human apolipoprotein C-I accounts for the ability of plasma high density lipoproteins to inhibit the cholesteryl ester transfer protein activity. J Biol Chem 275:37504–37509. doi:10.1074/jbc.M007210200
85. Dumont L, Gautier T, de Barros JP, Laplanche H, Blache D, Ducoroy P, Fruchart J, Fruchart JC, Gambert P, Masson D, Lagrost L (2005) Molecular mechanism of the blockade of plasma cholesteryl ester transfer protein by its physiological inhibitor apolipoprotein CI. J Biol Chem 28:38108–38116. doi:10.1074/jbc.M504678200
86. Kowal RC, Herz J, Goldstein JL, Esser V, Brown MS (1989) Low density lipoprotein receptor-related protein mediates uptake of cholesteryl esters derived from apoprotein E-enriched lipoproteins. Proc Natl Acad Sci USA 86:5810–5814. doi:10.1073/pnas.86.15.5810
87. Kowal RC, Herz J, Weisgraber KH, Mahley RW, Brown MS, Goldstein JL (1990) Opposing effects of apolipoproteins E and C on lipoprotein binding to low density lipoprotein receptor-related protein. J Biol Chem 265:10771–10779
88. Weisgraber KH, Mahley RW, Kowal RC, Herz J, Goldstein JL, Brown MS (1990) Apolipoprotein C-I modulates the interaction

of apolipoprotein E with beta-migrating very low density lipoproteins (beta-VLDL) and inhibits binding of beta-VLDL to low density lipoprotein receptor-related protein. J Biol Chem 265: 22453–22459
89. Roses AD (1996) Apolipoprotein E alleles as risk factors in Alzheimer's disease. Annu Rev Med 47:387–400. doi:10.1146/annurev.med.47.1.387
90. Morishima-Kawashima M, Oshima N, Ogata H, Yamaguchi H, Yoshimura M, Sugihara S, Ihara Y (2000) Effect of apolipoprotein E allele epsilon4 on the initial phase of amyloid beta-protein accumulation in the human brain. Am J Pathol 157: 2093–2099
91. Andreola A, Bellotti V, Giorgetti S, Mangione P, Obici L, Stoppini M, Torres J, Monzani E, Merlini G, Sunde M (2003) Conformational switching and fibrillogenesis in the amyloidogenic fragment of apolipoprotein a-I. J Biol Chem 278:2444–2451. doi:10.1074/jbc.M204801200
92. Westermark P, Mucchiano G, Marthin T, Johnson KH, Sletten K (1995) Apolipoprotein A1-derived amyloid in human aortic atherosclerotic plaques. Am J Pathol 147:1186–1192
93. Ban T, Hoshino M, Takahashi S, Hamada D, Hasegawa K, Naike H, Goto Y (2004) Direct observation of Abeta amyloid fibril growth and inhibition. J Mol Biol 344:757–767. doi:10.1016/j.jmb.2004.09.078
94. Collinge J (2001) Prion diseases of humans and animals: their causes and molecular basis. Annu Rev Neurosci 24:519–550. doi:10.1146/annurev.neuro.24.1.519
95. Manzano-León N, Mas-Oliva J (2006) Estrés Oxidativo, Péptido β-amiloide y Enfermedad de Alzheimer. Gac Med Mex 142: 229–238
96. Zhu X, Smith MA, Honda K, Aliev G, Moreira PI, Nunomura A, Casadesus G, Harris PL, Siedlak SL, Perry G (2007) Vascular oxidative stress in Alzheimer disease. J Neurol Sci 257:240–246. doi:10.1016/j.jns.2007.01.039
97. Lazar KL, Miller-Auer H, Getz GS, Orgel JP, Meredith SC (2005) Helix-turn-helix peptides that form alpha-helical fibrils: turn sequences drive fibril structure. Biochemistry 44:12681–12689. doi:10.1021/bi0509705
98. Zhang-Nunes SX, Maat-Schieman ML, van Duinen SG, Roos RA, Frosch MP, Greenberg SM (2006) The cerebral beta-amyloid angiopathies: hereditary and sporadic. Brain Pathol 16:30–39. doi:10.1111/j.1750-3639.2006.tb00559.x
99. Cabrejo L, Chassagne P, Doucet J, Laquerrière A, Puech N, Hannequin D (2006) Sporadic cerebral amyloidotic angiopathy. Rev Neurol (Paris) 162:1059–1067. doi:10.1016/S0035-3787(06)75118-9
100. Bukau B, Weissman J, Horwich A (2006) Molecular chaperones and protein quality control. Cell 125:443–451. doi:10.1016/j.cell.2006.04.014
101. Bence NF, Sampat RM, Kopito RR (2001) Impairment of the ubiquitin-proteasome system by protein aggregation. Science 292:1552–1555. doi:10.1126/science.292.5521.1552
102. Sherman MY, Goldberg AL (2001) Cellular defenses against unfolded proteins: a cell biologist thinks about neurodegenerative diseases. Neuron 29:15–32. doi:10.1016/S0896-6273(01)00177-5
103. Gross M, Wilkins DK, Pitkeathly MC, Chung EW, Higham C, Clark A, Dobson CM (1999) Formation of amyloid fibrils by peptides derived from the bacterial cold shock protein CspB. Protein Sci 8:1350–1357. doi:10.1110/ps.8.6.1350
104. Krebs MR, Wilkins DK, Chung EW, Pitkeathly MC, Chamberlain AK, Zurdo J, Robinson CV, Dobson CM (2000) Formation and seeding of amyloid fibrils from wild-type hen lysozyme and a peptide fragment from the beta-domain. J Mol Biol 300:541–549. doi:10.1006/jmbi.2000.3862
105. Pertinhez TA, Bouchard M, Tomlinson EJ, Wain R, Ferguson SJ, Dobson CM, Smith LJ (2001) Amyloid fibril formation by a helical cytochrome. FEBS Lett 495:184–186. doi:10.1016/S0014-5793(01)02384-5
106. Zurdo J, Guijarro JI, Jiménez JL, Saibil HR, Dobson CM (2001) Dependence on solution conditions of aggregation and amyloid formation by an SH3 domain. J Mol Biol 311:325–340. doi:10.1006/jmbi.2001.4858
107. Srisailam S, Kumar TK, Rajalingam D, Kathir KM, Sheu HS, Jan FJ, Chao PC, Yu C (2003) Amyloid-like fibril formation in an all beta-barrel protein. Partially structured intermediate state(s) is a precursor for fibril formation. J Biol Chem 278:17701–17709. doi:10.1074/jbc.M300336200
108. Fändrich M, Forge V, Buder K, Kittler M, Dobson CM, Diekmann S (2003) Myoglobin forms amyloid fibrils by association of unfolded polypeptide segments. Proc Natl Acad Sci USA 100:15463–15468. doi:10.1073/pnas.0303758100
109. Guijarro JI, Sunde M, Jones JA, Campbell ID, Dobson CM (1998) Amyloid fibril formation by an SH3 domain. Proc Natl Acad Sci USA 95:4224–4228. doi:10.1073/pnas.95.8.4224
110. Fowler DM, Koulov AV, Balch WE, Kelly JW (2007) Functional amyloid from bacteria to humans. Trends Biochem Sci 32:217–224. doi:10.1016/j.tibs.2007.03.003
111. Berson JF, Theos AC, Harper DC, Tenza D, Raposo G, Marks MS (2003) Proprotein convertase cleavage liberates a fibrillogenic fragment of a resident glycoprotein to initiate melanosome biogenesis. J Cell Biol 161:521–533. doi:10.1083/jcb.200302072
112. Fowler DM, Koulov AV, Alory-Jost C, Marks MS, Balch WE, Kelly JW (2006) Functional amyloid formation within mammalian tissue. PLoS Biol 4:e6
113. Lee ZH, Hou L, Moellmann G, Kuklinska E, Antol K, Fraser M, Halaban R, Kwon BS (1996) Characterization and subcellular localization of human Pmel 17/silver, a 110-kDa (pre)melanosomal membrane protein associated with 5,6,-dihydroxyindole-2-carboxylic acid (DHICA) converting activity. J Invest Dermatol 106:605–610. doi:10.1111/1523-1747.ep12345163
114. Perry VH, Cunningham C, Boche D (2002) Atypical inflammation in the central nervous system in prion disease. Curr Opin Neurol 15:349–354. doi:10.1097/00019052-200206000-00020
115. Maeda J, Ji B, Irie T, Tomiyama T, Maruyama M, Okauchi T, Staufenbiel M, Iwata N, Ono M, Saido TC, Suzuki K, Mori H, Higuchi M, Suhara T (2007) Longitudinal, quantitative assessment of amyloid, neuroinflammation, and anti-amyloid treatment in a living mouse model of Alzheimer's disease enabled by positron emission tomography. J Neurosci 27:10957–10968. doi:10.1523/JNEUROSCI.0673-07.2007
116. von Arnim CA, Spoelgen R, Peltan ID, Deng M, Courchesne S, Koker M, Matsui T, Kowa H, Lichtenthaler SF, Irizarry MC, Hyman BT (2006) GGA1 acts as a spatial switch altering amyloid precursor protein trafficking and processing. J Neurosci 26:9913–9922. doi:10.1523/JNEUROSCI.2290-06.2006
117. Morozova-Roche LA (2007) Equine lysozyme: the molecular basis of folding, self-assembly and innate amyloid toxicity. FEBS Lett 581:2587–2592. doi:10.1016/j.febslet.2007.05.023
118. Wetzel R (2006) Kinetics and thermodynamics of amyloid fibril assembly. Acc Chem Res 39:671–679. doi:10.1021/ar050069h
119. Magaki S, Raghavan R, Mueller C, Oberg KC, Vinters HV, Kirsch WM (2007) Iron, copper, and iron regulatory protein 2 in Alzheimer's disease and related dementias. Neurosci Lett 418: 72–76. doi:10.1016/j.neulet.2007.02.077
120. Kuo YM, Crawford F, Mullan M, Kokjohn TA, Emmerling MR, Weller RO, Roher AE (2000) Elevated A beta and apolipoprotein E in A betaPP transgenic mice and its relationship to amyloid accumulation in Alzheimer's disease. Mol Med 6:430–439

121. Matsubara E, Soto C, Governale S, Frangione B, Ghiso J (1996) Apolipoprotein J and Alzheimer's amyloid beta solubility. Biochem J 316:671–679
122. Alexandrescu AT (2005) Amyloid accomplices and enforcers. Protein Sci 14:1–12. doi:10.1110/ps.04887005
123. Lindahl B, Eriksson L, Lindhal U (1995) Structure of heparan sulfate from human brain, with special regard to Alzheimer's disease. Biochem J 306:177–184
124. Mas-Oliva J, Arnold KS, Wagner WD, Phillips DR, Pitas RE, Innerarity TL (1994) Isolation and characterization of a platelet-derived macrophage-binding proteoglycan. J Biol Chem 269: 10177–10183
125. Bussini S, Meda L, Scarpini E, Clementi E, Conti G, Tiriticco M, Bresolin N, Baron P (2005) Heparan sulfate proteoglycan induces the production of NO and TNF-alpha by murine microglia. Immun Ageing 2:11. doi:10.1186/1742-4933-2-11
126. Snow AD, Wight TN (1989) Proteoglycans in the pathogenesis of Alzheimer's disease and other amyloidoses. Neurobiol Aging 10:481–497. doi:10.1016/0197-4580(89)90108-5
127. Castillo GM, Ngo C, Cummings J, Wight TN, Snow AD (1997) Perlecan binds to the beta-amyloid proteins (A beta) of Alzheimer's disease, accelerates A beta fibril formation, and maintains A beta fibril stability. J Neurochem 69:2452–2465
128. Ancsin JB (2003) Amyloidogenesis: historical and modern observations point to heparan sulfate proteoglycans as a major culprit. Amyloid 10:67–79
129. Arrasate M, Pérez M, Valpuesta JM, Avila J (1997) Role of glycosaminoglycans in determining the helicity of paired helical filaments. Am J Pathol 151:1115–1122
130. Brückner G, Hausen D, Härtig W, Drlicek M, Arendt T, Brauer K (1999) Cortical areas abundant in extracellular matrix chondroitin sulfate proteoglycans are less affected by cytoskeletal changes in Alzheimer's disease. Neuroscience 92:791–805. doi:10.1016/S0306-4522(99)00071-8
131. Snow AD, Sekiguchi RT, Nochlin D, Kalaria RN, Kimata K (1994) Heparan sulfate proteoglycan in diffuse plaques of hippocampus but not of cerebellum in Alzheimer's disease brain. Am J Pathol 144:337–347
132. Snow AD, Sekiguchi R, Nochlin D, Fraser P, Kimata K, Mizutani A, Arai M, Scherier WA, Morgan DG (1994) An important role of heparan sulfate proteoglycan (Perlecan) in a model system for the deposition and persistence of fibrillar A beta-amyloid in rat brain. Neuron 12:219–234. doi:10.1016/0896-6273(94)90165-1
133. Kvansakul M, Hopf M, Ries A, Timpl R, Hohenester E (2001) Structural basis for the high-affinity interaction of nidogen-1 with immunoglobulin-like domain 3 of perlecan. EMBO J 20: 5342–5346. doi:10.1093/emboj/20.19.5342
134. Potter-Perigo S, Hull RL, Tsoi C, Braun KR, Andrikopoulos S, Teague J, Bruce Verchere C, Kahn SE, Wight TN (2003) Proteoglycans synthesized and secreted by pancreatic islet beta-cells bind amylin. Arch Biochem Biophys 413:182–190. doi:10.1016/S0003-9861(03)00116-4
135. Castillo GM, Cummings JA, Yang W, Judge ME, Sheardown MJ, Rimvall K, Hansen JB, Snow AD (1998) Sulfate content and specific glycosaminoglycan backbone of perlecan are critical for perlecan's enhancement of islet amyloid polypeptide (amylin) fibril formation. Diabetes 47:612–620. doi:10.2337/diabetes.47.4.612
136. Yamamoto S, Yamaguchi I, Hasegawa K, Tsutsumi S, Goto Y, Gejyo F, Naiki H (2004) Glycosaminoglycans enhance the trifluoroethanol-induced extension of beta 2-microglobulin-related amyloid fibrils at a neutral pH. J Am Soc Nephrol 15:126–133. doi:10.1097/01.ASN.0000103228.81623.C7
137. Suk JY, Zhang F, Balch WE, Linhardt RJ, Kelly JW (2006) Heparin accelerates gelsolin amyloidogenesis. Biochemistry 45: 2234–2242. doi:10.1021/bi0519295
138. Fraser PE, Nguyen JT, Chin DT, Kirschner DA (1992) Effects of sulfate ions on Alzheimer beta/A4 peptide assemblies: implications for amyloid fibril–proteoglycan interactions. J Neurochem 59:1531–1540. doi:10.1111/j.1471-4159.1992.tb08470.x
139. McCubbin WD, Kay CM, Narindrasorasak S, Kisilevsky R (1988) Circular-dichroism studies on two murine serum amyloid A proteins. Biochem J 256:775–783
140. Gupta-Bansal R, Frederickson RC, Brunden KR (1995) Proteoglycan-mediated inhibition of A beta proteolysis. A potential cause of senile plaque accumulation. J Biol Chem 270:18666–18671. doi:10.1074/jbc.270.31.18666
141. Ancsin JB, Kisilevsky R (1999) The heparin/heparan sulfate-binding site on apo-serum amyloid A. Implications for the therapeutic intervention of amyloidosis. J Biol Chem 274:7172–7181. doi:10.1074/jbc.274.11.7172
142. Jarrett JT, Berger EP, Lansbury PT Jr (1993) The C-terminus of the beta protein is critical in amyloidogenesis. Ann N Y Acad Sci 695:144–148. doi:10.1111/j.1749-6632.1993.tb23043.x
143. Selkoe DJ (1994) Cell biology of the amyloid beta-protein precursor and the mechanism of Alzheimer's disease. Annu Rev Cell Biol 10:373–403. doi:10.1146/annurev.cb.10.110194.002105
144. Sisodia SS (1992) Beta-amyloid precursor protein cleavage by a membrane-bound protease. Proc Natl Acad Sci USA 89:6075–6079. doi:10.1073/pnas.89.13.6075
145. Hardy JA, Higgins GA (1992) Alzheimer's disease: the amyloid cascade hypothesis. Science 256:184–185. doi:10.1126/science.1566067
146. Santiago-García J, Mas-Oliva J, Innerarity TL, Pitas RE (2001) Secreted forms of the amyloid-ß-precursor protein are ligands for the A scavenger receptor. J Biol Chem 276:30655–30661. doi:10.1074/jbc.M102879200
147. Manzano-León N, Delgado-Coello NB, Guaderrama-Díaz M, Mas-Oliva J (2006) Beta-adaptin: key molecule for microglial scavenger receptor function under oxidative stress. Biochem Biophys Res Commun 351:588–594. doi:10.1016/j.bbrc.2006.10.077
148. Varga J, Flinn MS, Shirahama T, Rodgers OG, Cohen AS (1986) The induction of accelerated murine amyloid with human splenic extract. Probable role of amyloid enhancing factor. Virchows Arch B Cell Pathol Incl Mol Pathol 51:177–185. doi:10.1007/BF02899027
149. Ganowiak K, Hultman P, Engström U, Gustavsson A, Westermark P (1994) Fibrils from synthetic amyloid-related peptides enhance development of experimental AA-amyloidosis in mice. Biochem Biophys Res Commun 199:306–312. doi:10.1006/bbrc.1994.1229
150. Soto C, Estrada L, Castilla J (2006) Amyloids, prions and the inherent infectious nature of misfolded protein aggregates. Trends Biochem Sci 31:150–155. doi:10.1016/j.tibs.2006.01.002
151. Prusiner SB (1997) Prion diseases and the BSE crisis. Science 278:245–251. doi:10.1126/science.278.5336.245
152. Cohen FE, Prusiner SB (1998) Pathologic conformations of prion proteins. Annu Rev Biochem 67:793–819. doi:10.1146/annurev.biochem.67.1.793
153. Ghetti B, Piccardo P, Frangione B, Bugiani O, Giaccone G, Young K, Prelli F, Farlow MR, Dlouhy SR, Tagliavini F (1996) Prion protein amyloidosis. Brain Pathol 6:127–145. doi:10.1111/j.1750-3639.1996.tb00796.x
154. Richardson EP, Masters CL (1995) The nosology of Creutzfeldt–Jakob disease and conditions related to the accumulation

of PrPCJD in the nervous system. Brain Pathol 5:33–41. doi:10.1111/j.1750-3639.1995.tb00575.x
155. DeArmond SJ, Prusiner SB (1995) Prion protein transgenes and the neuropathology in prion diseases. Brain Pathol 5:77–89. doi:10.1111/j.1750-3639.1995.tb00579.x
156. Giaccone G, Verga L, Bugiani O, Frangione B, Serban D, Prusiner SB, Farlow MR, Ghetti B, Tagliavini F (1992) Prion protein preamyloid and amyloid deposits in Gerstmann–Sträussler–Scheinker disease, Indiana kindred. Proc Natl Acad Sci USA 89:9349–9353. doi:10.1073/pnas.89.19.9349
157. Revesz T, Ghiso J, Lashley T, Plant G, Rostagno A, Frangione B, Holton JL (2003) Cerebral amyloid angiopathies: a pathologic, biochemical, and genetic view. J Neuropathol Exp Neurol 62:885–898
158. Liao YC, Lebo RV, Clawson GA, Smuckler EA (1986) Human prion protein cDNA: molecular cloning, chromosomal mapping, and biological implications. Science 233:364–367. doi:10.1126/science.3014653
159. Prusiner SB (1991) Molecular biology of prion diseases. Science 252:1515–1522. doi:10.1126/science.1675487
160. Pan KM, Baldwin M, Nguyen J, Gasset M, Serban A, Groth D, Mehlhorn I, Huang Z, Fletterick RJ, Cohen FE, Prusiner SB (1993) Conversion of alpha-helices into beta-sheets features in the formation of the scrapie prion proteins. Proc Natl Acad Sci USA 90:10962–10966. doi:10.1073/pnas.90.23.10962
161. Gasset M, Baldwin MA, Lloyd DH, Gabriel JM, Holtzman DM, Cohen F, Fletterick R, Prusiner SB (1992) Predicted alpha-helical regions of the prion protein when synthesized as peptides form amyloid. Proc Natl Acad Sci USA 89:10940–10944. doi:10.1073/pnas.89.22.10940
162. Büeler H, Fischer M, Lang Y, Bluethmann H, Lipp HP, DeArmond SJ, Prusiner SB (1992) Normal development and behaviour of mice lacking the neuronal cell-surface PrP protein. Nature 356:577–582. doi:10.1038/356577a0
163. Büeler H, Aguzzi A, Sailer A, Greiner RA, Autenried P, Aguet M, Weissmann C (1993) Mice devoid of PrP are resistant to scrapie. Cell 73:1339–1347. doi:10.1016/0092-8674(93)90360-3
164. Prusiner SB, McKinley MP, Bowman KA, Bolton DC, Bendheim PE, Groth DF, Glenner GG (1983) Scrapie prions aggregate to form amyloid-like birefringent rods. Cell 35:349–358. doi:10.1016/0092-8674(83)90168-X
165. DeArmond SJ, McKinley MP, Barry RA, Braunfeld MB, McColloch JR, Prusiner SB (1985) Identification of prion amyloid filaments in scrapie-infected brain. Cell 41:221–235. doi:10.1016/0092-8674(85)90076-5
166. Wasmer C, Lange A, Van Melckebeke H, Siemer AB, Riek R, Meier BH (2008) Amyloid fibrils of the HET-s(218-289) prion form a beta solenoid with a triangular hydrophobic core. Science 319:1523–1526. doi:10.1126/science.1151839
167. Hou X, Aguilar MI, Small DH (2007) Transthyretin and familial amyloidotic polyneuropathy. Recent progress in understanding the molecular mechanism of neurodegeneration. FEBS J 274:1637–1650. doi:10.1111/j.1742-4658.2007.05712.x
168. Costa PP, Figueira AS, Bravo FR (1978) Amyloid fibril protein related to prealbumin in familial amyloidotic polyneuropathy. Proc Natl Acad Sci USA 75:4499–4503. doi:10.1073/pnas.75.9.4499
169. Sousa MM, Cardoso I, Fernandez R, Guimäraes A, Saraiva MJ (2001) Deposition of transthyretin in early stages of familial amyloidotic polyneuropathy: evidence for toxicity of nonfibrillar aggregates. Am J Pathol 159:1993–2000
170. Monaco HL (2002) Three-dimensional structure of the transthyretin-retinol-binding protein complex. Clin Chem Lab Med 40:1229–1236. doi:10.1515/CCLM.2002.213
171. Redondo C, Damas AM, Saraiva MJ (2000) Designing transthyretin mutants affecting tetrameric structure: implications in amyloidogenicity. Biochem J 348:167–172. doi:10.1042/0264-6021:3480167
172. Jacobson DR, Pastore RD, Yaghoubian R, Kane I, Gallo G, Buck FS, Buxbaum JN (1997) Variant-sequence transthyretin (isoleucine 122) in late-onset cardiac amyloidosis in black Americans. N Engl J Med 336:466–473. doi:10.1056/NEJM199702133360703
173. Buxbaum JN, Tagoe CE (2000) The genetics of the amyloidoses. Annu Rev Med 51:543–569. doi:10.1146/annurev.med.51.1.543
174. Kelly JW, Colon W, Lai Z, Lashuel HA, McCulloch J, McCutchen SL, Miroy GJ, Peterson SA (1997) Transthyretin quaternary and tertiary structural changes facilitate misassembly into amyloid. Adv Protein Chem 50:161–181. doi:10.1016/S0065-3233(08)60321-6
175. Kelly JW (1998) The alternative conformations of amyloidogenic proteins and their multi-step assembly pathways. Curr Opin Struct Biol 8:101–106. doi:10.1016/S0959-440X(98)80016-X
176. Reixach N, Deechongkit S, Jian X, Kelly JW, Buxbaum JN (2004) Tissue damage in the amyloidoses: transthyretin monomers and nonnative oligomers are the major cytotoxic species in tissue culture. Proc Natl Acad Sci USA 101:2817–2822. doi:10.1073/pnas.0400062101
177. Kelly JW (1997) Amyloid fibril formation and protein misassembly: a structural quest for insights into amyloid and prion diseases. Structure 5:595–600. doi:10.1016/S0969-2126(97)00215-3
178. Nichols WC, Dwulet FE, Liepnieks J, Benson MD (1988) Variant apolipoprotein AI as a major constituent of a human hereditary amyloid. Biochem Biophys Res Commun 156:762–768. doi:10.1016/S0006-291X(88)80909-4
179. Gorevic PD, Munoz PC, Gorgone G, Purcell JJ Jr, Rodrigues M, Ghiso J, Levy E, Haltia M, Frangione B (1991) Amyloidosis due to a mutation of the gelsolin gene in an American family with lattice corneal dystrophy type II. N Engl J Med 325:1780–1785
180. Levy E, Haltia M, Fernandez-Madrid I, Koivunen O, Ghiso J, Prelli F, Frangione B (1990) Mutation in gelsolin gene in Finnish hereditary amyloidosis. J Exp Med 172:1865–1867. doi:10.1084/jem.172.6.1865
181. de la Chapelle A, Tolvanen R, Boysen G, Santavy J, Bleeker-Wagemakers L, Maury CP, Kere J (1992) Gelsolin-derived familial amyloidosis caused by asparagine or tyrosine substitution for aspartic acid at residue 187. Nat Genet 2:157–160. doi:10.1038/ng1092-157
182. Wisniewski T, Golabek A, Kida E, Wisniewski K, Frangione B (1995) Conformational mimicry in Alzheimer's disease. Role of apolipoproteins in amyloidogenesis. Am J Pathol 147:238–244
183. Maury CP, Kere J, Tolvanen R, de la Chapelle A (1990) Finnish hereditary amyloidosis is caused by a single nucleotide substitution in the gelsolin gene. FEBS Lett 276:75–77. doi:10.1016/0014-5793(90)80510-P
184. Kiuru S (1998) Gelsolin-related familial amyloidosis, Finnish type (FAF), and its variants found worldwide. Amyloid 5:55–66
185. Chen CD, Huff ME, Matteson J, Page L, Phillips R, Kelly JW, Balch WE (2001) Furin initiates gelsolin familial amyloidosis in the Golgi through a defect in Ca^{2+} stabilization. EMBO J 20:6277–6287. doi:10.1093/emboj/20.22.6277
186. Page LJ, Suk JY, Huff ME, Lim HJ, Venable J, Yates J, Kelly JW, Balch WE (2005) Metalloendoprotease cleavage triggers gelsolin amyloidogenesis. EMBO J 24:4124–4132. doi:10.1038/sj.emboj.7600872
187. Bhattacharya S, Latha JN, Kumresan R, Shashi S (2007) Cloning and expression of human islet amyloid polypeptide in cultured cells. Biochem Biophys Res Commun 365:8–15
188. Westermark P (1994) Amyloid and polypeptide hormones: what is their inter-relationship? Amyloid 1:47–60. doi:10.3109/13506129409148624

189. Koopmans SJ, Radder JK, Krans HM, Barge RM (1992) Biological action of pancreatic amylin: relationship with glucose metabolism, diabetes, obesity and calcium metabolism. Neth J Med 41:82–90
190. Cooper GJ, Day AJ, Willis AC, Roberts AN, Reid KB, Leighton B (1989) Amylin and the amylin gene: structure, function and relationship to islet amyloid and to diabetes mellitus. Biochim Biophys Acta 1014:247–258. doi:10.1016/0167-4889(89)90220-6
191. Edwards BJ, Morley JE (1992) Amylin. Life Sci 51:1899–1912. doi:10.1016/0024-3205(92)90106-Y
192. Nilsson MR, Raleigh DP (1999) Analysis of amylin cleavage products provides new insights into the amyloidogenic region of human amylin. J Mol Biol 294:1375–1385. doi:10.1006/jmbi.1999.3286
193. Anguiano M, Nowak RJ, Lansbury PT (2002) Protofibrillar islet amyloid polypeptide permeabilizes synthetic vesicles by a pore-like mechanism that may be relevant to type II diabetes. Biochemistry 41:11338–11343. doi:10.1021/bi020314u
194. Westermark P, Wernstedt C, Wilander E, Hayden DW, O'Brien TD, Johnson KH (1987) Amyloid fibrils in human insulinoma and islets of Langerhans of the diabetic cat are derived from a neuropeptide-like protein also present in normal islet cells. Proc Natl Acad Sci USA 84:3881–3885. doi:10.1073/pnas.84.11.3881
195. Rosano C, Zuccotti S, Bolognesi M (2005) The three-dimensional structure of β2 microglobulin: results from X ray crystallography. Biochim Biophys Acta 1753:85–91
196. Floege J, Ehlerding G (1996) Beta-2-microglobulin associated amyloidosis. Nephron 72:9–26. doi:10.1159/000188801
197. Gejyo F, Yamada T, Odani S, Nakagawa Y, Arakawa M, Kunitomo T, Kataoka H, Suzuki M, Hirasawa Y, Shirahama T, Cohen AS, Schmid K (1985) A new form of amyloid protein associated with chronic hemodialysis was identified as beta 2-microglobulin. Biochem Biophys Res Commun 129:701–706. doi:10.1016/0006-291X(85)91948-5
198. Gouin-Charnet A, Mourad G, Argilés A (1997) Alpha 2-macroglobulin protects some of the protein constituents of dialysis-associated amyloidosis from protease degradation. Biochem Biophys Res Commun 231:48–51. doi:10.1006/bbrc.1996.6019
199. Trinh CH, Smith DP, Kalverda AP, Philips SE, Radford S (1991) Crystal structure of monomeric human β-2-microglobulin reveals clues to its amyloidogenic properties. Proc Natl Acad Sci USA 99:9771–9776. doi:10.1073/pnas.152337399
200. McParland VJ, Kad NM, Kalverda AP, Brown A, Kirwin-Jones P, Hunter MG, Sunde M, Radford SE (2000) Partially unfolded states of beta(2)-microglobulin amyloid formation in vitro. Biochemistry 39:8735–8746. doi:10.1021/bi000276j
201. Ohhashi Y, Hagihara Y, Kozhukh G, Hoshino M, Hasegawa K, Yamaguchi I, Naiki H, Goto Y (2002) The intrachain disulfide bond of beta(2)-microglobulin is not essential for the immunoglobulin fold at neutral pH, but is essential for amyloid fibril formation at acidic pH. J Biochem 131:45–52
202. Gribbin JR (2004) Deep simplicity: bringing order to chaos and complexity. Random House Inc., New York, pp 1–304
203. Chapman MR, Robinson LS, Pinkner JS, Roth R, Heuser J, Hammar M, Normark S, Hultgren SJ (2002) Role of *Escherichia coli* curli operons in directing amyloid fiber formation. Science 295:851–855. doi:10.1126/science.1067484
204. Claessen D, Rink R, de Jong W, Siebring J, de Vreugd P, Boersma FG, Dijkhuizen L, Wosten HA (2003) A novel class of secreted hydrophobic proteins is involved in aerial hyphae formation in *Streptomyces coelicolor* by forming amyloid-like fibrils. Genes Dev 17:1714–1726. doi:10.1101/gad.264303
205. Mackay JP, Matthews JM, Winefield RD, Mackay LG, Haverkamp RG, Templeton MD (2001) The hydrophobin EAS is largely unstructured in solution and functions by forming amyloid-like structures. Structure 9:83–91. doi:10.1016/S0969-2126(00)00559-1
206. Coustou V, Deleu C, Saupe S, Begueret J (1997) The protein product of the het-s heterokaryon incompatibility gene of the fungus *Podospora anserina* behaves as a prion analog. Proc Natl Acad Sci USA 94:9773–9778. doi:10.1073/pnas.94.18.9773
207. King CY, Tittmann P, Gross H, Gebert R, Aebi M, Wüthrich K (1997) Prion-inducing domain 2-114 of yeast Sup35 protein transforms in vitro into amyloid-like filaments. Proc Natl Acad Sci USA 94:6618–6622. doi:10.1073/pnas.94.13.6618
208. Iconomidou VA, Vriend G, Hamodrakas SJ (2000) Amyloids protect the silkmoth oocyte and embryo. FEBS Lett 479:141–145. doi:10.1016/S0014-5793(00)01888-3
209. Iconomidou VA, Chryssikos GD, Gionis V, Galanis AS, Cordopatis P, Hoenger A, Hamodrakas SJ (2006) Amyloid fibril formation propensity is inherent into the hexapeptide tandemly repeating sequence of the central domain of silkmoth chorion proteins of the A-family. J Struct Biol 156:480–488. doi:10.1016/j.jsb.2006.08.011
210. Kobayashi T, Urabe K, Orlow SJ, Higashi K, Imokawa G, Kwon BS, Potterf B, Hearing VJ (1994) The Pmel 17/silver locus protein. Characterization and investigation of its melanogenic function. J Biol Chem 269:29198–29205
211. Kelly JW, Balch WE (2003) Amyloid as a natural product. J Cell Biol 161:461–462. doi:10.1083/jcb.200304074
212. DeLano WL (2002) The PyMOL molecular graphics system. DeLano Scientific, Palo Alto. http://www.pymol.org

Roche

Roche otorga el presente

Diploma

A: *Q.F.B. Víctor Guadalupe García González*

Por haber participado en el

Premio de Investigación Médica Dr. Jorge Rosenkranz

en el Área Básica; y hacerse acreedor al reconocimiento en la categoría *Investigador Consolidado* con el trabajo:

"Propiedades amiloidogénicas del péptido carboxilo-terminal de la Proteína Transferidora de Ésteres de Colesterol"

29 de septiembre de 2010

Dr. Jorge Tanaka Kido
Director Médico
Roche México